U.PORTO

FEUP FACULDADE DE ENGENHARIA
UNIVERSIDADE DO PORTO

IMPROVING RAILWAY TRACK MAINTENANCE USING POWER SPECTRAL DENSITY (PSD)

ABDUR ROHIM BOY BERAWI

A Dissertation Submitted in Partial Fulfillment of the Requirements for the Degree of

DOCTOR OF PHILOSOPHY IN TRANSPORT SYSTEMS

Supervisor: Professor Doctor Raimundo Delgado

Co-Supervisor: Professor Doctor Rui Calçada

AUGUST 2013

GENERAL TABLE OF CONTENTS

ABSTRACT

The implementation of Power Spectral Density (PSD) for assessing the track quality condition is relatively new in the area of railway tracks. Most of the Infrastructure Managers (IM's) tend to use the Track Quality Index (TQI) method, which is typically a statistical function of the standard deviation of each geometrical defect. In comparison with the PSD technique, TQI has some obvious disadvantages since, for example, it cannot indicate a specific problem that exists on a track whereas PSD can.

This research was conducted in response to a need for a rigorous approach to the development of a track degradation model for the purpose of track maintenance. The Power Spectral Density (PSD) forms the core focus for this research since it provides a systematic technique for evaluating track quality condition. To achieve the underlying objective, the research was divided into two major phases. The first phase attempted to examine the application of power spectral density in the track quality assessments. The investigation was then further continued by evaluating the existing relationship between various track geometry parameters. This phase is of particular importance towards establishing a reasonably accurate model of track degradation, which takes into account the interactions among various geometry variables. The second phase was conducted by developing a predictive degradation model which may capture the evolution of track quality in terms of statistical index and frequency spectrum. The results obtained from this model together with a track recovery model were then applied to analyze different maintenance scenarios.

The research findings indicate that some variables of track geometry are closely related. For instance, the strongest positive relationship can be found between the left and the right rails, in both longitudinal profile and alignment. Based on the coherence analysis, the variations of longitudinal profile in both rails are similar for wavelengths longer than 6 m while alignment exhibits a strong relationship for wavelengths longer than

66 m. Typically, the most detrimental wave among various track geometries can be found at a wavelength band between 6-30 m.

In correspondence with the application of the maintenance model, the results showed that the influence of the proposed track quality criteria (with TQI or PSD limits), the adopted variables of geometry defect (longitudinal profile or alignment) and selected maintenance strategies (preventive, delay, or the combination of regular and corrective maintenance) are key factors in determining the maintenance decision. From the analysis results, the preference for the track quality criteria of TQI may reduce the number of maintenance actions by 7% in relation to the use of PSD. A reduction in the number of tamping actions might also be achieved if the track maintenance solely considered defects in the longitudinal profile instead of in the alignment variable. The declination ranges up to 52% with respect to PSD criteria and 22% with respect to TQI criteria. Finally, the selected strategy of delayed maintenance has proven to be more efficient for tamping decision than preventive and the combination of regular and corrective maintenance.

Keywords: power spectral density; track quality index; ballasted track; track maintenance

RESUMO

A implementação de espectros de densidade de potência (PSD) para avaliação da condição da via é relativamente recente na área de vias ferroviárias. A grande maioria dos Gestores de Infraestruturas (IM's) utiliza o método do Índice de Qualidade da Via (TQI), o qual é tipicamente uma função estatística do desvio-padrão de cada defeito geométrico. Relativamente ao método PSD, a aplicação do TQI possui algumas desvantagens como, por exemplo, não ser possível indicar um problema específico existente na via. Por seu lado, o PSD consegue dar resposta a este tipo de problemas.

A presente investigação foi conduzida no sentido de satisfazer a necessidade de uma abordagem rigorosa ao desenvolvimento de um modelo de degradação da via para manutenção da via. O método PSD representa o principal foco de interesse da presente investigação uma vez que envolve uma metodologia sistemática para determinação da condição da via. Para atingir estes objectivos, o trabalho encontra-se dividido em 2 fases. A primeira fase contempla a análise da aplicação do método PSD na avaliação da qualidade da via. O trabalho continua com a avaliação da relação existente entre os vários parâmetros relativos à geometria da via. Esta fase assume especial importância para establecer um modelo de degradação da via de forma apropriada e precisa, uma vez que considera a interação entre as várias variàveis da geometria da via. A segunda fase do trabalho foca-se no desenvolvimento de um modelo preditivo de degradação com capacidade de captar a qualidade da via no que diz respeito aos parâmetros estatisticos e espectro de frequência. Os resultados obtidos deste modelo juntamente com o modelo de processo de recuperação são então aplicados para análise de diferentes cenários de manutenção.

As recentes descobertas indicam que algumas das variáveis da geometria da via estão relacionadas. Por exemplo, existe uma forte relação entre o alinhamento da direita e da esquerda, e também entre o perfil e o alinhamento. Baseado na análise, para comprimentos de onda maiores que 6 m a variação do perfil nos dois alinhamentos é

semelhante, enquanto o alinhamento apenas exibe uma forte relação para maiores que 66 m. Tipicamente, os comprimentos de onda entre 6 e 30 m, para várias geometrias de via, são os mais danosos.

Em correspondência com a aplicação do modelo de manutenção, os resultados mostram que a influência do critério proposto de qualidade da via (com limites obtidos através de TQI ou PSD), das variáveis de defeitos geométricos de preferência (perfil ou alinhamento) e determinadas estratégias de manutenção (preventiva, tardia, ou a combinação entre a manutenção regular e corretiva) são os factores-chave na determinação da decisão de manutenção. Através da análise dos resultados, o critério do índice de qualidade da via TQI poderá reduzir o número de ações de manutenção até 7% menos do que se usar o PSD. A redução do número de manutenções também poderá ser alcançado se for apenas considerado o perfil de irregularidade em vez do alinhamento. Esta redução pode atingir os 52% com o critério PSD e os 22% com o critério TQI. Finalmente, a estratégia adotada de manutenção tardia provou ser mais eficiente para decisões de manutenção do que a manutenção preventiva e a combinação entre a manutenção regular e corretiva.

Palavras-chave: espectros de potência; indice de qualidade da via; via balastrada; manutenção da via

ACKNOWLEDGEMENTS

Many people have contributed to the work described here, and the author would like to take the opportunity to thank them.

First and foremost, a big thank you to my supervisor Prof. Raimundo Delgado for the patient guidance, encouragement and valuable advice he has provided throughout my time as his student. His positive outlook and confidence in my research inspired me and gave me confidence.

Grateful appreciation is also expressed to my co-supervisor, Prof. Rui Calçada, for his assistance and constructive comment with many insightful suggestions. He spent countless hours proofreading my thesis and discussing new research ideas. His encouragement and kindness will never be forgotten. I also wish to thank to Dr. Cecilia Vale for her advice and technical input during various stages of my study. Without her involvement, this work would not have been possible.

I gratefully acknowledge the funding received towards my PhD from the Fundação para a Ciência e a Tecnologia (FCT). The support and direction offered by the MIT Portugal Program are greatly appreciated. The author would also like to thank the support of the Portuguese Railway Administration (REFER) for the access to railway information data.

Utmost gratitude is also forwarded to Prof. Alvaro Costa and Prof. Jorge Pinho, Director of MIT Portugal – University of Porto Program for their supports. Thanks must also go to Prof. Isabel Ribeiro for helping me when needed. I would like to thank Prof. Cristiana who spent endless hours proofreading my thesis.

My parents, brothers and sisters deserve a warm and special acknowledgement for their love and care. It would certainly have been much difficult without my colleagues, lending me their shoulders to lean on and providing invaluable moments of friendship.

TABLE OF CONTENTS

LIST OF FIGURES

LIST OF TABLES

ABBREVIATIONS

AI	Alignment Index
AL	Alert Limit
AMPL	A Mathematical Programming Language
CEN	European Committee for Standardization
DFT	Discrete Fourier Transform
FFT	Fast Fourier Transform
FRA	Federal Railroad Administration
GI	Gauge Index
GPS	Global Positioning System
IAL	Immediate Action Limit
IL	Immediate Limit
ILP	Integer Linear Programming
IM	Infrastructure Manager
IP	Integer Programming
LCC	Life Cycle Cost
LP	Linear Programming
M&R	Maintenance and Renewal
MAE	Mean Absolute Error

MGT	Million Gross Ton
MILP	Mixed Integer Linear Program
ORE	Office for Research and Experiments
PSD	Power Spectrum Density
RMSE	Root Mean Squared Error
SD	Standard Deviation
SNCF	Société Nationale des Chemins de Fer Français
TGI	Track Geometry Index
TI	Twist Index
TQI	Track Quality Index
TRC	Track Recording Car
UI	Unevenness Index

LIST OF NOTATIONS

I. Latin Letters

Chapter 2

A	-	Amplitude of auto spectrum density; Indication of the state of rail surface
A_a	-	Roughness coefficient; Scale factor for alignment
A_i	-	Reverse check method
A_p	-	Scale factor for longitudinal profile
A_v	-	Roughness coefficient
a	-	Coefficient Chinese PSD; One half of track gauge
a_0	-	Coefficient factor (ORE Model)
a_1	-	Coefficient factor (ORE Model)
b	-	Coefficient Chinese PSD; Constant factor (ORE Model); Width of sleeper in longitudinal direction; Rate of deterioration
C_1	-	Constant factor (ITDM Model)
c	-	Coefficient Chinese PSD; Total number of section samples
$\Delta cross\ level$	-	Difference of cross level or superelevation irregularity between two points
d	-	Coefficient Chinese PSD
e	-	Coefficient Chinese PSD

e_1	-	Settlement after the first cycle load
e_T	-	Track settlement after an operational load T
e_N	-	Ballast settlement; Settlement after N cyclic loading
F_e	-	Equivalent wheel set load
F_i	-	Static wheel-set load type i
EI	-	Flexural rigidity of rail
F	-	Normal force
$F(k)$	-	Continuous Fourier transform
$F(m)$	-	The m-th DFT output of the sampled component
$F_n(m)$	-	Discrete Fourier transform
$F_n^*(m)$	-	Complex conjugate
f	-	Wavenumber (PSD China)
$f(n)$	-	Sequence of input samples
$f(x)$	-	Continuous waveform.
$G_{rr}(n)$	-	PSD vertical irregularity
$G_{rr}(n_0)$	-	Scale factor of rail roughness
G_{xx}	-	Auto power spectral density
h	-	Amount of track improvement given by the tamping machine
$\Delta horz.level$	-	Difference of horizontal level between two points
i	-	Sequential number

J	-	Synthetic Track Quality Coefficient
j	-	Imaginary unit
K	-	Condition Index (Banverket); Factor to describe the track structure; Track stiffness
k	-	Coefficient Chinese PSD; Number of samples of assessment sections exceeding the allowable value; Analysis wavenumber; Determined variable (FRA PSD)
k_h	-	Parameter (ITDM Model)
k_{l_hrtop}	-	Lubrication factor
k_{l_lrtop}	-	Lubrication factor
$k_{l\_hrgauge}$	-	Lubrication factor
k_w	-	Wear coefficient
k_1	-	Rail pad
L	-	Rail influence factor; Measurement distance; Total track length studied
L_e	-	Elastic length
L_o	-	Fixed length of track segment
L_s	-	Traced length of space curve
Σl	-	Sum of track length where all σ values are below
M	-	Structure factor
M_{sub}	-	Subgrade modulus

m	-	Intermediate mass consisted of sleeper, ballast and subgrade; Index of the DFT output in the wavenumber domain
N	-	Total number of axles; Number of cyclic loading; The number of samples of the input sequence and the number of wavenumber points in the DFT output
N_i	-	Number of wheel-set load type *i.*
Nr	-	Number of window or block data
ΔN	-	Number of axles in the initial period of settlement
n	-	Index of spatial domain of input samples; Number of signals registered in the analyzed track section; Cyclic wavenumber
$nfft$	-	Number of spectral lines
n_0	-	Coefficient (SNCF PSD and Braun PSD)
P	-	Influence factor for sub-grade; Lateral load; Contact pressure between wheel and rail
P_b	-	Maximum sleeper pressure due to a wheel load
P_l	-	Lateral load
p	-	Ballast pressure
Q	-	Condition Index (Banverket); Track quality represented by MDZ number
Q_0	-	Initial track quality
R	-	Curve radius; Set of real numbers
S	-	Average growth of irregularities in section; Relative value of

settlement; Standard deviation

SDA_{maint}	-	Standard deviation for maintenance of alignment
SDA_{mes}	-	Standard deviation value of alignment
SDA_n	-	Standard deviation of newly laid track for alignment
SDG_{maint}	-	Standard deviation for maintenance of gauge
SDG_{mes}	-	Standard deviation value of gauge
SDG_n	-	Standard deviation of newly laid track for gauge
SDT_{maint}	-	Standard deviation for maintenance of twist
SDT_{mes}	-	Standard deviation value of twist
SDT_n	-	Standard deviation of newly laid track for twist
SDU_{maint}	-	Standard deviation for maintenance of unevenness
SDU_{mes}	-	Standard deviation value of unevenness
SDU_n	-	Standard deviation of newly laid track for unevenness
S_e	-	Standard deviation of track gauge
S_w	-	Standard deviation of track twist
S_y	-	Standard deviation of horizontal irregularities
S_z	-	Standard deviation of vertical irregularities
SD_{left}	-	Standard deviation for left longitudinal profile
SD_{right}	-	Standard deviation for right longitudinal profile
$S(f)$	-	Track irregularity Chinese PSD

$S_{al}(\Omega)$	-	PSD of track lateral alignment irregularity
$S_{av}(\Omega)$	-	PSD of track vertical alignment irregularity
$S_{cl}(\Omega)$	-	PSD of cross level or superelevation irregularity
$S_{gauge}(\Omega)$	-	PSD of track gauge irregularity
$S_v(\Omega)$	-	PSD of track longitudinal profile irregularity
$\|\|s\|\|$	-	Sliding distance
T	-	Passed tonnage (t)
t	-	Time or tonnage
V	-	Average running speed
v	-	Train speed
$\Delta vert.level$	-	Difference of vertical level between two points
W	-	Coefficient of parameter defectiveness; Vertical wheel load
W_e	-	Defectiveness of track gauge
W_g	-	Defectiveness of superelevation (cross level)
W_w	-	Defectiveness of twist
W_x	-	Arithmetic averages for vertical defectiveness
W_y	-	Arithmetic averages for horizontal defectiveness
W_5	-	Five Parameters of Defectiveness
w	-	Volume lost due to wear; Waviness
w_{hr_gauge}	-	Wear for high rail gauge face

w_{hr_top}	-	Wear for top of the high rail
w_{lr_top}	-	Wear for top of the low rail
x	-	Longitudinal distance; Average value of track irregularity; Repeated number of loading or tonnage
x_i	-	Value of parameter at point i
Δx	-	Sampling interval
y	-	track settlement
Δy	-	Difference between two measurement
Z	-	Set of integers

Chapter 3

f_j	-	Predicted value
n	-	Number of predictors
y_j	-	Actual value

Chpter 4

A_k	-	Amplitude coefficient of random series
$G_{rr}(n_k)$	-	Power Spectral Density Standard
N	-	Total number increments in the range of upper and lower waves
n_{low}	-	Lower wavelength

n_k - Center wavenumber

n_{up} - Upper wavelength

Δn - Wave band

$r(x)$ - Stationary stochastic process

Chapter 5

L - Length of track irregularity signal

M - Half width of Hanning window

N - Number of data points

$P_{sg}(\lambda)$ - Cross power spectrum density between signal x and y

$P_{ss}(\lambda)$ - Power spectrum of signal g

p - Cross correlation coefficient

$R_{ss}(m)$ - Auto-correlation of sampled signal *s(x)*

$R_{ss}(\tau)$ - Auto-correlation of signal *s(x)*

$R_{sg}(m)$ - Cross correlation function

S - Average power of the input waveform

$s(n)$ - Space domain of track irregularity

$s(x)$ - Continuous random of track irregularity

m - Number of lag sample

x - Distance

II. Greek Letters

Chapter 2

Ω	-	Spatial wave-number
$\Omega_c, \Omega_s, \Omega_\gamma$	-	Critical wavenumber
a	-	Coefficient (Sato's model)
β	-	Coefficient (Sato's model)
γ	-	Coefficient (Sato's model)
δ	-	Wear depth
λ	-	Wavelength
ψ	-	Angle of attack between wheel set to the track
σ_H	-	Standard deviation of height / longitudinal profiles
σ_S	-	Standard deviation for interaction
$\sigma_{H_{lim}}$	-	Standard deviation limit of longitudinal profile in a given track class
$\sigma_{S_{lim}}$	-	Standard deviation limit for interaction in a given track class

Chapter 4

θ_k	-	Phase angle
Ω_l	-	Uppermost limits
Ω_n	-	Discrete angular wavenumber
Ω_u	-	Uppermost limit

Chapter 5

α	-	Desired level of confidence
τ	-	Lag distance
γ^2	-	Coherence function
$\gamma^2_{1-\alpha}$	-	Confidence level

1

INTRODUCTION

1.1 INTRODUCTION

In recent years, studies on track degradation in railways have attracted a great deal of attention. Intensive research activities have been carried out by many organizations with the aim of securing a high level of safety and reliability of the infrastructure system. New technologies and stringent safety standards are constantly being introduced for several reasons, not only to prevent the assets from failure or damage but also to minimize the main sources of problems associated with the performance degradation in terms of quality, comfort and safety of each journey.

Since failure on the railway system will result in significant economic losses, many Infrastructure Managers (IMs) spend a substantial proportion of budget on Maintenance and Renewal (M&R) of the tracks, which makes up a considerable part of the total railway operating cost, accounting for up to 70% of the total life cycle cost (LCC) of track infrastructure [Jianmin, 2007]. For instance, a single track of 1 km long in typical European countries requires an average of 30,000 euro for a 1-year maintenance period [Gines, 2008]. With this massive amount of financial expenditure, a small reduction in the cost of maintenance will undoubtedly bring a significant impact, particularly to the overall LCC.

As degradation is one of the prime issues in this matter, it becomes important to understand the complexity of degradation mechanisms, its likelihood of occurrence in the railway track, as well as the variables affecting the degradation. The recognition of any changes in the track condition over time and the consequences of maintenance actions on the track performance will enable to predict the residual life time of the asset. The accurate life cycle including any necessary maintenance activities throughout the service life can thus be drawn and by doing so, the railway company is capable of systematically reducing the operation and maintenance expenditures without affecting traffic safety.

1.2 PROBLEM DESCRIPTION

Nowadays, efforts have been made to develop effective maintenance and renewal policies. The goal of maintenance management is to reduce the adverse effects of failure and to maximize the availability of the railway network at minimum cost [Lofsten, 1999]. In this case, the railway infrastructure managers (IMs) play an important role. They are challenged to optimize each stage of the maintenance procedure and to analyze the best alternative maintenance strategies (inspection frequency, interval of tamping, etc.) with respect to cost effectiveness and safety issues.

In order to assure the operational services, there are two main maintenance strategies that may be applied [Holmgren, 2005]. The first one is preventive maintenance, where the intervention is performed at a predetermined interval and/or on a continuous basis. The primary goal of this typical maintenance is to prevent the consequences of failure or the degradation of the functioning items. The second strategy is known as corrective maintenance, where the intervention is carried out after particular equipment has suffered failure. This type of maintenance is unplanned and repairs are intended to bring the system back to work in order; however, it is neither practical nor economically feasible to perform both methods. Regular maintenance of a large infrastructure network is costly and fairly time-consuming because it might be done even when it is unnecessary. On the other hand, the corrective maintenance can be extremely costly since the disruption of traffic operation due to the system failure will have an adverse

effect at an additional cost, namely involving delay costs, train cancellations and penalties imposed by traffic operators to the IMs. To be able to manage these issues, a prediction model of track degradation is needed to make the best decision in maintenance and replacement strategies, to account for costs and risks over the life cycle of a railway track.

Analyses and detailed studies on track degradation have been done by many researchers and various predictive models have been proposed, from simple deterministic to the most elaborated stochastic models. Based on the literature review, the main railway degradation models are those developed by Bing and Gross [1983], Shenton [1984], Sato [1995] and TU Muenchen [Demharter, 1982]. The models were built based on empirical analysis, in which the settlements were mainly considered as the controlling degradation factors.

More recent developments in track degradation models refer the use of rail geometry data to provide the characterization of track geometry irregularities. By computing the rail variance, for individual or a set of geometrical parameters (such as longitudinal profile, alignment, gauge, twist and cross level or superelevation irregularity), the quantitative value, named Track Quality Index (TQI), can be derived. The progress of changes in TQI may help the track manager to predict the future quality of a unit section [Bing and Gross, 1983]. In spite of its principal role, which is to portray the track condition, TQI may not reflect the wavelength contents of geometry defect, which is inherently related to the particular issue of train-track interaction.

In order to overcome this drawback, as an alternative for assessing rail irregularity, power spectrum graph may be used [Zhiping *et al*., 2009]. Such graph provides information concerning track irregularity in the frequency domain, with horizontal and vertical axes representing the spatial frequency and Power Spectrum Density (PSD), respectively [Zhiping *et al*. (2009), Zhiping and Shouhua (2009), Zhiqiang *et al*. (2009)]. Both of these axes can be used as indicators for track quality. The higher the PSD values, the poorer the track quality will be, while the lower the PSD values mean

the opposite situation. An analysis on the horizontal axis can also help to detect which wavelengths have contributed to the geometry defect [El-Sibaie and Zhang, 2004]. The PSD application, however, is not as widely used as the previous aforementioned technique. The expertise and knowledge required to process and to interpret information regarding the Power Spectral Density is the main drawback in the development of this method.

Following these shortcomings, this dissertation aims to develop a logical model for the deterioration of track geometry and to incorporate the proposed model as basis for optimizing maintenance in practice. The Power Spectral Density (PSD) forms a core focus of the studies since it involves a systematic technique for evaluating track quality condition. For the purpose of analysis, a particular segment of the Portuguese Northern Railway Lines with 33.4 km in length will be considered and multivariate statistical analyses will be employed in some geometric parameters. The results will be used to derive the optimization model for scheduling track maintenance by means of tamping in a given period of time.

The application of maintenance model will consider the deterioration of two geometrical parameters that most influence the vehicles and the track dynamics in the vertical and horizontal directions, which are the longitudinal profile and the alignment. Several track maintenance strategies will also be analysed in order to obtain the most efficient approach to reduce the number of maintenance actions while keeping the safety level. In this case, a new proposed maintenance strategy called Delay Maintenance (DM) will be introduced and will be compared with the conventional approaches in the track maintenance management. The core of this strategy is taken from the benefit of delaying the time to perform the maintenance operations, so thus the recovery effectiveness can be much higher than the conventional one. The track maintenance optimization model will be detailed in Chapter 6.

1.3 RESEARCH GOALS AND OBJECTIVES

The primary goals of this research are:

1. To investigate the application of Power Spectral Density in the assessment of railway track quality. For this purpose, PSD standards developed in various countries will be analyzed and those methods will then be implemented in real field assessments.
2. To quantify the degree of interdependency and to establish the similarity of one track geometry variable to another. For evaluating the existing relationship between each of them, correlation analyses will be employed in this research.
3. To develop an optimization model for scheduling track maintenance in ballasted tracks. The proposed model will consist of two parts: the predictive degradation model that may able to capture the evolution of track quality in terms of statistical index and frequency spectrum, and the track recovery model due to tamping operations. The results obtained from the optimization model will then be applied to analyze different maintenance scenarios.

1.4 SCOPE AND LIMITATIONS

The scope and limitations of this research are as follows. Firstly, the research is focused on developing a degradation model in the context of operation and maintenance stages of a track life cycle system, with a predefined design and situation. Any changes in the design structure and characteristics of the railway components made towards a better performance should be conducted separately. The reason for this limitation is the size and complexity of the research area.

Secondly, not all factors that may influence the track degradation process will be considered in the prediction model development. This is due to the insufficiency and unavailability of information related to some of these factors in the database (e.g. environment, type of materials, *etc*).

1.5 OUTLINE OF THE DISSERTATION

This study is organized in 7 chapters. Chapter 1 presents a brief introduction to the background of the research study followed by problem description. The purpose of the research, objectives, scope and limitations are also outlined in this chapter.

In chapter 2, a review is given with respect to literature closely related to the present work. The literature review deals with the current models associated with track degradation assessment, including track structural index, track quality index and power spectral density. This information provides the basis for developing the optimization model proposed in the research. In the rest of the chapter, a step-by-step procedure to calculate the optimization problem in the given model is described.

Chapter 3 details the methodology used in the study. The different phases and conceptual frameworks of research are explained, including research approach, data collection, research protocols, analysis and validation of the research model.

Chapter 4 presents the application of power spectral density in the track quality assessments. In this chapter, various PSD standards are compared in order to define the characteristic features contained in each particular standard. The implementation and procedure used to quantify the state of railway irregularity will be also described with an application case study.

Chapter 5 provides the results of the analysis of the relationship between various track geometry parameters. A comprehensive correlation study has been conducted to determine the degree of interdependency and to establish the similarity of one geometry variable to another. Such studies are necessary to support the research findings obtained in chapter 6.

Chapter 6 is the core of the research. It provides a chronological overview of the development of the maintenance models together with a discussion of relevant assumptions. Several analyses are carried out in this chapter, such as the identification of relationship between track quality index and power spectral density, and the establishment of an alternative criteria of threshold limit based on power spectral density. The results are used to improve the maintenance decision strategies, and then followed by validation with some performance criteria.

Chapter 7 summarizes the main conclusions of this doctoral research and formulates the recommendations for further research.

2

LITERATURE REVIEW

2.1 INTRODUCTION

This chapter provides a literature review concerning the present subject under investigation. It further includes an introduction to the methods of track quality assessment as well as an overview on various maintenance strategies of railway tracks.

2.2 RAILWAY TRACK SYSTEM

The railway infrastructure comprises a wide array of elements intended to support and guide the train in a safe and economic manner. Typically, the track structure can be grouped in two main categories: superstructure and substructure. The superstructure consists of rails, fastening system, rail-pads and sleepers, while the substructure consists of ballast, sub-ballast and sub-grade. Figure 2.1 shows the track design and the components included in a ballasted track structure.

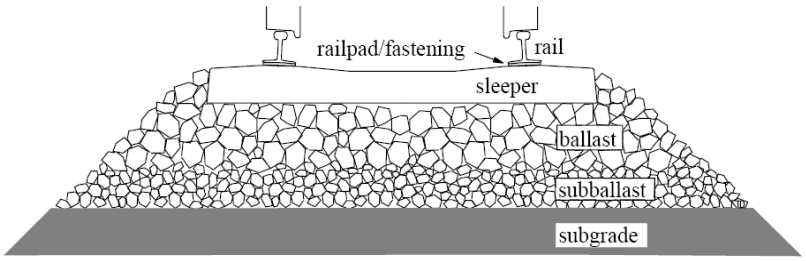

Figure 2.1 – Track Design of a Ballasted Track [Dahlberg, 2003]

Some important parameters that describe the layout and path of the track are defined as "track geometry". By design, track geometry should contain the specific criteria so as to ensure the optimal comfort and safety for train operation. For this reason, the European Standards [prEN 13848-5] have specified the requirements for the homologation of track geometry including longitudinal profile, alignment, gauge, cross level (or superelevation irregularity) and twist. Figure 2.2 illustrates a schematic description regarding these geometry variables.

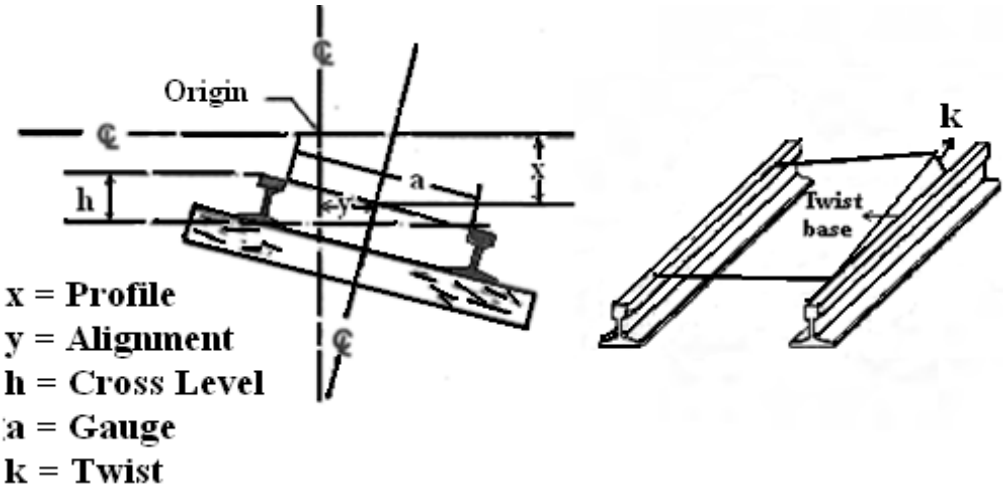

Figure 2.2 – Track Geometry Parameters [Bing and Gross,1983]

Longitudinal profile and alignment are delineated with the track geometry of each rail projected longitudinally against the vertical and horizontal plane, respectively. Any change in the elevation of the two rails relative to a designated level is called longitudinal profile deviation. For an upward vertical deviation, the sign is denoted as positive while a downward deviation is expressed by a negative value. The alignment irregularity is caused by the lateral variation of the rails from a given centerline of the track. If the lateral deviation bends to the left, the sign is symbolized as positive while a negative value is given when the track deviates to the opposite direction.

Gauge specifies the inner distance between two rails measured at 16 mm below the top surface of the railhead. In Portugal, the gauge for primary railway lines is 1.668 mm, although a wide variety of gauges are used around the world. The term of gauge irregularity, therefore, refers to the deviation of the track from its specified value. The other parameter, cross level or cant irregularity, measures the amount of vertical deviation between two flat rails from the design value. This design value, commonly called super-elevation, helps to compensate the centrifugal force of the vehicle on a given curve. Consequently, cross level is not considered a defect unless it deviates from the predefined super-elevation. The last geometry variable, twist, is also associated with super-elevation. It measures the difference in the super-elevation between two points taken at a separate fixed distance along the track.

2.3 ASSESSMENT OF TRACK CONDITION

The track geometry is subjected to atmospheric influences and dynamic stresses due to the operational loads. These processes lead to the modification of the track geometry, which, if not controlled to a certain degree, may result in safety risk and derailment. In order to prevent the track from these issues, the railway network should be inspected as well as regularly maintained in accordance with the railway engineering standards.

The following section will briefly describe the strategies and applications used for assessing the railway track geometry.

2.3.1 TRACK INSPECTION CAR

Prior to the maintenance works, the measurement of the track geometry parameters is normally carried out within a specific time interval. The results are recorded as numerical values, which can be used to indicate the level of track quality. For obtaining these values, the rail operator may apply two common methods of measurement. In the first method, the measurement is conducted manually, by workers who walk along the track to detect the existence of any geometry problems [Lichtberger, 2005]. However, this technique is considered inefficient, particularly in terms of time and labor cost, due

to the extent and large scale of the railway network. The accuracy of this method is questionable as well, since not all rail defects can be directly detected by the human eye. With the advancement of technology, the application of sophisticated cars has been incorporated as supplement to the previous technique. The use of the track inspection car has proven to be efficient, yielding more outputs in the track information data.

In Portugal, track condition monitoring for high speed and conventional lines is performed by the Track Recording Car (TRC) EM 120 (Figure 2.3). This machine is able to acquire traditional geometry parameters, such as gauge, cross level or superelevation irregularity, twist, alignment and longitudinal profiles with a sampling rate of 0.25 m, and provides the calculation of the track quality index from the derived parameters.

In order to perform those functions, the machine is embedded with two main modules: a car with real time measurement module and a stationary data storage module [Cacho, 2009]. The first module is designed to read any gap in the geometry parameters from the predefined design and then sends the results to the second module for storage purposes. The computer program, which links to the Global Positioning System (GPS) receiver, will analyze the data and give the information according to customer specifications.

Figure 2.3 – Track Recording Car EM 120 [Comboios.org, 2007]

The irregularity data provided by EM 120 is based on the measurement of a 10 m chord-versine. The principle of this technique is to assess the gap corresponding to the observed roughness of a straight-line in the center point of the track in the 10 m distance measurement. This gap is then defined as track geometry irregularity. The following figure illustrates how the track geometry parameters are measured by EM 120.

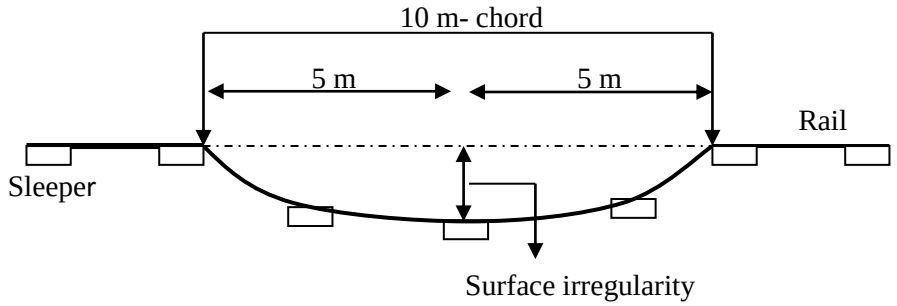

Figure 2.4 – Track Surface Irregularity [Oyama, 2006]

2.4 TRACK DEGRADATION

It has been observed that the condition of a railway track degrades rapidly over a period of time. Having the knowledge of the degradation process will aid in the estimate of the future state of a track condition and in the mitigation of the problems associated with operational safety. The following section presents the theoretical framework and the current practices related with railway track degradation.

2.4.1 GENERAL CONCEPT

Track degradation is a complex process. The mechanism involves many influencing parameters such as axle load, traffic speed, climate, track characteristics and topography (Figure 2.5). Today, research efforts have been carried out not only to address the degradation problems, but also to determine the contribution of each parameter to the entire process.

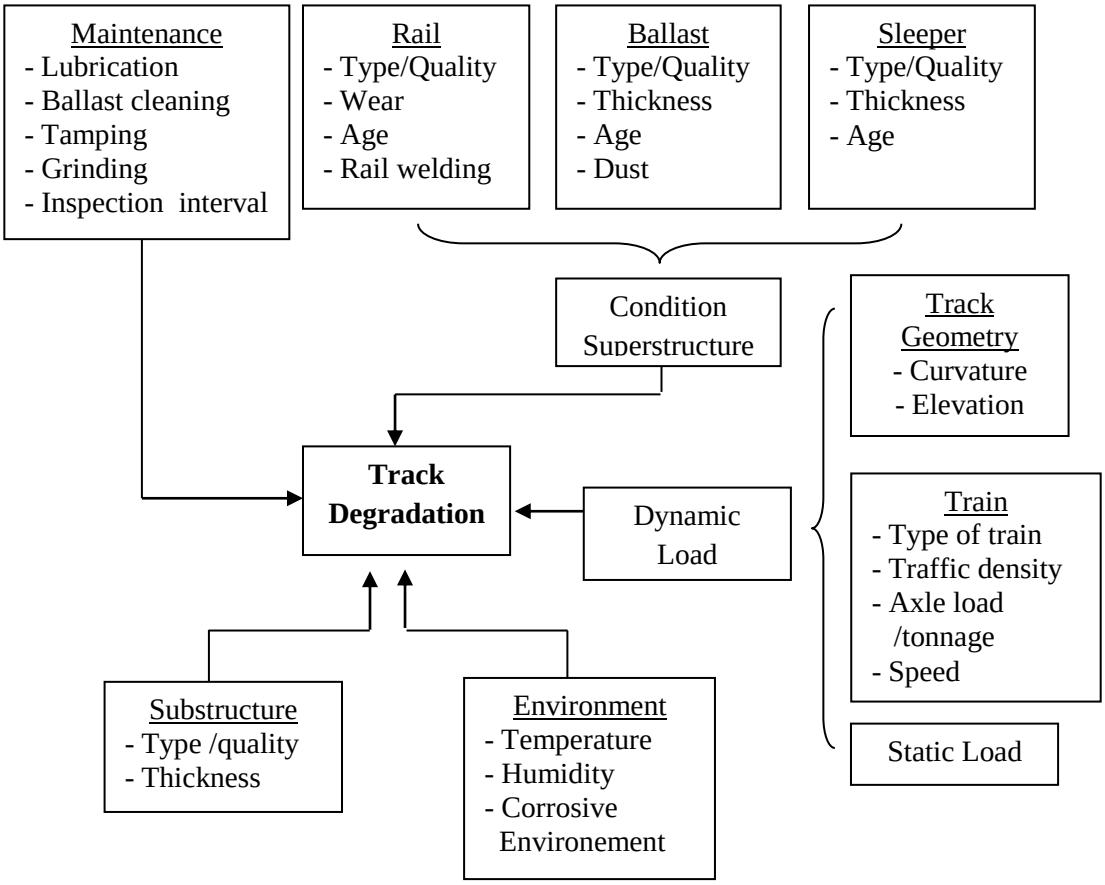

Figure 2.5 – Influencing Parameters to the Track Degradation

Ferreira & Murray [1997] have investigated the physical factors that may have impact on track deterioration. According to the results, the authors argue that the declination in the track quality is mainly driven by three parameters, i.e. dynamic forces, axle load and train speed. Speed contributes to the deterioration process by increasing the dynamic forces at high speeds and decreasing those at low speeds. Load contributes to increased rail wear and fatigue, wheel wear, and strains in rails and sleepers. As a consequence, cracks in the rail and sleepers will occur, the railhead will be worn out, the rail fastening will be loosen, and the ballast load will thus be redistributed. These situations will lead to reduce travel safety and comfort, and increase track components deterioration and delays.

Later work reported by Larson [2004] has found that wear and fatigue damage are considerably affected by the existence of curvature. The shape and radius of curvature can determine the rail defect with the following relationship:

- Narrow curves implies wear (ahead of fatigue)
- Tangent track implies fatigue (ahead of wear)

Using the Swedish railway data, Larson then attempted to correlate various ranges of curvature with the state of track condition:

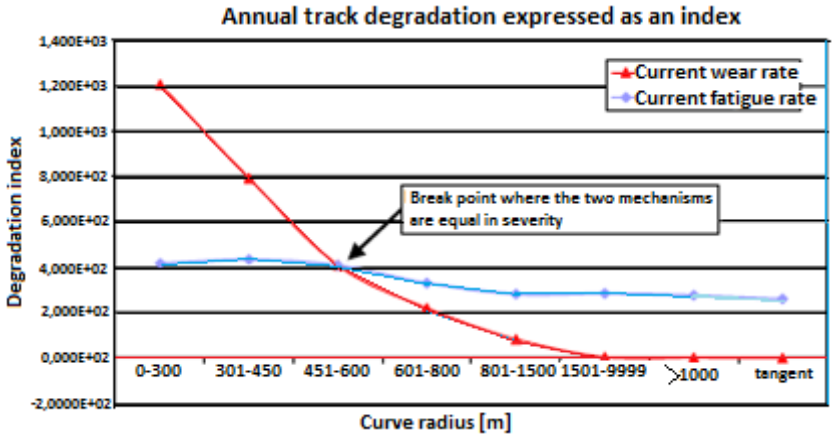

Figure 2.6 – Wear and Fatigue mechanisms as a function of Curve Radii [Larson, 2004]

As indicated in the figure, the narrow curve has caused a higher degradation index compared to the plain track. Higher index means shorter service life of the rails. Wear, in this case, governs the rail degradation with short life span, while fatigue drives the rail degradation with long life span [Zarembski, 1991].

Pita *et al.* [2004] and Berggren [2005] later investigated the influence of track stiffness to the track degradation. Based on their experimental study, the authors found that an increase in vertical stiffness produces a negative effect, especially in vertical stresses exerted by the vehicles on the rail. However, having a very flexible track may enhance

the energy dissipated from vehicles running at high speed. Considering this duality, an attempt was made to define the optimum value for the vertical stiffness, which minimizes the maintenance cost on the one hand, and the cost due to the dissipated energy on the other. The equilibrium of these two costs is achieved when the vertical stiffness of the track stands at about 70-80 kN/mm for lines on which trains run at high speed.

Similarly, the application of maintenance (consisting of tamping, grinding, lubrication, etc.) could improve the quality of railway track. When the tamping action is performed, the ballast under the ties is re-compacted and the area of contact increases. The larger the areas of contact, the better the ties distribute the weight of the rail and rolling stock, which in turn may impede the acceleration of track to face deterioration. Likewise, the application of preventive grinding also leads to a significant increase in the rail service life, since it slows down the rail corrugation growth and decreases traffic noise. From the experience gained in practice, the combination of maintenance methods, such as rail grinding and lubrication, may extend the life span and the limit of rail components from 50% to 300% [Judge, 2002].

Some other factors contributing to track deterioration have also been examined by many researchers. Lichberger [2001] discussed the effect of initial track quality to preserve the track from rapid degradation. Johansson *et al*. [2008], Witt [2008] and Lundvist [2005] argued that the selection of under sleeper pad could help reduce the ground vibration and minimize track misalignment. The preferences in choosing the material quality are also essential to attenuate the distortion on the track performance. Poor materials can cause more track degradation, while good materials will enhance the resistance of the track to failure [Zwanenburg, 2006].

2.4.2 TRACK DEGRADATION CURVE

In order to define where the quality limit is and to decide when the intervention is required, it is therefore necessary to understand the degradation behavior. Normally, the

degradation line will exhibit a “saw tooth” shape, in which the quality deteriorates between two subsequent maintenance activities [Jovanovich, 2004]. This process is schematically shown in the following figure:

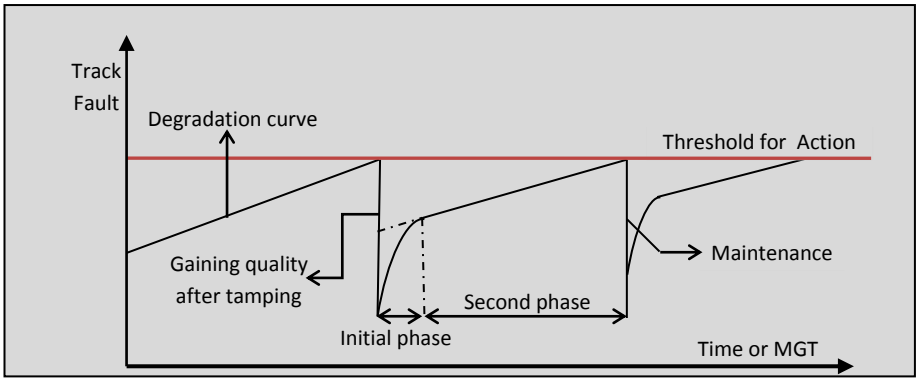

Figure 2.7 – General Trend Degradation Model [Lichtberger, 2001]

The railway track commences with an initial quality from a newly constructed line or previous maintenance action. During the train operation, the track quality starts to degrade as a result of interaction of several effective parameters, such as the cumulative of track loads (MGT), time, speed, etc. When the defect of the track reaches the threshold limit, tamping should be carried out to reduce the amount of standard deviation, leading the track geometry to deterioration in two major phases.

The first phase occurs directly after tamping, around the first 0.5-2 MGT of traffic borne. This period is followed by a rapid exponential track failure, characterized by the breaking off of the points of ballast stone that settle into a more compact position [Lichtberger, 2001]. Once the track has been sufficiently established, the second phase of degradation takes place. The track faults will deteriorate slowly and increase linearly in proportion to the number of load cycles [Lyngby, 2009]. Several mechanisms of ballast and sub-grade behavior are governed during this process. Continuous volume

reduction due to particle rearrangement and sub-ballast or sub-grade penetration into ballast voids are examples of such characteristics.

Subsequently, the efficiency of maintenance will decrease in time and the period between two tampings becomes shorter. When tamping is considered ineffective to repair the geometry faults, line reconstruction should be carried out.

2.5 TRACK DEGRADATION MODELS: CURRENT PRACTICES AND APPLICATIONS

In the past few years, several attempts have been made to build a track degradation model, from the simple one that relies on a single parameter to a comprehensive one which embraces several influencing variables. From the reviews on the available literature, these models can be classified into two different aspects [Sadeghi and Asgarinejad, 2007]:

- Track degradation considered from a structural viewpoint
- Track degradation considered from a geometrical viewpoint

From a structural viewpoint, the model development is based on the progression of defects in the physical structure, such as ballast settlement, wear and corrugation. Shenton [1984], Sato [1997], Chrismer and Selig [1993] and TU Munich [Demharter, 1982] have developed models in this area. From a geometrical viewpoint, the reflection of the actual state of track condition uses geometrical parameters, such as longitudinal profile, alignment, etc. Some of the developers of this model are Bing and Gross [1983] and recently, the practical use of the model has been adopted by many countries. In fact, both viewpoints are correlated. Any deviation in the geometry parameters is known as a result from the track structural problems [Berggren, 2005].

2.5.1 MODELS OF STRUCTURAL DEGRADATION OF THE TRACK

This section contains a brief and general description of 8 models dealing with the structural degradation of the track.

A. Sato track degradation model

The study on track deterioration due to ballast settlement has produced an equation proposed by Sato [1995]. The following equation is used to estimate the settlement of the track under repeated loading on both heavy haul narrow gauge and high standard gauge:

$$y = \gamma \cdot (1 - e^{-ax}) + \beta \cdot x \tag{2.1}$$

where:

y = track settlement (mm)

x = repeated number of loading or tonnage carried by track (cycles or tons)

a, β, γ = coefficients

Sato divides the model into two major parts. The first part refers to the initial track settlement imposed by the compaction of the ballast, which occurs directly after maintenance. The settlement in this phase is relatively fast and it can be best modeled using an exponential function ($\gamma \cdot (1 - e^{-ax})$). As soon as the ballast is consolidated, the second stage will occur. The settlement increases linearly in proportion with the cyclic loading ($\beta \cdot x$), which is called the long term settlement. The severity of settlement depends on the quality and behavior of the ballast, the sub-ballast and the sub-grade.

The coefficient γ expresses the level of settlement and a indicates the steepness of the initial function. β defines how quickly the track settlement grows in the second phase.

B. Shenton settlement model

Various parameters influencing track degradation have been investigated by Shenton. The research was conducted on different tracks spread in many countries, such as Britain, USA and several European countries. By combining the theories of functionality followed by hypotheses testing in practice, he derived a general equation that may quantify the ballast settlement [Shenton, 1984]. The proposed model is defined by:

$$e_N = K \cdot \frac{F_e}{10} \cdot [(0.69 + 0.028 \cdot h) \cdot N^{0.2} + 2.7 \cdot 10^{-6} \cdot N] \qquad (2.2)$$

where:

e_N = ballast settlement (mm)

K = a factor to describe the track structure(≈ 1.1)

F_e = equivalent wheel set load (kN)

h = amount of track improvement given by the tamping machine (mm)

N = total number of axles (-)

Furthermore, Shenton suggested an equivalent wheel-set load (F_e) according to the following equation:

$$F_e = \left(\frac{\sum F_i^5 \cdot N_i}{\sum N_i} \right)^{0.2} \qquad (2.3)$$

where:

F_e = equivalent wheel-set load (kN)

F_i = static wheel-set load type *i* (kN)

N_i = number of wheel-set load type *i* (-)

The implementation of Shenton model confirmed the absence of some influencing parameters, such as train speed and dynamic load.

C. Sugiyama Model

Sugiyama examined the growth of vertical defect within 100 days of train operation in Japan. By applying the regression theory, he proposed the degradation model as a function of passage tonnage, rail factors and vehicle speed [Iwnicki *et al.*, 1999].

$$S = 2.09 \cdot 10^{-3} \cdot T^{0.31} \cdot V^{0.98} \cdot M^{1.1} \cdot L^{0.21} \cdot P^{0.26} \quad (2.4)$$

where:

S = average growth of irregularities in section (mm /100 days)

T = passed tonnage (MGT/year)

V = average running speed (km/h)

M = structure factor

L = rail influence factor (1 for CWR and 10 for jointed rail)

P = influence factor for sub-grade (1 for good and 10 for bad)

The structure factor is derived from the following equation:

$$M = \frac{P_b \cdot \sqrt{k_1}}{\sqrt{m \cdot EI \cdot K}} \quad (2.5)$$

where:

P_b = maximum sleeper pressure due to a wheel load (Pa)

k_1 = rail pad (N/m)

m = intermediate mass consisting of sleeper, ballast and subgrade (ton)

EI = flexural rigidity of the rail (Nm^2)

K = track stiffness (N/mm)

As indicated in the formula, M is defined as a relative value. The lower the value of M, the lower the track deterioration will be.

D. ORE Model

Based on an extensive study in the field, ORE has developed several models used for estimating track degradation. One of them was published in the 1970's, which considered the settlement as a logarithmic function [Lichtberger, 2005]. The model is divided into two parts. The first part expresses the deterioration directly after tamping, whilst the second part describes the deterioration as a proportion of traffic volume (cyclic loading). The ORE degradation model is given by the following formula:

$$e_N = e_1 \cdot (1 + b \cdot \log N) \tag{2.6}$$

where:

e_N = settlement after N cyclic loading (mm)

e_1 = settlement after the first cycle load (mm)

N = number of cyclic loading

b = constant (0.2 for an individual sleeper and 0.43 for the track grid)

In the subsequent report published in 1975, ORE released another settlement model. The equation presents deterioration as a function of operational loads, axle load and railway track condition.

$$e_T = a_1 + a_0 \cdot \log \frac{T}{2 \cdot 10^6} \tag{2.7}$$

where:

e_T = track settlement after an operational load T (mm)

T = passed tonnage (t)

a_1 & a_0 = coefficient factors which depend on the track quality condition (Table 2.1)

Table 2.1 – Ranges of the coefficients [Lichtberger, 2005]

Track Condition	a_0 [mm]	a_1 [mm]
High quality track	2-4	6-10
Average track	4-6	10-15
Poor track	6-10	15-20

E. TU Munich Model

An experiment under well-controlled laboratory condition was conducted by TU Munich to calculate the rate of track settlement for vehicles passing on a dipped joint. Ballast pressure was multiplied by the logarithmic of the number of axle passes as follows [Demharter, 1982]:

$$\begin{aligned} S_{opt} &= 1.57 \cdot p \cdot \Delta N + 3.04 \cdot p^{1.21} \cdot \ln N \\ S_{med} &= 1.89 \cdot p \cdot \Delta N + 5.15 \cdot p^{1.21} \cdot \ln N \\ S_{pess} &= 2.33 \cdot p \cdot \Delta N + 15.20 \cdot p^{1.21} \cdot \ln N \end{aligned} \tag{2.8}$$

where:

S = relative value of settlement (optimistic, medium and pessimistic value)

p = ballast pressure (Pa)

ΔN = number of axles in the initial period of settlement. It should be <= 10,000 axle passes (-)

N = number of axles in the second period of settlement (-)

The ballast pressure should be calculated by Zimmerman method, as follows:

$$p = M_{sub} \cdot \frac{V_0}{2000 \cdot b \cdot M_{sub} \cdot L_e} \cdot \sum_{axles} \frac{sin\left({}^{x}/_{L_e}\right) + cos\left({}^{x}/_{L_e}\right)}{e^{{}^{x}/_{L_e}}} \tag{2.9}$$

where:

M_{sub} = sub-grade modulus (N/m^3)

b = width of sleeper in longitudinal direction (m)

x = longitudinal distance between load and the position where the deflection will be calculated if not directly under the load

L_e = elastic length (m) $= \sqrt[4]{\frac{4 \cdot EI}{b \cdot M_{sub}}}$

According to Equation (2.8), the degradation model is divided in two major parts. The first part refers to the initial settlement immediately after a maintenance action, whilst in the second part the settlement occurs gradually in proportion to the number of axle passes.

F. TU Graz Model

TU Graz has suggested a model to represent the track settlement using a quality number called MDZ [Hummitszch, 2005]. In order to obtain this number, all changes in the vehicle acceleration due to the track imperfection should be summed up and then, by examining the progress of MDZ over the time, the degradation trend is fitted with an exponential function:

$$Q = Q_0 \cdot e^{-b \cdot t} \tag{2.10}$$

where:

Q = track quality represented by MDZ number (-)

Q_0 = initial track quality (-)

b = rate of deterioration

t = time or tonnage

The initial cost and maintenance effort are of great importance in this model, as Q_0 is the result of capital expenditure and $e^{-b \cdot t}$ represents the track deterioration behavior. To obtain the MDZ number, equation 2.11 is given:

$$MDZ = c \cdot \frac{1}{L} \cdot v^{0.65} \cdot \sum_{i=1}^{L/\Delta x} \sqrt{(\Delta vert.level)^2 + (\Delta horz.level + \Delta cant)^2} \qquad (2.11)$$

where:

$\Delta vert.level$ = difference of vertical level between two points (mm)

$\Delta horz.level$= difference of horizontal level between two points (mm)

$\Delta cross\ level$= difference of cross level or superelevation irregularity between two points (mm)

v = train speed (km/h)

c = coefficient (-)

L = measurement distance (m)

Δx = sampling interval (m)

G. ITDM Model

A model for estimating wear degradation has been proposed by Queensland University. The function takes into account the angle of attack between the wheel-set of the vehicle and the railway track, and it can be used for predicting wear defect, either on rail top or gauge separately [Zhang *et al*., 1999].

Wear for top of the high and low rail:

$$w_{hr\_top} = 7.6 \cdot 10^{-6} \cdot k_h \cdot k_{l\_hrtop} \cdot W_{hr\_top} \cdot \sin\psi$$
$$w_{lr\_top} = 9.5 \cdot 10^{-6} \cdot k_h \cdot k_{l\_lrtop} \cdot W_{lr\_top} \cdot \sin\psi \qquad (2.12)$$

Wear for high rail gauge face:

$$w_{hr\_gauge}(R) = \begin{cases} 12.1 \cdot 10^{-6} \cdot k_h \cdot k_{l_{hrgauge}} \cdot C_1 \cdot P_l \cdot \sin\psi & \Leftarrow \quad R \leq 500 \\ 12.1 \cdot 10^{-6} \cdot k_h \cdot k_{l\_hrgauge} \cdot C_1 \cdot P_l \cdot \sin\psi \ (1.7 - 0.0014R) & \Leftarrow \ 500 < R < 1200 \end{cases} \quad (2.13)$$

where:

$k_{l\_hrtop}, k_{l\_lrtop}, k_{l\_hrgauge}$ = lubrication factor (ranging from 0.115 for well lubricated condition and 0.497 for dry friction)

k_h = $51.05 \cdot e^{-0.0152H}$, where H is the rail hardness

W_{hr_top}, W_{lr_top} = vertical wheel load (kN)

C_1 = constant factor (-)

P_l = lateral load (kN)

ψ = angle of attack between wheel set and the track (rad)

R = curve radius (m)

H. Archard Wear Model

The Archard model establishes the lost volume of wear in proportion to the normal tension applied to the surface and to the local slip modulus, but inversely to the material hardness of the rail [Archard, 1953]. The equation is given as follows:

$$w = \frac{k_w}{H} \cdot F \cdot \|s\| \quad (2.14)$$

where:

w = volume lost due to wear (m^3)

k_w = wear coefficient (m^2/N)

F = normal force (N)

H = material hardness (Pa)

$\|s\|$ = sliding distance (m)

The equation above can also be rewritten to measure the wear depth or wear rate on a particular rail:

$$\delta = \frac{k_w}{H} \cdot P \cdot \|s\| \tag{2.15}$$

where:

δ = wear depth (m)

P = contact pressure between wheel and rail (Pa)

The wear coefficient is influenced by many factors, including mixed or boundary lubricated contacts, sliding velocity and temperature. This factor can be found by experimental research.

2.5.2 MODELS OF GEOMETRICAL DEGRADATION OF THE TRACK

Nowadays, the utilization of geometrical parameters is a common practice, especially for monitoring the behavior of track performance and to determine different repair and maintenance strategies. This approach, called Track Quality Index (TQI), is explained in the following sections.

A. Synthetic Coefficient

The synthetic coefficient *J* is an indicator of track quality developed by the Polish Railways [Madejski & Grabczyk, 2002]. The formula is based on the standard deviation of four different geometry parameters as given by:

$$J = \frac{S_z + S_y + S_w + 0.5 \cdot S_e}{3.5} \tag{2.16}$$

where:

J = synthetic Track Quality Coefficient (mm)

S_z = standard deviation of vertical irregularities (mm)

S_y = standard deviation of horizontal irregularities (mm)

S_w = standard deviation of track twist (mm)

S_e = standard deviation of track gauge (mm)

The standard deviation for each measured parameter is calculated using the following formula:

$$S = \sqrt{\frac{1}{n}\sum_{i=1}^{n}(x_i - \bar{x})^2} \tag{2.17}$$

where:

n = number of signals registered in the analyzed track section (-)

x_i = value of parameter at point *i* (mm)

$\bar{x}$ = average value of track irregularity (mm)

This synthetic coefficient also specifies the allowable deviation for different line speeds (Table 2.2). If any values are exceeded, a remedial action is required to bring the track back to the appropriate level.

Table 2.2 – Allowable deviations for *J* coefficient [Madejski&Grabczyk, 2002]

Speed (km/h)	J Coeff. (mm)	Speed (km/h)	J Coeff. (mm)
80	7	150	2.3
90	6.2	160	2
100	5.5	170	1.7
110	4.9	180	1.6
120	4	190	1.5
130	3.5	200	1.4
140	2.8	220 *)	1.1

**) Calculated through extrapolation*

B. Track Geometry Index (TGI)

The Track Geometry Index (TGI) was developed by the Indian Railways, which aimed to quantify the level of track condition. This model relies on the standard deviation of various geometry parameters over segments of 200 m in length. The average value of such segments per km gives the general TGI value [Talukdar *et al.*, 2006].

TGI can be calculated with the following formula:

$$TGI = \frac{2 \cdot UI + TI + GI + 6 \cdot AI}{10} \tag{2.18}$$

where UI, TI, GI, and AI are the indices for unevenness, twist, gauge, and alignment, respectively. The calculations for the different parameters are obtained by:

$$UI\ (\ Unevenness\ Index) = \ 100\ \cdot\ e^{-\ (SDUmes\ -\ SDUn\ /SDUmaint\ -\ SDUn)}$$

$$TI\ (\ Twist\ Index\ ) = \ 100\ \cdot\ e^{-\ (SDTmes\ -\ SDTn\ /SDTmaint\ -\ SDTn)}$$

$$GI\ (\ Gauge\ Index\ ) = \ 100\ \cdot\ e^{-\ (SDGmes\ -\ SDGn\ /SDGmaint\ -\ SDGn)}$$

$$AI\ (\ Alignment\ Index\ ) = \ 100\ \cdot\ e^{-\ (SDAmes\ -\ SDAn\ /SDAmaint\ -\ SDAn)}$$

where:

$SDU_{mes}\ /\ SDT_{mes}\ /\ SDG_{mes}\ /\ SDA_{mes}$ = measured standard deviation value of unevenness, twist, gauge and alignment, respectively (mm)

$SDU_n\ /\ SDT_n\ /\ SDG_n\ /\ SDA_n$ = standard deviation prescribed for newly laid track for unevenness, twist, gauge and alignment, respectively (mm)

$SDU_{maint}\ /\ SDT_{maint}\ /\ SDG_{maint}\ /\ SDA_{maint}$ = standard deviation prescribed for maintenance of unevenness, twist, gauge and alignment, respectively (mm)

SDU_{mes} and SDA_{mes} are obtained from the average of the measured standard deviations of the left and the right rails.

$$SD_{mes} = \frac{SD_{left} + SD_{right}}{2} \tag{2.19}$$

where :

SD_{left} = standard deviation of the left longitudinal profile (mm)

SD_{right} = standard deviation of the right longitudinal profile (mm)

Table 2.3 specifies the SD values used for newly laid track and for urgent maintenance tracks. The classification of track condition with corresponding maintenance is given in Table 2.4.

Table 2.3 – Standard Deviation (SD) values [Sadeghi & Asgarinejad, 2008]

Parameters	Chord Length (m)	SD for newly laid track (mm)	SD for maintenance with max. speed ≥ 105 km/h (mm)	SD for maintenance with max. speed < 105 km/h (mm)
Unevenness	9.60	2.5	6.2	7.2
Twist	3.60	1.75	3.8	4.2
Gauge	1.00	1.00	3.6	3.6
Alignment	7.20	1.50	3.0	3.0

Table 2.4 – TGI Classification for Maintenance [Talukdar *et al.*, 2006]

No	TGI Value	Maintenance requirement
1	TGI > 80	No maintenance required
2	50 < TGI < 80	Need basic maintenance
3	36 < TGI < 50	Planned maintenance
4	TGI < 36	Urgent maintenance

C. European Regulation Standard [prEN 13848-5:2005]

The European Committee for Standardization (CEN) has created a group of standards, prEN 13848, which consist of five parts of technical specifications. This series of standards aims to define a unique approach for evaluating track geometrical quality in various member countries. First part of the integrated standard provides the terminology and a framework for specification of track geometry parameters, including track gauge, longitudinal profile, alignment, superelevation irregularity (or cross level) and twist. Parts 2 to 4 of the standard cover the measuring system, track recording vehicle [Part 2], track construction and maintenance machine [Part 3], and manual and light weight devices [Part 4]. The remaining part of the European Standard, Part 5, specifies the minimum requirements for the quality levels of track geometry, and gives the safety-related limits for each parameter as defined in Part 1.

For addressing operational safety and ensuring the interoperability of train services, the Standard has set up three different quality levels. The maintenance strategies are relatively dependent on these levels, as explained in the Table 2.5. The specific parameters assigned to the quality levels are provided in Table 2.6.

Table 2.5 – Track Quality Levels

Track Quality Levels	
Alert Limit (AL)	If a limit value is exceeded, an action to correct the error has to be considered in the regularly planned maintenance.
Intervention Limit (IL)	If a limit value is exceeded, an action to correct the error has to be done immediately before the next inspection
Safety Limit (IAL)	If a limit value is exceeded, an action should be done to reduce the risk of derailment (closing the line, reducing speed, immediate tamping, *etc*.)

Table 2.6 – The Quality Level defined in the European Standard [Puzavac *et al*., 2011]

Parameters	Nominal to peak value			Nominal to mean value			Mean to peak value			Standard Deviation		
	SL	IL	AL	SL	IL	AL	SL	IL	AL	SL	IL	AL
Longitudinal Profile							✔	✔	✔			✔
Alignment							✔	✔	✔			✔
Gauge	✔	✔	✔	✔	✔	✔						
Superelevation Irregularity							✔	✔	✔			
Twist							✔	✔	✔			

As specified in Table 2.6, the European Standard used the standard deviation of the track geometry irregularity, in either longitudinal profile or alignment with the corresponding wavelengths between 3-25 m (D1). This indicator represents the dispersion of geometry defects (position of the measured points along the track), in relation to the mean signal (mean position of the track) over a 200 m-segment section (see equation 2.17). The higher the value of SD, the poorer the track quality will be; the lower values of SD correspond to the opposite situation.

A track quality can also be assessed according to the number of isolated track geometry defects per unit of track length, typically over 1 km or more. It may also be counted over 100 m or 200 m of track [Tzanakakis, 2013]. Three main levels have to be considered; Alert Limit (AL), Intervention Limit (IL) and Safety Limit (SL). For each limit, the standard defines the track geometry quality based on wavelength spans of $3 < \lambda \leq 25$ m (D1) and $25 < \lambda \leq 70$ m (D2). Tables 2.7 to 2.9 provide the permissible levels for those aforementioned parameters (longitudinal profile and alignment).

Table 2.7 – SD Threshold values for Longitudinal Profile and Alignment – Alert Limit

	Wavelength domain	
Speed (km/h)	Longitudinal Profile D1 (mm)	Alignment D1 (mm)
V ≤ 80	2.3 - 3	1.5 – 1.8
80 < V ≤ 120	1.8 – 2.7	1.2 – 1.5
120 < V ≤160	1.4 - 2.4	1.0 – 1.3
160 <V≤ 220	1.2 – 1.9	0.8 – 1.1
220 < V≤ 300	1.0 – 1.5	0.7 – 1.0

**The standard deviations are only given for Alert Limit.*

Table 2.8 – Isolated Defects SD for Longitudinal Profile - Mean to peak value

Speed (km/h)	Alert Limit (AL)		Intervention Limit (IL)		Safety Limit (SL)	
	Wavelength range (in mm)		Wavelength range (in mm)		Wavelength range (in mm)	
	D1	D2	D1	D2	D1	D2
V ≤ 80	12-18	N/A	16-20	N/A	29	N/A
80 < V ≤ 120	10-16	N/A	12-18	N/A	26	N/A
120 < V ≤ 160	8-15	N/A	10-17	N/A	24	N/A
160 < V ≤ 220	7-12	14-20	9-14	18-23	20	33
220 < V ≤ 300	6-10	12-18	8-12	16-20	17	28

Table 2.9 – Isolated Defects SD for Alignment- Mean to peak value

Speed (km/h)	Alert Limit (AL)		Intervention Limit (IL)		Safety Limit (SL)	
	Wavelength range (in mm)		Wavelength range (in mm)		Wavelength range (in mm)	
	D1	D2	D1	D2	D1	D2
V ≤ 80	12-15	N/A	14-16	N/A	22	N/A
80 < V ≤ 120	8-11	N/A	10-12	N/A	17	N/A
120 < V ≤ 160	6-9	N/A	8-10	N/A	14	N/A
160 < V ≤ 220	5-8	10-15	7-9	14-17	12	24
220 < V ≤ 300	4-7	8-13	6-8	12-14	10	20

N/A = Not Applicable

The analyses of track quality with respect to the isolated defect limits will be mainly discussed in Chapter IV while the quality assessments based on the standard deviation will be conducted in Chapter VI.

D. Track Quality Index (TQI)

The other quality measurement, TQI, was initiated by the Federal Railroad Administration, in the United States [El-Sibaie and Zhang, 2004]. The basic concept of this TQI is the use of the space curve length to represent track quality. As shown in Figure 2.8, for a specific track segment length, the rougher the track surface, the longer the space curve will be when stretched to a straight line:

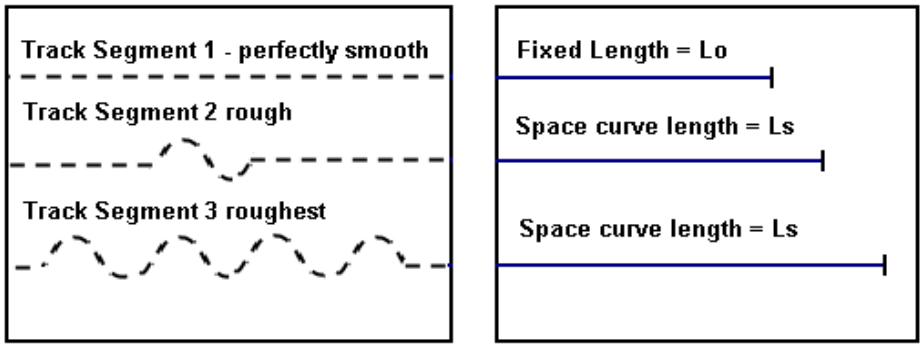

Figure 2.8 – Theoretical definition for fixed length (Lo) and traced length (Ls)

The TQI formula, for each longitudinal profile, alignment, cross level or superelevation irregularity and gauge, is expressed by the following equation:

$$TQI = \left[\frac{L_s}{L_0} - 1\right] \cdot 10^6 \tag{2.20}$$

where:

TQI = Track Quality Index for each individual track geometry parameter

L_s = traced length of space curve (feet)

L_0 = fixed length of track segment (feet)

The traced space curve length L_s is calculated by summing up the distance between any two points within the track segment:

$$L_s = \sum_{i=1}^{n} \sqrt{\Delta y_i^2 + \Delta x_i^2} \tag{2.21}$$

where:

Δy = difference between two measurements (feet)

Δx = sampling interval along the track (feet)

i = sequential number (-)

n = number of data points in the segment (-)

E. Q value

Banverket, the Swedish Railway company, has a number of indices that are used to express the state condition of their infrastructure facilities. Some of the main condition indices are known as K-value and Q-value [Anderson, 2002]. The Q-value is a weighted index of the standard deviation of the geometric parameters from its comfort limits set for a specific track class.

The Q value, therefore, is calculated per kilometer track using the following expression:

$$Q = 150 - 100 \cdot \left[\frac{\sigma_H}{\sigma_{H_{lim}}} + 2 \cdot \frac{\sigma_S}{\sigma_{S_{lim}}} \right] / 3 \qquad (2.22)$$

where:

σ_H = standard deviation of height / longitudinal profiles (mm)

σ_S = standard deviation for interaction (calculated as a combined effect from superelevation irregularity and side position of the rail (mm)

$\sigma_{H_{lim}}$ = standard deviation limit of longitudinal profile in a given track class (mm)

$\sigma_{S_{lim}}$ = standard deviation limit for interaction in a given track class (mm)

The Q-value is represented as a percentage. The lower value of the state condition indicates that the train may shake and be perceived uncomfortable by the passengers and vice versa.

F. K Value

The other main condition index that has been used by Banverket is the K-value [Anderson, 2002]. However, the application of K-value is not suitable for shorter track sections. The mathematical formulation for K-value is expressed by:

$$K = \frac{\Sigma l}{L} \cdot 100\% \tag{2.23}$$

where:

Σl = sum of track length where all σ values are below (superior) the allowable limit in a given track class (m)

L = total track length studied (m)

G. Five Parameters of Defectiveness

The five parameters of defectiveness (W_5) is a quality measure of line sections developed by the Polish Railways [Madejski & Grabczyk, 2002]. The formula treats the defectiveness of each geometry parameter as an independent event in practice. Considering the arrangement of the parameters, the following formula was created:

$$W_5 = 1 - (1 - W_e) \cdot (1 - W_g) \cdot (1 - W_w) \cdot (1 - W_x) \cdot (1 - W_y) \tag{2.24}$$

where:

W_5 = Five Parameters of Defectiveness

W_e = defectiveness of track gauge

W_g = defectiveness of superelevation (cross level)

W_w = defectiveness of twist

W_x = arithmetic averages for vertical defectiveness, as determined from the defectiveness of left and right rails, respectively

W_y = arithmetic averages for horizontal defectiveness, as determined from the defectiveness of left and right rails, respectively

The defectiveness for each measured track parameter is calculated from the relation:

$$W = \frac{k}{c} \tag{2.25}$$

where:

W = coefficient of parameter defectiveness

k = number of samples of assessment sections exceeding the allowable value

c = total number of section samples

Thus, to calculate the coefficient of parameter defectiveness, the allowable deviation for each track geometry element is defined according to the following line speed categories:

Table 2.10 – Allowable limits of parameter defectiveness [Madejski & Grabczyk, 2002]

Speed	Irregularities		Twist	Deviation of rail gauge			Superelevation
	Horizontal	Vertical	on 5 m	Widening	Narrowing	Gradient	Irregularity
(km/h)	(mm)	(mm)	(mm)	(mm)	(mm)	(mm)	(mm)
80	17	18	16	10	8	2	20
90	15	16	15	10	8	2	18
100	13	14	14	10	7	2	15
110	11	12	13	9	7	1	15
120	9	10	12	9	7	1	12
130	8	9	11	8	6	1	12
140	7	8	10	8	5	1	12

Speed	Irregularities		Twist on 5 m	Deviation of rail gauge			Superelevation Irregularity
	Horizontal	Vertical		Widening	Narrowing	Gradient	
150	6	7	9	7	4	1	10
160	6	6	8	6	3	1	8
170	5	5	7	6	3	0.5	8
180	5	4	6	5	3	0.5	6
190	3	3	5	5	3	0.5	6
200	4	3	5	4	3	0.5	5

The qualification for line maintenance depending on the W_5 defectiveness value is specified in Table 2.11.

Table 2.11 – Quality Qualifications of Track Lines [Madejski & Grabczky, 2002]

Evaluation of line	W_5 value
New lines	$W_5 < 0.1$
Lines in good condition	$W_5 < 0.2$
Lines in sufficient condition	$W_5 < 0.6$
Lines indicating insufficient condition	$W_5 > 0.6$

2.5.3 MODELS OF TRACK POWER SPECTRAL DENSITY (PSD)

The initial motivation for performing PSD calculations in railways is the practicality in the dynamic analysis of the train-track coupling system [Andren, 2006]. However, many researchers noted that the PSD would also be an appropriate method to classify the track roughness and deterioration, as it can show the characteristics of track irregularities by

means of wavelength and amplitude [Zhang *et al.*, 2010]. These quality indicators are usually provided in a power spectrum graph, a continuous curve with the ordinate representing spectral density and the abscissa as spatial frequency. Lower power spectra indicate better track irregularities, whereas higher power spectra demonstrate the opposite situation. Changes in track irregularities over a determined span are also indicative of particular problems existing on the track. A slow change of track irregularities (known as a long wave defect) may affect the vertical and lateral body vibration resulting in poor journey quality. On the contrary, a short wave defect may cause shock and high frequency vibrations that can lead to the risks of derailment and noise emission.

Basically, to derive the power spectrum graph, a signal should be transformed from the time-based domain to the frequency-based domain using the corresponding algorithm, called Fourier Transform. A similar analogy can also be imposed for the track geometry irregularity that is commonly described in the spatial domain. The transformation via the use of the Fourier transform will result in the wavenumber-based spectra, which is often called spatial frequency of a wave (Figure 2.9). This new domain defines which wavelengths are present in the original waveform.

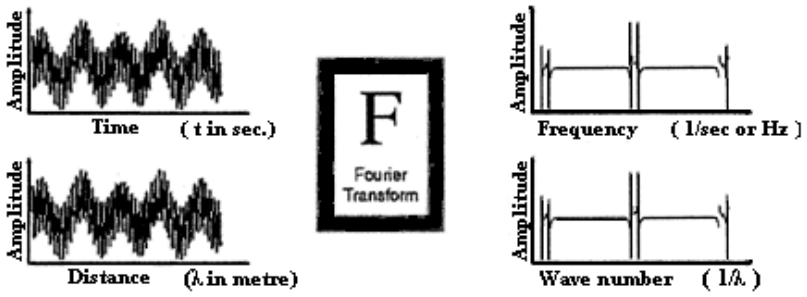

Figure 2.9 – Fourier Transform [Lindner, 1999]

Provided that $\int_{-\infty}^{\infty}|f(x)|dx < \infty$, where $f(x)$ is a continuous waveform, the transformation from the space-based domain to the wavenumber-based domain of the Fourier transform can be given by:

$$F(k) = \int_{-\infty}^{\infty} f(x) \cdot e^{-j2\pi kx} dx \tag{2.26}$$

where:

$F(k)$ = continuous Fourier transform

$f(x)$ = continuous space domain waveform

k = analysis wavenumber, where $k = {}^{1}/_{\lambda}$ and λ is wavelength

x = distance

j = $\sqrt{-1}$

In the discrete or sampled sense, the wavenumber domain sequence $F(m)$ is approximated in the sampled data $f(n)$ by:

$$F(m) = \sum_{n=0}^{N-1} f(n) \cdot e^{-j2\pi nm/N} \;\; ; m = 0, \dots, N-1 \tag{2.27}$$

where:

$F(m)$ = the m-th DFT output of the sampled component

$f(n)$ = the sequence of input samples; $f(0), f(1), f(3), .. etc.$

m = index of the DFT output in the wavenumber domain

n = index of spatial domain of input samples

j = $\sqrt{-1}$

N = the number of samples of the input sequence and the number of wavenumber points in the DFT output

The Discrete Fourier Transform (DFT) is an incredibly useful tool. It can provide information concerning certain frequencies that might occur and relative changes in amplitude. However, the only drawback with the technique is the amount of time

required to compute the output. As the number of points in the DFT increases, the amount of necessary computation becomes excessive. Therefore, to reduce the calculation time, a mathematical procedure, namely Fast Fourier Transform (FFT), is implemented.

There are many distinct FFT algorithms involving a wide range of mathematics, from simple to complex numbers. Such an example of FFT equation is given in the following formula:

$$F(m) = \sum_{n=0}^{(\frac{N}{2})-1} f(2n) \cdot W_N^{2nm} + W_N^m \cdot \sum_{n=0}^{(\frac{N}{2})-1} f(2n+1) \cdot W_N^{2nm} \qquad (2.28)$$

where $W_N = e^{-j2\pi/N}$. The reduction is obtained by splitting the input signal $f(n)$ into two shorter interleaved sequences; one of the odd numbers and one of the even numbers, as given above. Using this method, FFT only takes (N log N) operations for the computation of a DFT of N points, while DFT takes (N^2) operations.

In order to perform a discrete Fast Fourier Transform (FFT), a Matlab software tool is used and applied to each window or block of data. The auto spectrum is then calculated and the results are averaged. The formula for calculating the single sided auto-spectrum of a discrete frequency spectrum is given by:

$$G_{xx} = \frac{2}{Nr} \sum_{n=1}^{Nr} F_n^*(m) \cdot F_n(m) \qquad (2.29)$$

where:

G_{xx} = auto power spectral density (one sided)

Nr = number of window or block data

$F_n(m)$= discrete Fourier transform (DFT)

$F_n^*(m)$ = complex conjugate of $F_n(m)$

For scaling the auto-spectrum, the equation below is used:

$$A = \frac{2}{nfft} \cdot \sqrt{2 \cdot G_{xx}} \tag{2.30}$$

where:

A = amplitude of auto-spectrum density

$nfft$ = number of spectral lines

Stationary Check

The technique of Fast Fourier Transform (FFT) is based on the stochastic (or random) stationary hypothesis. According to this concept, the joint probability distribution of any subset of the sequence of random variables should be invariant with respect to a shift in time or distance. To have a clear view on this concept, a stochastic process is assumed as a finite sequence of random variables, e.g., $X_{-n}, X_{-n+1}, \dots, X_0, X_1, X_2, \dots, X_n$, and the joint probability distribution is represented by:

$$Pr\{(X_1 = x_1, X_2 = x_2, \dots, X_n = x_n)\} = p(x_1, x_2, \dots, x_n) \tag{2.31}$$

The stochastic process is said to be stationary if:

$$Pr\{X_1 = x_1, \dots, X_n = x_n\} = Pr\{\underbrace{X_{1+l} = x_1, \dots, X_{n+l} = x_n}_{\text{Time shift by } l}\} \tag{2.32}$$

for every n and shift l and for $x_1, \dots, x_n$.

Therefore, the first step to analyze the track irregularity using FFT is to check whether the measured data can be classified stationary or not. The common technique, that is easy to apply and useful for verification, consists of using the turn check method and reversed order check method [Zhiping and Shouhua, 2009]. If the random sign is stationary, the measured data should be stochastic and there will be no trend component.

The procedure for reverse check method is as follows. Consider a sequence of N observations of random variable x, where the observations are denoted by x_i, in which $i = 1,2,3, \dots, N$. Then count the number of times that $x_i > x_j$ for $i < j$. The sum of such inequality is called reverse check method (A_i), as defined by Equation (2.33):

$$h_{ij} = \begin{cases} 1 & if\ x_i > x_j \\ 0 & otherwise \end{cases}$$

then,

$$A_i = \sum_{j=i+1}^{N} h_{ij} \tag{2.33}$$

The total number of A_i from a set of observation is then denoted A, as follows:

$$A = \sum_{i=1}^{N-1} A_i \tag{2.34}$$

Considering the hypothesis that the observation is independent and there is no trend component, a confidence interval is given to A by:

$$A_{N;1-\alpha/2} < A < A_{N;\alpha/2} \tag{2.35}$$

If the number of turn check (A) drops into the confidence interval, the measured data is stationary.

Waveform Filtering

Filters play a vital role in removing selected wavelengths from an incoming waveform and minimizing random contributions called "noise". An ideal filter will have an amplitude response that is unity for the wavelengths of interest (called *pass band*) and zero everywhere else (called *stop band*). The wavelength at which the response changes from pass band to stop band is referred to as the "*cutoff wavelength*". Figure 2.10 shows the sample of Chebyshev filters used to limit the wave irregularities within the interval of 3 to 25 m.

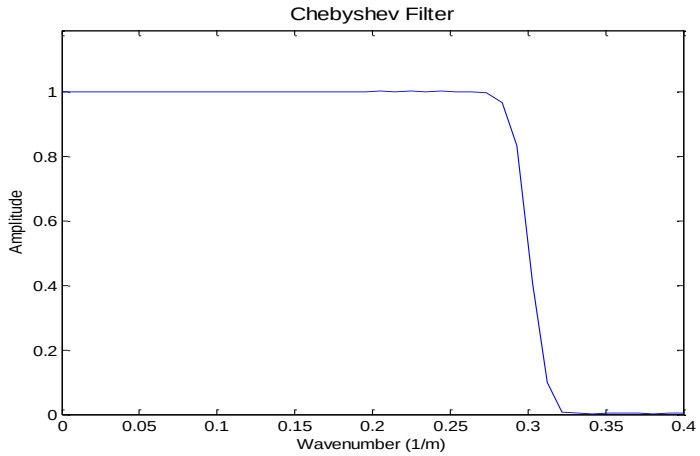

a) Chebyshev Low-Pass Filter

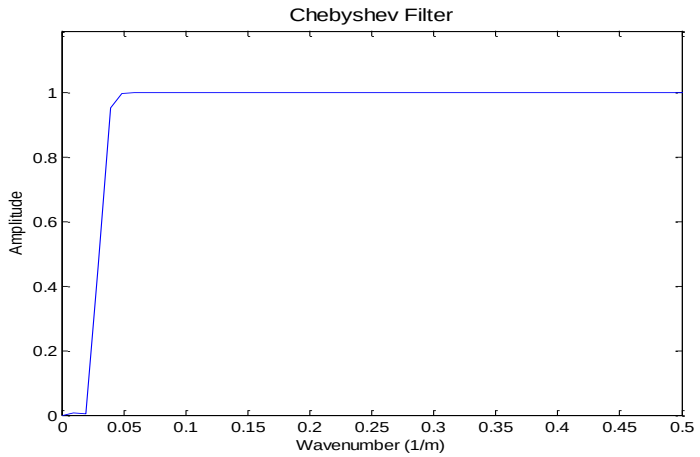

b) Chebyshev High-Pass Filter

Figure 2.10 – Chebyshev Filters

A low-pass Chebyshev filter is designed to pass the low wavelengths of track irregularity, from zero to a certain cut-off wavelength, 3 m (k = 0.33), and to block high wavelengths.

A high-pass Chebyshev filter is designed to pass the high wavelengths of track irregularity, from a certain cut-off wavelength, 25 m (k = 0.04), to λ (analysis wavelengths), and to block low wavelengths.

TRACK POWER SPECTRAL DENSITY (PSD) STANDARDS

Comprehensive evaluations of the track irregularity spectrum have been made in several countries such as Britain, Germany, USA and China [Zhipping and Shouhua, 2009]. Various analytical expressions of the PSD function have been proposed, depending on the characteristics of the track measured in each specific country. Those studies are described in the following sections.

A. The FRA PSD Standards (United States)

The US Federal Railroad Administration (FRA) has classified the railway track into 9 categories of track classes, in which Classes 1 to 6 are designed for ordinary tracks and Classes 7 to 9 are dedicated for high speed railways. For each track classes, the random track irregularity is described using a one-sided power spectral density (PSD) function. It also has to be noted that due to the limitation in the measurement equipment, the function is only applied to the wavelength range of 1.524 m to 304.8 m [Liu *et al*., 2011]. The empirical formula of PSD is as follows:

For vertical alignment:

$$S_{av}(\Omega) = \frac{k \cdot A_v \cdot \Omega_c^2}{\Omega^2 \cdot (\Omega^2 + \Omega_c^2)} \tag{2.36}$$

For lateral alignment:

$$S_{al}(\Omega) = \frac{k \cdot A_a \cdot \Omega_c^2}{\Omega^2 \cdot (\Omega^2 + \Omega_c^2)} \tag{2.37}$$

For gauge and superelevation irregularity (cross level):

$$S_{gauge/cl}(\Omega) = \frac{4 \cdot k \cdot A_v \cdot \Omega_c^2}{(\Omega^2 + \Omega_c^2) \cdot (\Omega^2 + \Omega_s^2)} \tag{2.38}$$

where:

$S_{av}(\Omega)$ = PSD of track vertical alignment irregularity [cm^2 / (rad/m)]

$S_{al}(\Omega)$ = PDS of track lateral alignment irregularity [cm^2 / (rad/m)]

$S_{gauge/cl}(\Omega)$ = PSD of track gauge or superelevation irregularity (cross level) [cm^2 / (rad/m)]

Ω = spatial wave-number [rad/m]

Ω_c, Ω_s = critical wavenumber [rad/m]

A_v, A_a = roughness coefficient related to the line grade [cm^2·rad / m]

k = a determined variable (≈ 0.25)

The spatial wavenumber (Ω) is related to the frequency per time unit f_h (Hertz) by the following relation $\Omega = 2 \cdot \pi \cdot f_h / V$. Table 2.12 presents the parameters used in Equations (2.36) to (2.38).

Table 2.12 – Coefficients for Power Spectral Density (PSD) function [Xia, 2002].

Line Grade	Max. line speed		A_v [cm^2.rad / m]	A_a [cm^2.rad / m]	Ω_c [rad/m]	Ω_s [rad/m]
	Freight (km/h)	Passenger (km/h)				
1	16	24	1.2107	3.3634	0.8245	0.6046
2	40	48	1.0181	1.2107	0.8245	0.9308
3	64	97	0.6816	0.4128	0.8245	0.852
4	97	129	0.5376	0.3027	0.8245	1.1312
5	129	145	0.2095	0.0762	0.8245	0.8209
6	177		0.0339	0.0339	0.8245	0.438

Note: the coefficients of track classes 7 to 9 are not defined yet by the FRA

B. German PSD Standard

The German track PSD spectrum is widely used for dynamic simulations of railway vehicles, especially in the European countries [Zhiqiang *et al*., 2009]. The model is characterized by a single-sided spectrum and is best represented by track irregularities in the range of $0.01 \cdot 2\pi$ to $0.4 \cdot 2\pi$ (rad/m) [Zhang *et al*., 2010]. The PSD function is expressed by:

For longitudinal profile:

$$S_v(\Omega) = \frac{A_p \cdot \Omega_c^2}{(\Omega^2 + \Omega_\gamma^2) \cdot (\Omega^2 + \Omega_c^2)} \tag{2.39}$$

For lateral alignment:

$$S_{al}(\Omega) = \frac{A_a \cdot \Omega_c^2}{(\Omega^2 + \Omega_\gamma^2) \cdot (\Omega^2 + \Omega_c^2)} \tag{2.40}$$

For cross level or superelevation irregularity:

$$S_{cl}(\Omega) = \frac{(A_p \cdot \Omega_c^2 / a^2) \cdot \Omega^2}{(\Omega^2 + \Omega_\gamma^2) \cdot (\Omega^2 + \Omega_c^2) \cdot (\Omega^2 + \Omega_s^2)} \tag{2.41}$$

where:

$S_v(\Omega)$ = PSD of track longitudinal profile irregularity [m^2 / (rad/m)]

$S_{al}(\Omega)$ = PSD of track lateral alignment irregularity [m^2 / (rad/m)]

$S_{cl}(\Omega)$ = PSD of cross level or superelevation irregularity [m^2 / (rad/m)]

Ω = $2\pi/\lambda$ denotes spatial wavenumber [rad/m]

$\Omega_c, \Omega_\gamma, \Omega_s$ = critical wavenumber [rad/m]

a = 0.75 m (one half of track gauge)

A_p = scale factor for longitudinal profile [m^2·rad / m]

A_a = scale factor for alignment [m^2·rad / m]

The parameters for the above equations are given in Table 2.13, which represent the track irregularity with low and high levels of perturbation.

Table 2.13 – Track PSD parameters [Lin *et al*., 2004]

Parameters	A_a [10^{-7}·m^2·rad / m]	A_p [10^{-7}·m^2·rad / m]	Ω_c [rad/m]
Low Disturbance	2.119	4.032	0.820
High Disturbance	6.125	10.80	0.820

Parameters	Ω_γ [rad/m]	Ω_s [rad/m]
Low Disturbance	0.0206	0.438
High Disturbance	0.0206	0.438

C. Chinese PSD Standard

Various spectra of track irregularities (also referred as PSD Standards) were published by the Chinese Academy of Railway Science (CARS). The standards are created for evaluation and diagnosis of track quality, which are suitable for three different operational speed classes: 200 km/h, 160 km/h, and 120 km/h [Xianmai *et al*., 2008]. For each of these, the spectrum range is given to accommodate the disparity of spectral amplitude that may vary from one track section to another. The track condition with a certain spectrum is usually fitted with one of these ranges. The closer the spectral curve of the track section to the lower limit of the reference value, the higher the track quality; conversely, the closer the spectral curve to the upper limit of the reference value, the lower the track quality.

The Chinese PSD function is based on single-sided spectrum, which relies on 6 different coefficients as shown below:

$$S(f) = \frac{af^2 + b}{cf^2 + df^4 + ef^2 + k} \tag{2.42}$$

where $S(f)$ denotes track irregularity PSD in unit [mm^2 / (1/m)] and f is wavenumber, often called spatial frequency of a wave, measured in 1/m.

The spectral coefficients for Equation (2.42) are given in Table 2.14 to 2.16.

Table 2.14 – Spectral Parameters for line speed of 200 km/h [Xianmai *et al*., 2008]

Track Irregularity		a	b	c	d	e	k
Gauge	Upper	362.2681	0.2393	15370.860	681.2174	10.2670	-0.0007
	General	54.0439	0.0357	8254.682	365.8602	5.5139	-0.0004
	Lower	119.2536	0.0783	36295.990	1619.269	24.2936	-0.0018
Cross level (Superelevation defect)	Upper	951.449	2.1747	47442.79	2121.780	25.473	0.0112
	General	35.4842	0.0811	6369.446	284.8838	3.4199	0.0015
	Lower	238.6205	0.5418	85347.970	3842.441	45.8306	0.02
Alignment	Upper	0.0	0.00699	0.0	1.0	0.01893	0.00003
	General	0.0	0.00194	0.0	1.0	0.01894	0.00003
	Lower	0.0	0.00097	0.0	1.0	0.01893	0.00003
Longitudinal Profile	Upper	0.0	0.00353	0.0	1.0	0.00752	0.0
	General	0.0	0.00098	0.0	1.0	0.00788	0.0
	Lower	0.0	0.00047	0.0	1.0	0.00783	0.0

Table 2.15 – Spectral Parameters for line speed of 160 km/h [Xianmai *et al*., 2008]

Track Irregularity		a	b	c	d	e	k
Gauge	Upper	612.3768	0.4046	8660.944	383.8376	5.7852	-0.0004
	General	213.1331	0.1408	10851.220	480.9504	7.2484	-0.0005
	Lower	187.2267	0.1238	31792.310	1407.659	21.23	-0.0015
Cross level (Superelevation defect)	Upper	1890.022	4.2158	19981.090	984.2226	18.5928	0.0011
	General	94.9519	0.2118	3613.811	178.0026	3.3627	0.0002
	Lower	511.6737	1.1433	65036.82	3191.977	60.4676	0.0036
Alignment	Upper	0.0	0.01751	0.0	1.0	0.01893	0.00003
	General	0.0	0.00486	0.0	1.0	0.01893	0.00003
	Lower	0.0	0.00146	0.0	1.0	0.01893	0.00003
Longitudinal Profile	Upper	0.0	0.01016	0.0	1.0	0.00704	0.0
	General	0.0	0.0029	0.0	1.0	0.00758	0.0
	Lower	0.0	0.00084	0.0	1.0	0.0075	0.0

Table 2.16 – Spectral Parameters for line speed of 120 km/h [Xianmai *et al*., 2008]

Track Irregularity		a	b	c	d	e	k
Gauge	Upper	640.740	0.4233	6524.507	289.1726	4.3582	-0.0003
	General	255.976	0.1691	7819.645	346.5745	5.2233	-0.0004
	Lower	325.929	0.2151	28425.14	1261.602	18.9956	-0.0015
Cross level (Superelevation	Upper	1830.68	7.3882	20908.35	1028.226	30.9382	0.008
	General	110.624	0.44649	2527.1	124.2566	3.73927	0.00097

Track Irregularity		a	b	c	d	e	k
defect)	Lower	1077.07	4.3434	70234.04	3460.220	103.9562	0.027
Alignment	Upper	0.0	0.02622	0.0	1.0	0.01893	0.00003
	General	0.0	0.00874	0.0	1.0	0.01893	0.00003
	Lower	0.0	0.00306	0.0	1.0	0.01893	0.00003
Longitudinal Profile	Upper	0.0	0.01351	0.0	1.0	0.00687	0.0
	General	0.0	0.00478	0.0	1.0	0.00739	0.0
	Lower	0.0	0.00166	0.0	1.0	0.00721	0.0

Note:

Although PSD provides a limit range of the spectral amplitude, this does not mean that the track spectrum cannot be lower or higher than the threshold limit value. The range is proposed based on the expected amplitude span of the Chinese track irregularity spectra.

D. SNCF PSD Standards (France)

Through an investigation on the railway track in France, SNCF proposed a single-sided PSD, which is valid for vertical alignment. The equation, defined as a function of cyclic wavenumber [cycles / m], presents the track irregularities within the range of 2 m ≤ L ≤ 40 m [Broeck (2001), Fryba (1996)]. The SNCF model is as follows:

For vertical irregularity:

$$G_{rr}(n) = \frac{A}{\left(1 + {}^{n}/_{n_0}\right)^3} \tag{2.43}$$

where:

A = Indication of the state of rail surface [m^3] or [m^2 / (cycle/m)]

$\begin{cases} 308 \times 0.509 \cdot 10^{-6} \text{ for a good state} \\ 308 \times 1.790 \cdot 10^{-6} \text{ for a good state} \end{cases}$

n_0 = coefficient, equal to 0.0489 [cycle/m]

n = cyclic wavenumber [cycle/m]

E. The Braun PSD Standard

The International Organization for Standardization (ISO) provides a uniform method for measuring vertical surface of roads, highways, and off-road terrain. Braun, as cited by Broeck [2001], has then adapted the model for road condition from ISO to the context of the railway. The Braun PSD model has two different limits; upper and lower limit values, and it is basically characterized by single-sided spectra. The Braun model is described by the following equation:

For vertical irregularity:

$$G_{rr}(n) = Grr(n_0) \cdot \left(\frac{n}{n_0}\right)^{-w} \tag{2.44}$$

where:

$G_{rr}(n_0)$ = scale factor of rail roughness [m^3] or [m^2 / (cycle/m)]

- $5 \cdot 10^{-7}$ for the upper limit
- $1.0 \cdot 10^{-7}$ for the lower limit

n_0 = 1 / (2π) [cycle/m]

w = waviness, with values usually ranging from 1.5 to 3.5

n = cyclic wavenumber [cycle/m]

Table 2.17 presents a summary of all track degradation models and power spectral density functions obtained from the literature review.

Table 2.17 – Summary of Track Degradation Model & PSD– Literature Review

No	Structural Index	Developer	Formulation
1	Shenton settlement model	Shenton	$e_n = K \cdot \frac{F_e}{10} \cdot [(0.69 + 0.028 \cdot h) \cdot N^{0.2} + 2.7 \cdot 10^{-6} \cdot N]$
2	Sato degradation model	Sato	$y = \gamma \cdot (1 - e^{-\alpha x}) + \beta \cdot x$
3	Sugiyama model	Sugiyama	$S = 2.09 \cdot 10^{-3} \cdot T^{0.31} \cdot V^{0.98} \cdot M^{1.1} \cdot L^{0.21} \cdot P^{0.26}$
4	ORE model	ORE	$e_n = e_1 \cdot (1 + b \cdot \log N)$
5	TU Munich model	TU Munich	$S = A \cdot p \cdot \Delta N + B \cdot p^{1.21} \cdot \ln N$
7	Archard Model	Archard	$w = \frac{k_w}{H} F \lVert s \rVert$
8	ITDM Model	Queensland University	$w = A \cdot k_h \cdot k_l \cdot W_h \cdot \sin \psi$
9	TU Graz model	TU Graz	$Q = Q_0 \cdot e^{-b \cdot t}$
	Geometry Index	Developer	Formulation
10	J synthetic coefficient	Polish Railway	$J = \frac{S_z + S_y + S_w + 0.5 S_e}{3.5}$
11	Track Geometry Index	Indian Railway	$TGI = \frac{2UI + TI + GI + 6AI}{10}$
12	European Standards (EN 13848-5)	CEN	SD and Mean
13	Track Quality Index	US railway	$TQI = \left[\frac{L_s}{L_0} - 1\right] \cdot 10^6$
14	Q value	Swedish Railway	$Q = 150 - 100 \cdot \left[\frac{\sigma_H}{\sigma_{H_{lim}}} + 2 \cdot \frac{\sigma_S}{\sigma_{S_{lim}}}\right] / 3$

15	K value	Swedish Railway	$K = \frac{\Sigma l}{L} \cdot 100\%$
16	Five Parameter Defectiveness (W5)	Polish Railway	$W_5 = 1 - (1 - W_e) \cdot (1 - W_g) \cdot (1 - W_w) \cdot (1 - W_x) \cdot (1 - W_y)$
	PSD	Developer	Formulation
17	FRA	United Stated	$S_{av}(\Omega) = \frac{k \cdot A_v \cdot \Omega_c^2}{\Omega^2 \cdot (\Omega^2 + \Omega_c^2)}$
18	German	Germany	$S_v(\Omega) = \frac{A_p \cdot \Omega_c^2}{(\Omega^2 + \Omega_v^2) \cdot (\Omega^2 + \Omega_c^2)}$
19	Chinese	China	$S(f) = \frac{af^2+b}{cf^2+df^4+ef^2+k}$
20	SNCF	France	$G_{rr}(n) = \frac{A}{\left(1 + {}^{n}/_{n_0}\right)^3}$
21	Braun	ISO	$G_{rr}(n) = Grr(n_0) \cdot \left(\frac{n}{n_0}\right)^{-w}$

2.6 TRACK MAINTENANCE

The maintenance management system is considered one of the aspects standing out as particularly important to guarantee a high level of safety and reliability of the infrastructure system. The concept relies on the combination of all features of technical and administrative actions, including track supervision, intervention and monitoring [Zoetaman & Esveld, 2005].

In this section, a schematic overview on maintenance management will be discussed. The existing methods and technologies used in track maintenance will be briefly presented.

2.6.1 LEVEL OF MAINTENANCE

When the track state falls below the acceptable limit value, an appropriate action should be conducted to fix the defect and to ensure that the railway track meets the required safety and quality standards [Esveld, 2001]. Intervention has to be done in a systematic way, i.e. avoiding any potential conflict that can disrupt the operation of train services.

Several levels of maintenance actions have therefore been identified according to the application timing. Such interventions are classified as:

- Corrective Maintenance

  This type of maintenance can be considered as the oldest intervention activity in the railway systems. It is carried out based on the occurrence of failure or worn out of the structural elements and is, therefore, performed at unpredictable intervals.

The corrective maintenance may be twofold: replacement of fault components and repair action. Preferences between these alternatives are based on the cost and benefits resulting from each option.

- Preventive Maintenance

  Preventive maintenance is contradictory to the previous type of intervention. The activity is performed according to a regular scheduled time which aims to prevent the breakdown and failure of the railway system. When proposing this intervention work, one should consider the economical aspect as the main criteria.

- Predictive Maintenance

  The predictive maintenance attempts to forecast the "future" condition of the equipments. By implementing this strategy, maintenance can be performed at a scheduled point in time when the maintenance activity is the most cost-effective or before the performance of the system drops to a threshold limit.

  In order to determine the intervention time, statistical processes, such as regression analysis and probability methods, are used.

2.6.2 TRACK MAINTENANCE ACTIVITIES

According to its purpose, track maintenance can be divided into two distinct categories [Shimatake, 1997]. The first category refers to the repair of defects which occurred in the railway geometry caused by the deformation of supporting materials such as ballast and sleepers. To remove this defect, a particular track intervention known as tamping is applied by using either manual or automatic tamper machine. In the second category, the maintenance is carried out to repair the mechanical parameters which in most cases could not be restored without parts replacement.

Normally, in lines with average traffic loads, the intervention to restore the defects in geometrical parameters is taken after 40-50 million gross load tons while the repair in the mechanical parameters such as rail unit occurs after about 500-600 million gross tons [Profillidis, 2000].

Various methods of intervention, repair and replacement applied to the track maintenance are briefly described in the following sections. The description includes the procedure and technology used in the current management technique.

1) Tamping

Tamping is the most common railroad maintenance activity. It is operated by the tamping machine which aims to correct the geometry faults and to compact the ballast beneath the sleepers. The most sophisticated machine, currently available, is capable of adjusting the ballast position simultaneously at a speed of up to 1.6 km per hour, providing the efficiency of 50 manual workers [Lichtberger, 2005].

Figure 2.11 – Tamping Machine [Plasser and Theurer, 2013]

The principle of operation of such tamping machine comprises several procedures:

A. The tamping machine takes the position over the sleeper to be tamped

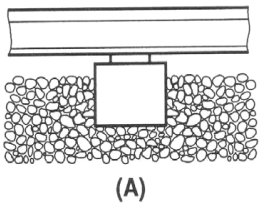

B. The lifting rollers elevate the sleeper and rails to the adjusted level, leaving a void beneath the sleeper

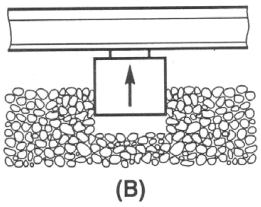

C. The machine arms bars are pushed down vertically into the ballast in either side of the sleepers

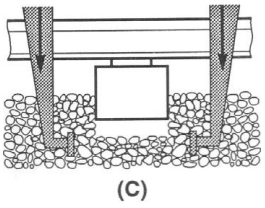

D. By squeezing and vibrating the arms, the ballast fills the void beneath the sleeper and its packing is improved.

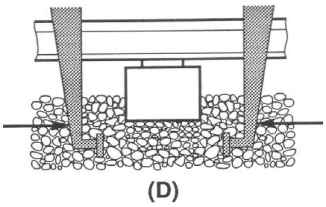

E. The arms are withdrawn from the ballast and the machine is moved forward to the next sleeper to repeat the cycle operation

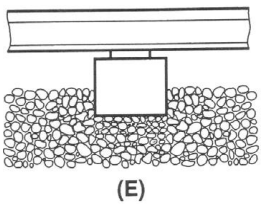

Figure 2.12 – Tamping Process [Selig, 1994]

Some undesired effects may occur during the tamping procedure. The vibration generated by tamping may, for instance, result in completely disturbed and loosened ballast bed. The disturbed ballast thus leads to lateral track instability, putting the track at risk of safety. In order to reduce this drawback, the infrastructure manager usually performs the subsequent activities of re-compaction of the ballast after tamping, using mechanical stabilization.

2) Dynamic Track Stabilization

The lateral track instability commonly occurs due to the loss of compaction of the ballast as a side effect of the vibration induced during the tamping operation. To mitigate this problem, the dynamic track stabilizer is used to consolidate ballast more densely and to provide an optimum homogenous settlement of the track. By imposing the DTS technique, the track will gain a settlement corresponding to 70,000 ton up to 100,000 ton of train loads [Lichtberger, 2005].

Figure 2.13 – Dynamic Track Stabilizer [Unitedindustrial, 2013]

The dynamic track stabilizer consists of 4 axle wagon fitted with a diesel engine and pressurized cylinders on the stabilizing unit. When the stabilizing action is carried out, the machine generates a vertical force beneath the track with an approximate load of 356 kN. The vibration that is transmitted to the ballast, lies in the natural frequency range and caused the stones to settle closer together within the cavities. This method allows the track to settle more uniformly and systematically, resulting in a 30% extension in the maintenance cycle [Grabe & Maree, 1997].

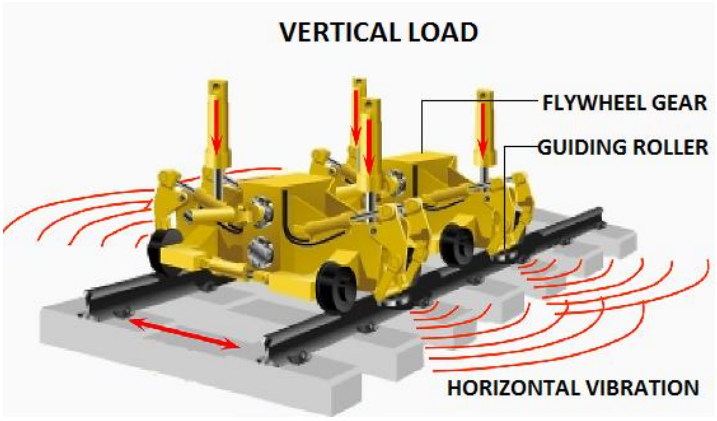

Figure 2.14 – Dynamic track stabilization equipment's [Total Track, 2013]

3) Ballast Cleaning

Ballast becomes degraded due to the repeated passage of trains and to very intense compression during wheel-track interactions. Such ballast crushes into small particles of stones known as fines. When the fines combine with water, the ballast loses its primary function of support to the track bed, as well as its drainage capability.

In order to remove the fines, ballast cleaning can be performed using an automated machine with adjustable excavating chain. The ballast is transferred upwards to the machine frame to be vibrated in order to eliminate the dirt and any other particles smaller than 35 mm. Afterwards, the conveyor arrangement distributes the clean coarse materials back to the ballast bed.

Figure 2.15 – Ballast Cleaning Machine [Remtech, 2010]

4) Rail Grinding

Irregularities in the geometry of the rails can cause a very high dynamic load. These irregularities partly occur due to faults in the manufacturing process or as a result of the train operation activities [Magel & Kalousek, 2002]. This special type of track imperfection is the so called rail corrugation, which is a periodic vertical irregularity on the railhead. Although rail corrugations do not pose a risk of immediate derailment, some undesirable problems can occur, such as increase in noise and in the vibrations experienced by passengers, ballast deterioration and higher maintenance cycles [Kumar, 2006].

At present, grinding can be considered the most effective maintenance practice to remove the irregularities and to restore the original rail profile. There are two types of rail grinding strategies. The first one is preventive grinding, which serves to prevent the development of defects growing from the surface or into the subsurface of the rail. In this method, the maintenance operation relies on the application of one pass of a large production grinder or multiple passes of a lighter grinder. The second strategy is the implementation of corrective grinding with the purpose of removing the defects on the

surface after they have shown significant presence in the rail [Sroba, 2004]. The operation usually involves multiple passes of a large production grinder.

Typically, the grinding machine consists of a series of vehicles equipped with grinding wheels. As it moves along the track, the equipment performs a grinding operation on the rail surface while it re-profiles the rail [Cope, 1993]. When it is used for grinding operation, several grinding units are blocked in one angle plane while performing the re-profiling operation; the grinding wheels are set at different angles so that a polygonal profile is achieved.

Figure 2.16 – Rail Grinding machine [Plasser and Theurer, 2013]

An accurate application of the rail grinding will produce several impacts:

- Overall improvement in rail life
- Reduction in rolling contact fatigue
- Reduction in rail wear
- Reduction in corrugation
- Reduction in energy dissipation
- Reduction in noise

5) Rail Lubrication

Rail lubrication is a technique to reduce the friction and wear that occurs between the flange part of the wheel and the gauge side of curved tracks [Alp *et al*., 1996]. Using lubrication, the wear rate can be reduced about 10 to 15 times in the 300-400 meter curve radius and 2 to 5 times in 600 meter curve radius [Jendel, 1999]. Figure 2.17 shows a machine dedicated to perform lubrication.

Lubrication may also be made by automatic applicators which are installed in the track or mounted on the motive stock. The selection of the application method will depend on the combination of economic factors, the nature of the railway network and the traffic levels.

Figure 2.17 – Rail lubrication equipment [Memolub, 2013]

6) Replacement

Traditionally, replacement simply consists of replacing the worn-out track components by new ones. As technology steps forwards, the estimate of the service life of a track structure or of a particular component can be easily determined. The replacement strategy is then conducted based on the prediction of the economic life span of the track materials. In this section, some replacement methods commonly used in the track maintenance will be briefly described.

- Rail Replacement

  Prior to rails replacement, new welded rails are transported to the site using a train vehicle. When these arrive, the rails are brought down and placed beside the defected track for installation. A rail exchanger is then used to take out the old rails from ties and insert the new rails to the sequence.

- Ballast Replacement

  A ballast replacement machine and its technique are quite similar to ballast cleaning. However, when the ballast replacement is carried out, a number of hopper wagons are normally attached in the sequence of the machine as storage and supplier of the new ballast. When the wagon arrives at the excavated site, the bottom of a bucket is then opened and the ballast falls down to the track.

2.7 REVIEW OF OPTIMIZATION MODELS

The optimization model for scheduling a preventive maintenance by mathematical programming is a relatively new concept. However, there are already some contributions on this theme by some scholars.

For example, Martland *et al*. [1994] proposed a technique to assist a rail manager in determining the best allocation for maintenance activities by minimizing the maintenance cost. The authors considered route geometry, track conditions, traffic

volume along with the life cycle costing strategy as decision variables in the target functions. They examined the effect of these costs in an optimal maintenance schedule in a numerical example.

A mathematical formulation for optimizing the maintenance works was also developed by Budai *et al*. [2004]. The objective of their model is to minimize the time required for maintenance, which is expressed by a cost function. For obtaining the nearly–optimal solution, they used a heuristic approach.

Redy *et al*. [2006] presented a simulation model and developed a statistical analysis considering different types of lubrication and grinding strategies. Throughout the simulation, the impacts on various costs, such as grinding cost, operational risk, replacement and lubrication were analyzed to find the proper time interval for interventions.

In another study conducted by Grimes [1995], an optimum schedule for track maintenance was obtained using the technique called Genetic Programming (GP). Financial aspects, such as the cost of maintenance and profit for maintaining quality, were the main considerations in generating the intervention action. Based on the comparison with other maintenance tools, GP provided a satisfactory performance.

Lyngby *et al*. [2008] later used the procedure of Markov Chain to determine the optimum number of maintenance interventions required in the track segments. Three aspects were considered in the model development, i.e. punctuality cost, accident cost and extra maintenance cost, due to reduced track quality.

In the works presented by Oyama and Miwa [2006], the maintenance schedule was developed through the use of integer programming algorithms. By taking into consideration the cost and the level of degradation, they developed a multi-criteria

optimization model to find the optimal preventive tamping intervals for broad railway networks.

Another approach was also introduced by Hokstad *et al.* [2005] with the assistance of a computer software application namely Maple. Utilizing the combination of preventive maintenance and condition monitoring, the generated maintenance was scheduled by minimizing the conflict with train operation hours.

Finally, Vale *et al*. [2010] developed an approach which made use of a mixed integer programming model specifically for scheduling tamping on ballasted tracks. The optimal solution was obtained by considering some technical aspects, such as the track gradual degradation, the track layout, the level of recovery and the allowable limits for intervention.

Determining optimal maintenance intervals during the projected horizons, while assuring the safety and satisfying certain constraints are the objectives of this thesis. To achieve these objectives, a mathematical model designed to optimize maintenance schedule is formulated as mixed integer programming (MILP). The fundamental concept and the general nature of this model are described in the next sections.

2.7.1 MIXED INTEGER LINEAR PROGRAMMING (MILP)

Linear programming (LP) is a branch of applied mathematics that deals with finding an optimal solution to a given linear function over a set defined by linear inequalities and equations. This technique was developed in 1947 by George Dantzig, an American mathematical scientist who invented an efficient method called simplex algorithms for solving linear problems. Shortly after, many scholars contributed to the field of linear programming in different ways, including theoretical development, computational aspects and exploration of new applications of the subject [Bazaraa *et al*., 1990].

Basically, linear programming contains several essential elements, which are:

1. Decision Variables
2. Linear Objective function
3. Linear Constraints

The first element represents the level of quantity undertaken by the respective unknown variables (number of items to produce, amount of money to invest, etc.). These variables are usually represented using symbols, such as $X_1, X_2, X_3, \dots, X_n$.

The second element deals with the goal or objective of a particular problem, such as minimizing the expenses or maximizing the profits. It consists of a certain number of variables which form a total objective value (Z) equal to $c_1X_1 + c_3X_2, + \cdots + c_nX_n$. The parameter of c_i expresses the contribution of each unit $X_i(i = 1,2, \dots, n)$ to the objective function.

The last element denotes limitations that restrict alternatives available to the decision makers. There are three types of constraints: less than or equal to (≤), greater than or equal to (≥) and simply equal to (=). The constraint "≤" ensures the solution used less than or equal the number of resources available. A "≥" constraint specifies minimum resources that must be utilized in the final solution. And the "=" constraint is more restrictive in the sense that it specifies the amount of some resource variables.

Given these definitions, the standard formulation of LP can be written as follows:

$$\text{Max} \quad c^T x + d^T y \tag{2.45}$$

$$Subject\ to \quad Ax + By \leq b \tag{2.46}$$

$$x, y \geq 0 \tag{2.47}$$

where x and y deal with the vector of decision variables, which are needed to be determined. c, d and b are defined as the coefficient vectors. A and B are the matrix coefficients and $(.)^T$ is the matrix transpose. The expression of $c^T x + d^T x$ can also be called the objective function, while the inequalities $Ax + By \leq b$ and $x, y \geq 0$ represent the constraints, which determine a set of feasible solutions.

If all of the decision variables are restricted to be integers, then the LP problem is called a (pure) integer linear programming (ILP). However, when the decision variables are binary and can take only the values of 0 or 1, the problem is designated as a zero-one linear program.

Another type of LP problem considers the combination of those two aforementioned types with the standard LP form (some variables are integers and the others are continuous). The problem, which is called mixed integer linear program (MILP), can be written as follows:

$$\text{Max} \quad c^T x + d^T y \tag{2.48}$$

$$Subject\ to \quad Dx + Ey \leq f \tag{2.49}$$

$$l_1 \leq x \leq u_1 \text{ and } l_2 \leq y \leq u_2 \tag{2.50}$$

$$x \in R^p \tag{2.51}$$

$$y \in Z^n \tag{2.52}$$

where R is the set of real numbers (continuous) and Z is the set of integers. Integer variables with bounds $0 \leq y \leq 1$ are called binary variables. $c \in R^p$,$d \in R^n$,$D \in R^{m \cdot p}$, $E \in R^{m \cdot n}$ *and* $f \in R^m$. l_1 and l_2, u_1 and u_2 are simple lower and upper bounds of the problem variables x and y.

For that reason, the concept of LP relaxation plays a key role in the solution of MILP problem. Three general procedures are identified throughout the concept:

a) Derive the LP relaxation from the MILP by removing the integrality constraints ($y \in Z^n$). This is the basis for LP relaxation strategy.
b) Solve the LP relaxation and identify the continuous optimum point.
c) Add special constraints that iteratively modify the LP solution in a manner that will eventually render an optimum extreme point which fulfills the integer requirements.

It should be noted that by simply rounding the continuous solutions to the nearest integer values as mentioned in step (*c)*, does not always yield an optimal solution. In fact, the rounded solutions may result in an optimal and, at worst, an infeasible objective goal [see Hamdy, 1997]. Accordingly, for generating special constraints specified in the procedure (*c)*, the following methods were developed:

- Branch and Bound method
- Cutting plane method

Each of these algorithms has different procedures, as explained in the following sections.

A. Branch and Bound Method

The branch and bound method is a solution technique that may be applied to a number of different types of problems. The principle of this technique is based on the partition of the total set of feasible solutions into smaller subsets of solutions. The result, schemed by a tree structure, can then be evaluated systematically until the best solution is found.

For example, the explicit enumeration of all possible solution of a problem has one general integer variable x_1 and two binary variables x_2 with the ranges $1 \leq x_1 \leq 3$, $0 \leq x_2 \leq 1$ and $0 \leq x_3 \leq 1$, respectively (Figure 2.18). The tree starts from the top of

the node, called “root node”, and represents the sets of all possible solutions (12 numbers). Each branch representing each solution. The chain on the left, for instance, demonstrates the partial solution in which $x_1 = 1, x_2 = 0$ and $x_3 = 0$.

Although the structure in Figure 2.18 displays a complete enumeration of all possible solutions, some nodes might be infeasible due to other constraints in the model.

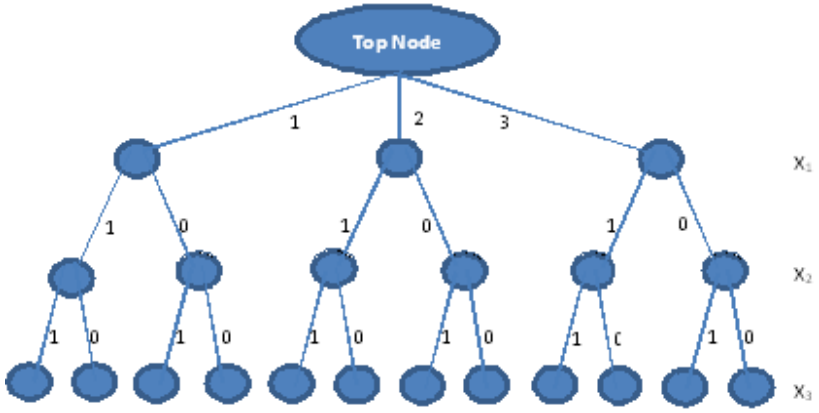

Figure 2.18 – Tree Structures

The branch and bound methods can also be customized to handle any special situations, including MILP problem. In this case, the first step that should be made is to drop the integrality restriction using the LP relaxation method and solve the associated linear program. The LP solution, which is usually produced-fraction variables, is then divided into feasible regions in an attempt to make integral. If any stage of the entire current LP solutions is integer, then the optimal solution is found.

Note that the important aspect of the branch and bound method is to avoid as much as possible the growing of the tree. In order to restrict the tree to grow only at the most promising nodes, it is necessary to specify the policies concerning how to select the next node and the next variable, how to prune (cut off and disregard the nodes) and when to stop.

B. Cutting Plane Method

The cutting plane method is another alternative to solving problems associated with integer programming. However, it does not divide the feasible region into subdivisions, as in the branch and bound, but instead works with a single linear program, which is refined by adding a new constraint. The new constraint is then used to successively reduce the feasible solution until an integer optimal solution is obtained.

Figure 2.19 presents an example of the cutting plane method. The feasible solution of LP relaxation lies inside the polygon. If a part of the polygon is shaved, it might possibly find an optimal integer solution. However, this additional cutting should not disturb any feasible integer solutions to the problems.

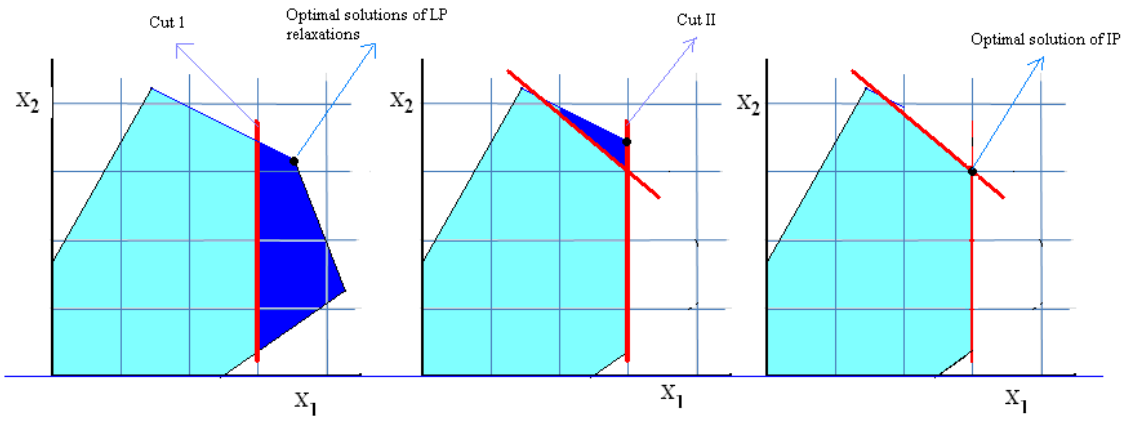

Figure 2.19 – Example of Cutting Plane Method

The rationale behind this technique consists of several steps:

1. Solve the LP relaxation by ignoring the integrality constraints
2. If by chance the optimal basic variables are all integers, the optimum solution has, therefore, been found.

   Otherwise:

   2(a). Generate a cut, i.e., a constraint which is satisfied by all feasible integer solutions but not by LP relaxation solutions.

2(b). Add a new constraint obtained in step 2(a) and repeat step 1

Using the two aforementioned techniques, the optimization routine for solving the LP problems can be very powerful, though it would also be time consuming and expensive for real application. Indeed, some optimization problems may also have a mixed LP problem in large scale considering the number of integer variables, multiple constraints, etc. The development of fast, relatively inexpensive and sophisticated software would thus be of great benefit to many users.

2.8 OPTIMIZATION SOFTWARE

In this section, the details of the software utilized to solve the mathematical integer programming will be discussed.

2.8.1 CPLEX OPTIMIZATION SOFTWARE

CPLEX is a product developed by ILOG used for solving relatively large mathematical optimization problems. This software employs AMPL programming language to formulate the projected problem and then proposes the optimal solutions using CPLEX solver.

In CPLEX, there are several ways to visualize the mathematical problems. One of the simplest ways is to create a text file using a text editor, such as Microsoft notepad. Figure 2.20 presents an example of the CPLEX application.

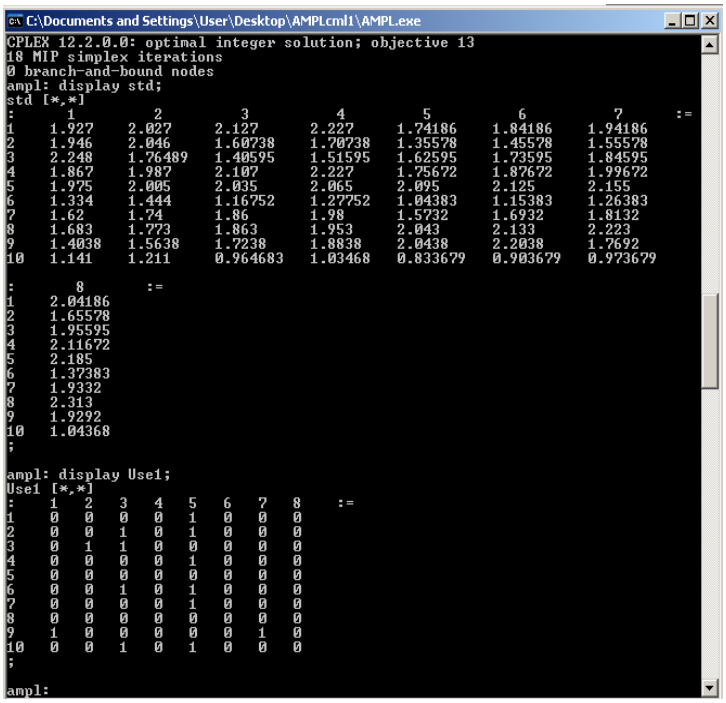

Figure 2.20 – The CPLEX Solver

For solving the problems, CPLEX uses a solution procedure called branch and bound method. In this concept, if a feasible solution is found at a node, the values will be recorded as the incumbent solutions. The node, where the values are found, is then known as the incumbent node and the objective values will be recorded as the incumbent objectives. Afterwards, the search is continued to the other nodes that have not yet been examined. Any nodes with lower objective values than the incumbent will be disregarded, while those larger than the incumbent will then be installed as new incumbent. The obtained incumbent at the end of the search, well ahead, becomes the solution to the problem.

2.9 SUMMARY

Maintaining and controlling the quality of the railway infrastructure are essential to ensure the availability of the system. These aims should be followed by the implementation of a track maintenance strategy with respect to the balance between safety level and economic aspects. In such case, a comprehensive understanding of the track degradation process and knowledge of all causes to rail degradation can help Infrastructure Managers (IM's) predict the track change behavior and prevent failures in the system.

This chapter provided a general review of the track degradation mechanisms, the analytical models used for assessing the track geometry condition, followed by the common techniques for carrying out track maintenance. In the end of chapter, the fundamental concept and general nature of mathematical integer programming, to be used as a basis for finding the optimal tamping schedule, is described.

From a review on the available literature, the assessment of railway track quality can be classified into two different approaches: assessment by considering the structural aspect (consists with settlement, wear and fatigue) and assessment by considering the geometrical aspect. The last approach measures a railway track quality from the progression of statistical and power spectral density of geometry defects (see Table 2.17).

Satoh, Shenton, ORE and TU Munich have developed track degradation models from a structural perspective. Settlement is the main consideration in the models, governing the behavior and performance of railway tracks. The expression given for the deterioration is distinguished by two major phases: the first phase is related to the rapid settlement after maintenance and the second phase is associated with the long term settlement. However, this approach lacks the implementation of some influencing parameters such as train speed and dynamic load. The more comprehensive degradation model is then given by Sugiyama, who took into account the factors of train speed and track structure.

The model is of particular use for predicting track degradation for 100 days of train operation and it considers a cumulative of one year passage tonnage rather than individual axle load. In the TU Graz model, the initial track quality is of the highest importance as it may determine the behavior of the railway track over its entire period of service. To calculate the track quality, this model should be combined with measurements of geometry parameters obtained from the track recording car.

Archard wear equation is a simple model and the base for a number of refined wear models. However, the wear coefficient, as used in this model, is difficult to estimate due to the need of detailed information from both laboratory and field tests. An alternative approach for analyzing wear is the ITDM model, which is more sophisticated and more complex. It endeavors to embrace all the major factors which may influence service life of track components such as material hardness, wheel forces and rail lubrication.

Further reviews were also made to other models, namely the Track Quality Index (TQI), that utilized geometrical parameters for track quality assessment purposes. Most of the models depend on the statistical evaluation of track geometry defects over a particular distance. The quantitative value of track quality can be varied from one model to the others, due to the diverse type of measurements conducted by railway companies, such as the mid chord of measurements (used to measure deflection of geometry defect) and the weighted value for each single geometry parameter.

Similarly to the TQI model, the track quality assessments based on PSD are considerably varied among the countries. Usually the model is developed to represent the railway track spectrum in a particular country. The characteristic features of each PSD model as well as its comparison will be discussed in Chapter 4.

In the area of track maintenance, several methods and technologies used to repair and to correct the track defects have been identified. Such maintenance is diverse according to the mechanisms and the consequences of improvement. Tamping, for instance, is widely

used to correct the geometry defect caused from deformation in the track structural bed, while rail grinding is used particularly to remove the defect in the rails caused by manufacturing or the nature of operations. The combination of maintenance methods can result in a higher performance of the track infrastructure.

Finally, the fundamental concept and general nature of mixed integer programming model are explained. This kind of problem has proved to be useful to address diverse types of problems in planning, routing and scheduling of railway track maintenance. The branch and bound method and cutting plane method are the main techniques in order to derive the optimum solution from the constructed mathematical problems. The application of this problem in an actual railway network will be presented in Chapter 6

3

RESEARCH METHODOLOGY

3.1 INTRODUCTION

This chapter outlines the research methodology designed to achieve the aim and objectives of the thesis. It begins with an explanation of the research strategy and objectives, followed by the research structure. This chapter also explains the processes employed and provides a justification for the selection of methodologies and for preparation of the conclusions.

As stated in the introductory chapter, this research aims to develop an optimization model for scheduling track maintenance with respect to safety and reliability issues. The Power Spectral Density (PSD) forms a core focus of the studies since it involves a systematic technique for evaluating track quality condition. To achieve the underlying objective, the research begins by examining the application of power spectral density in track quality assessments. Investigation is then continued further by seeking the relationship and degree of interdependency of one geometry variable to the others. These steps are of particular importance towards establishing a foundation for planning an effective maintenance decision as well as for providing a reasonably accurate model of track degradation, which takes into account interactions among various geometrical parameters. The development of a proposed model is then validated in practice.

3.2 RESEARCH STRATEGY

Research strategy can be defined as the way in which the research objectives are achieved. There are two general strategies within the context of research, namely 'quantitative research' and 'qualitative research' [Greene and Caracelli, 1997]. Deciding on which type of research will be conducted depends on the purpose of the study, the available resources, and the type and availability of information [Bouma and Atkinson, 1995].

- *Quantitative research*

  Quantitative research refers to the systematic empirical investigation of a given problem, based on testing a hypothesis or a theory composed of variables, measured with numbers, and analysed with statistical procedures or computational techniques, in order to determine whether the hypothesis or theory holds true [Creswell, 1994]. Quantitative data is, therefore, not abstract, it is solid and reliable, and presented in numerical format such as statistics, percentages, quantities, etc.

- *Qualitative Research*

  Qualitative research refers to a method of inquiry employed in many different academic disciplines, which emphasizes meanings, experiences and understanding the complexity of the problems [Strauss and Corbin, 1998]. The information gathered in qualitative research may facilitate the interpretation of the relationships between variables.

In order to take advantage of the strengths of both aforementioned methods, this research employed a combination of quantitative and qualitative approaches. The quantitative approach is used since the data analysis comprises many numbers, counts and statistical procedures to derive a base model for maintenance optimization.

The qualitative approach is conducted using a case study to help attain a deeper understanding of the interaction of different geometry variables associated with track deterioration. This method also enables to draw conclusions emerged from the data, to form a theory that explains a pattern in the base model and at the same time validates the theories in practice.

3.3 RESEARCH OBJECTIVE

Research can be classified into several categories depending upon the knowledge on a certain area and the intended solution [Kumar, 2006]:

- ✓ *Exploratory Research*

  Exploratory research is practically used for a problem that has not been clearly defined or when the researcher does not have sufficient knowledge on the area of study. The focus in this research is to gain a deep insight and familiarity on the issues for further investigation.

- ✓ *Descriptive research*

  This research category attempts to describe the situation or phenomena of an issue in a systematic manner. There are many methods involved in this study, such as conducting surveys to describe the status-quo and developmental studies seeking to observe changes in the behaviour of a phenomenon.

- ✓ *Explanatory research*

  When an issue is already known and there is some description of it, this research category can help identify its "why" and "how". This type of research looks for causes and reasons for such situation or phenomenon. For example, a descriptive research may discover that the wheel-rail interaction is one of the factors which play an important role in track geometry degradation, whereas the explanatory research is more interested in learning why or how the interaction between wheel and rail can influence the degradation process.

- ✓ *Correlational research*

  Correlational research is used to discover the relationship or interdependency between two or more aspects of a situation. It attempts to identify the causal of a phenomenon on one hand and the impact on the other hand, for instance the relationship between the track stiffness and the level of degradation.

In the current analysis, the selected methodologies are descriptive and correlational researches. Descriptive research is used in the early studies to describe the mechanism of changing of track performance behaviour as well as to explain the parameters influencing track degradation. The correlational research seeks to identify the relationship among various track geometry parameters as a foundation for developing the optimization model.

3.4 RESEARCH PROTOCOLS

A conceptual framework was developed to specifically guide and monitor the activities of the research in a systematic way. The framework contains the descriptions of several main elements on how projects and activities are expected to work to accomplish the objectives.

Figure 3.1 shows the sequence of the research methods. The research begins by conducting a comprehensive literature survey to address the research aim and objectives as described in chapter one. The research aim is to develop a logical model for the deterioration of track geometry and to incorporate the proposed model as basis for optimizing maintenance in practice.

The research is divided into two phases. The first phase is to investigate the application of power spectral density in the track quality assessments. Various PSD standards are compared in order to define the characteristic features contained in each particular standard. The implementation and procedure used to quantify the state of railway

irregularity will be also described with an application of case study. The investigation is then continued further in the second phase. A comprehensive correlation study is conducted to determine the degree of interdependency and to establish the similarity of one geometry variable to another. Using constructive knowledge, a predictive degradation model containing several geometry parameters is then developed. The model is able to forecast the future progress behavior of the track irregularity in the statistical and frequency domain.

Each of the research phases contains several main activities. The following section is dedicated to explain how the research aim and objectives are achieved.

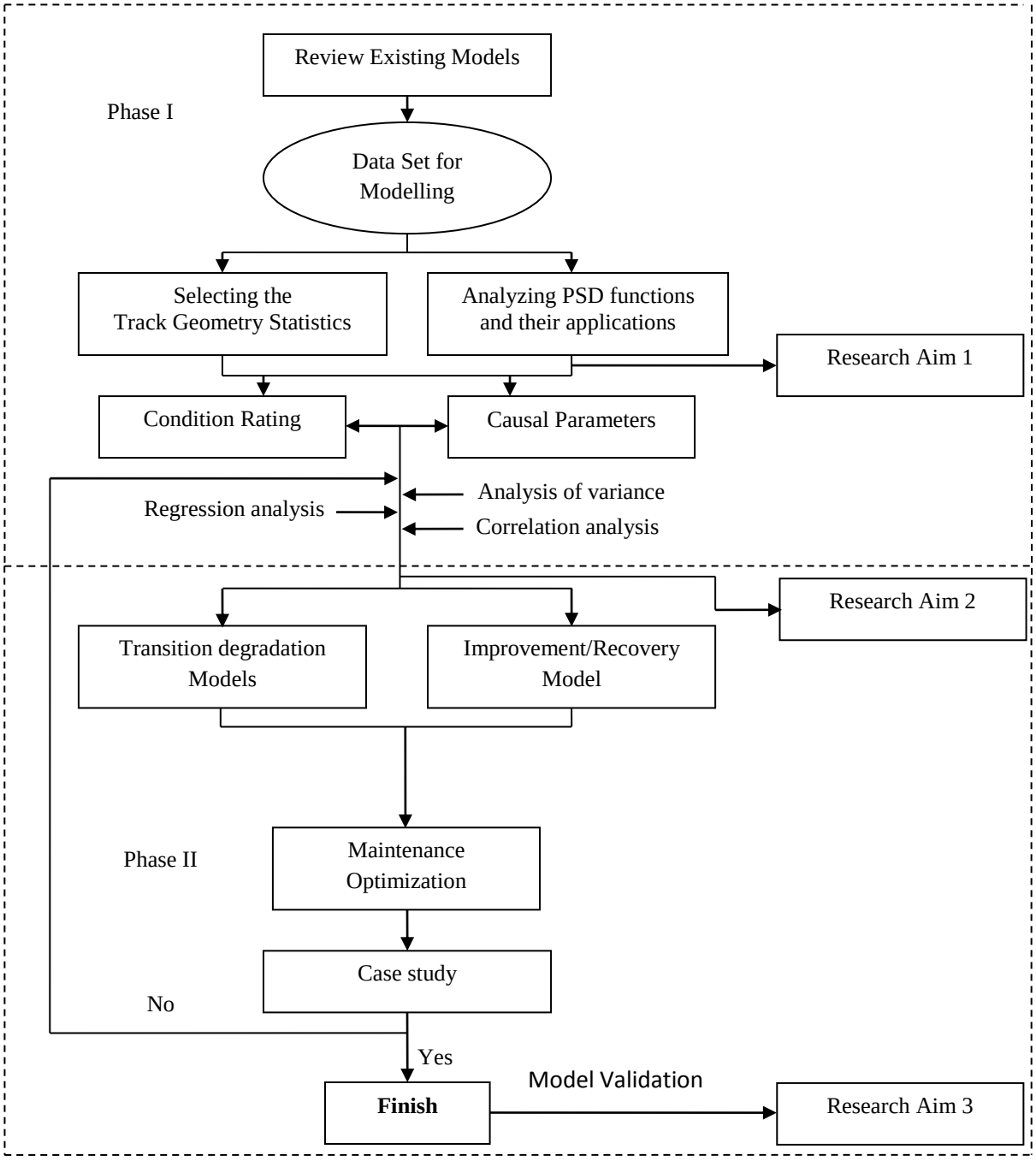

Figure 3.1 – Schematic Diagram of the Research Methodology

Phase I

This section discusses the activities shown in Figure 3.1 that relate to phase I of the research methodology. Such activities include literature review, data collection, research approaches and procedures used to develop the optimization model.

The literature survey was carried out within (1) the concept of track degradation and (2) the application of existing methodologies for assessing track quality, including track quality index and power spectral density approaches. The aims are to develop a comprehensive understanding of the track degradation mechanism, to systemize the normative aspects that should be taken into account in the framework modelling, and to identify the feasibility of current approaches in adapting the changes in track performance behaviour.

In order to obtain this information, different databases from many sources were explored. These data can be classified as primary and secondary data. The data collected by the researcher for the purpose of study through various experiments or from the on-site data recording are called primary data. The data taken by the researcher from secondary sources, internal and external, are called secondary data.

In the context of this study, the primary data were collected from REFER databases. It consisted of measurement reports conducted by Track Recording Car EM 120, which comprised all information about the geometrical quality of the track, such as longitudinal profile, horizontal alignment, gauge, super-elevation, network topography, etc. Over 8 years of inspection records were acquired from October 2003 to January 2009. For the secondary data, the full text of many journal articles and books were found in electronic databases, such as Elsevier, Emerald, ASCE, Transportation Research Record, etc. Some technical standards from European Committee for Standardization (CEN) were also examined. The researcher also studied relevant reports, master thesis and PhD dissertations from various universities.

Furthermore, from the literature research in the field of track degradation models, it appears that there is a lack of studies employing the methodology of power spectral density to assess the quality of railway geometry.

Phase II

This section discusses the activities shown in Figure 3.1 that relate to phase II. These include analyzing data and developing methodologies for optimizing the maintenance strategy to be subsequently validated in practice.

The data analysis comprises the inspection, transformation, and modeling of the data with the purpose of highlighting useful information for the proposition of the study. The statistical approaches, such as correlation analysis, and variance and regression analyses are used to obtain the analytical representation of the statistical relationship among the track geometry parameters. Such studies are necessary to determine the scale of relationship among various geometry variables.

The establishment of statistical relationships is the main aim of this research, which will enable to provide a rational model to predict the future value of track irregularity and at the same time, to create the transition model of track degradation. The proposed models are then used as the basis to obtain an optimal schedule of track maintenance with respect to various necessary aspects of the system. Finally, the research problem in phase II can be concluded when the estimation model has been validated.

3.5 VALIDATION OF THE MODEL

Model validations are needed to provide the confidence associated with the accuracy and reliability of the output predictions. The evaluation criteria, namely Root Mean Squared Error (RMSE) and Mean Absolute Error (MAE), are the common standards used for evaluating the model performance. Both of these criteria can range from 0 to ∞, where a lower value corresponds to a better performance.

The Root Mean Squared Error can be defined by:

$$RMSE = \sqrt{\frac{1}{n}\sum_{j=1}^{n}(f_j - y_j)^2} \quad (3.1)$$

while the Mean Absolute Error can be defined by:

$$\text{MAE} = \frac{1}{n}\sum_{j=1}^{n}|f_j - y_j| \quad (3.2)$$

where n represents the number of predictors, f_j stands for predicted value and y_j corresponds to the actual value.

In fact, there is no absolute criterion for a "good" value of RMSE or MAE. Such indicators simply show how close the observed data points are in relation to the predicted values.

The other method used for model validation is the comparison of the predictive performance of the models [Heiji *et al.*, 1995]. The data should be randomly divided into two parts: one part is used to construct the model, called estimation sample, and the other part is used to evaluate the prediction, called prediction sample. The models are estimated using data from the first sub-sample, and the estimated models are then used to predict the values in the prediction sample. The accuracy between actual and prediction values is measured by the forecast error.

3.6 SUMMARY

In this chapter the research methods, data collection and analysis procedures were outlined. The chapter explained how the research was structured, the justification behind the selected research methodology, how data was collected and analyzed, and how the verification of the research was achieved. This chapter underpins the next chapter where research findings and discussions are presented.

4

THE APPLICATION OF POWER SPECTRAL DENSITY (PSD) IN TRACK QUALITY ASSESSMENTS

4.1 INTRODUCTION

The implementation of Power Spectral Density (PSD) for assessing the track quality condition is relatively new in the area of railways. Most of the Infrastructure Managers (IMs) tend to use the Track Quality Index (TQI) method, which is typically a statistical function of the standard deviation of each geometrical defect. Compared to the PSD technique, TQI has some obvious disadvantages, for example, it cannot reflect the wavelength contents of the geometry defect, which is inherently related to the particular issue in train-track interaction. PSD can also be used to identify the occurrence of rail wear that is hardly detected by visual inspection [Cai, 2009]. However, the required expertise/knowledge to process and to interpret information regarding the Power Spectral Density is known as a drawback in the development of this method [Andren, 2006].

Some PSD standards proposed by many organizations and countries have been presented in Chapter 2. According to the literature, the analytical expressions of the PSD function are considerably different depending on the characteristics of the track measured in the country to which each PSD belongs to. The comparative studies

between various PSD standards for four random variables (longitudinal profile, alignment, gauge and twist) have been conducted and the feature of each PSD standard has been investigated. Then, the use of a PSD standard for the purpose of track geometry assessments is carried out on a stretch of Portuguese railway network data. Such assessments are conducted in two different ways: simulation of rail geometry irregularity and curve fitting method.

4.2 THE COMPARISON OF PSD STANDARDS

Various countries such as USA, China, France and Germany have modeled their own spectra of railway track irregularity (see chapter 2.5.3). Each form of PSD spectrum, represented by a PSD standard, has different characteristics and features such as the wave span of interest, the weighted value of track geometry parameter (coefficient factor) and the dedicated line speed.

Figures 4.1 to 4.4 present the comparison among PSD standards available in four aforementioned countries. Each standard is given according to their respective wavelength range of interest, with horizontal and vertical axes representing the spatial wavenumber and Power Spectral Density (PSD), respectively. Prior to analysis, normalization was conducted to convert a spatial wavenumber unit (rad/m) into cyclic wavenumber ($1/m$). The inversion of the cyclic wavenumber then gives an axis corresponding to the wavelength (m).

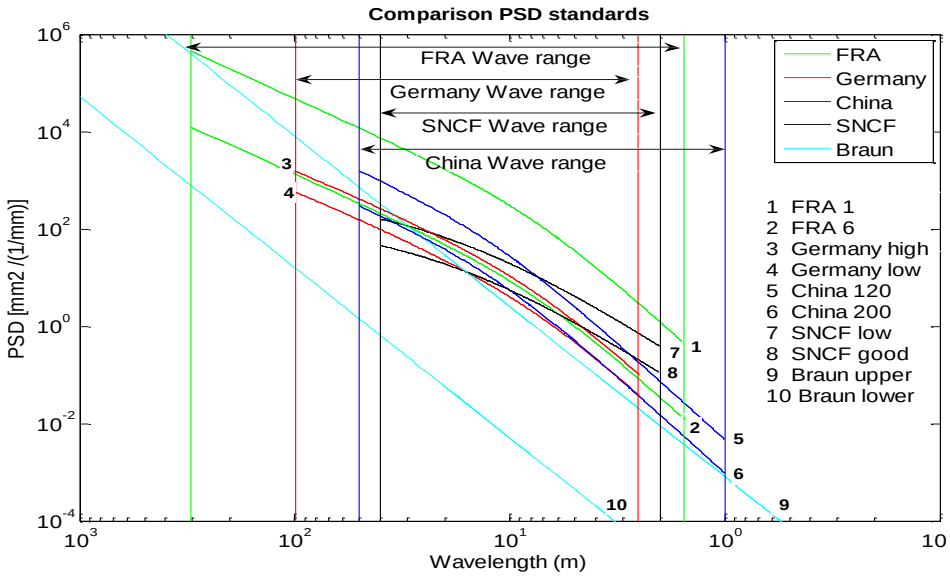

**There is no wavelength range found for Braun PSD*

Figure 4.1 – Comparison of Various PSD Standards - PSD Longitudinal Profile*

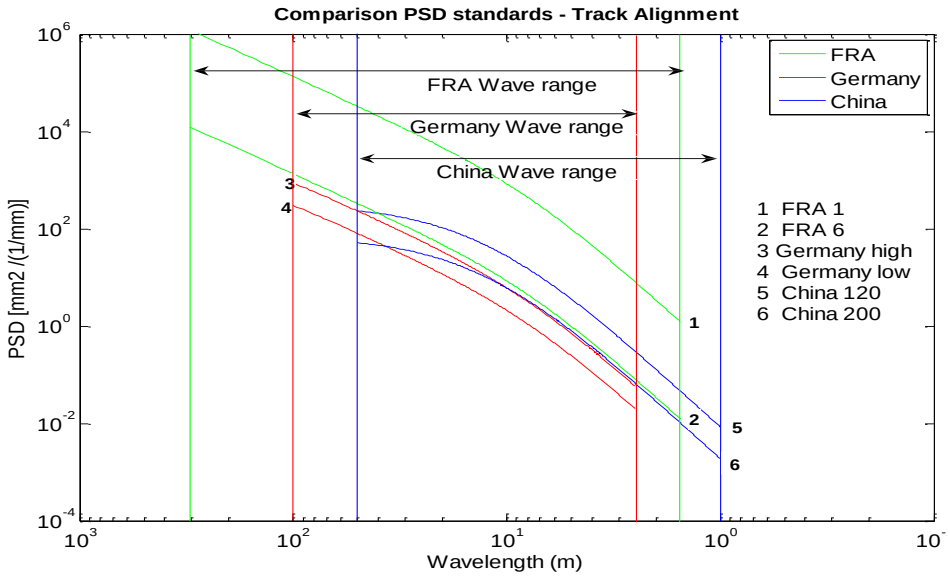

Figure 4.2 – Comparison of Various PSD Standards - PSD Alignment*

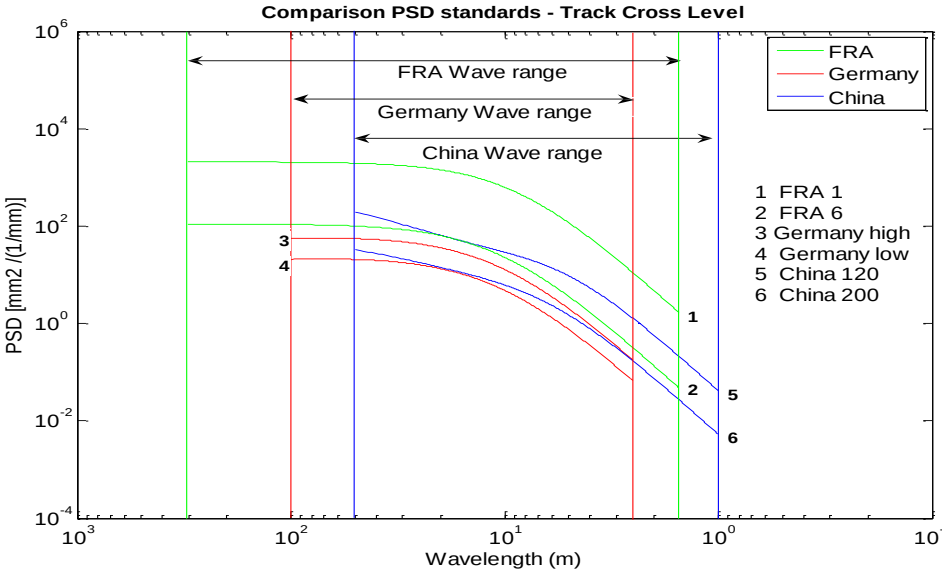

Figure 4.3 – Comparison of Various PSD Standards - PSD Cross Level or Superelevation irregularity*

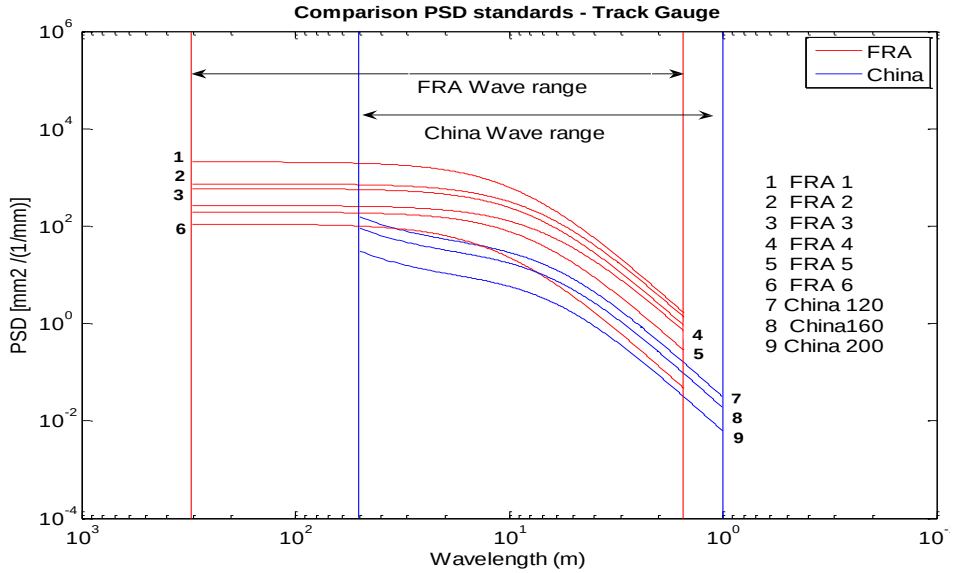

Figure 4.4 – Comparison of Various PSD Standards - PSD Gauge*

*) *the number of PSD standards in each particular geometry variable depends on the availability of PSD functions*

Figure 4.1 shows the comparison of longitudinal profile among PSD standards. Braun's track irregularity has less value than (or is superior to) the other standards, particularly for the short wave defects, of less than 16 m. For wavelength below 4 m, the curve of "Chinese 200" PSD expresses the same magnitude as "German low disturbance" spectrum and is superior to SNCF and FRA power spectral density. An opposite result is given by France spectrum ("SNCF good"), which is stricter for long wave irregularities, especially for those above 16 m.

The PSD comparison for track alignment irregularities is further detailed in Figure 4.2, which is supported by the function from FRA, German, and Chinese PSD standards. For wavelengths below 38 m, the magnitude of "German low disturbance" is lower than the other two standards, which indicates more restriction to the allowable tolerance imposed by German high speed lines. Similar PSD value is seen in "Chinese 200", "German high disturbance" and "FRA PSD 6" (177 km/h), particularly for wavelengths below 10 m.

A similar view is also given in Figure 4.3 for PSD Cross level (Superelevation irregularity), where the PSD of "German low disturbance" has lower spectral magnitude (superior) than the PSD of China and USA, for both short and long wave irregularities. For defects below the wavelength of 2 m, the magnitude of the PSD of "Chinese 200" is overlapping the PSD of "German high disturbance" and is lower than the PSD of "FRA 6", which indicates the superiority of the track quality construction in German and China. Furthermore, the figure also shows that for a line speed of 177 km/h (Class 6), FRA has better control than "China 120".

Figure 4.4 presents the PSD comparison of track irregularities for gauge variable. It is argued that the tolerance value of the Chinese spectrum is likely to be equal to the FRA standard, especially when it is analyzed based on the travelling speed. The spectrum of "FRA 6" (177 km/h), for example, lies between the "Chinese 200" and "Chinese 160" (wavelength < 7 m).

The comparisons of all these different standards have revealed that the German PSD is generally stricter to the geometry errors of longitudinal profile, alignment, and cross level or superelevation irregularity, which indicates a better quality control applied by German railway standards. The Chinese and FRA PSD are also showing the same characteristics in terms of curve trends as well as spectra amplitude, particularly for the wave irregularities below 10 m.

4.3 PROCEDURES FOR APPLYING PSD STANDARDS

This section deals with the procedure used to generate an artificial irregularity resulting from PSD standards as well as the techniques for finding the best fitting curve of the track irregularity spectra to a particular PSD standard. Both approaches are beneficial to determine the state of the track condition in the later stages.

4.3.1 TRANSFORMATION OF PSD INTO RAIL GEOMETRY IRREGULARITY

Broeck [2001], Xia [2002], Lei & Noda [2002], Zhang *et al.* [2001], Song *et al.* [2003], Ju *et al*. [2010] and Gupta [2008] have all employed a similar method for creating an excitation force in the vehicle dynamic analysis. The steps of the procedure are explained below.

Supposing a stationary stochastic process $r(x)$ with zero mean and variance, σ_k^2, the sample function of the stochastic process $r(x)$ can be simulated by:

$$r(x) = \sum_{k=1}^{N} A_k \cos(2\pi n_k x - \theta_k) \tag{4.1}$$

where:

A_k = Gaussian random variable with zero mean and variance, σ_k^2, as defined by:

$$\sigma_k^2 = 2 \cdot G_{rr}(n_k)\Delta n, \qquad k = 1,2, \dots N$$

$G_{rr}(n_k)$ = Power Spectral Density Standard

θ_k = Phase angle distributed between 0 and 2л randomly

n_k = Center wavenumber. In order to attain this value, a wave band, Δn, can be defined as:

$$\Delta n = \frac{n_{up} - n_{low}}{N}$$

therefore, $n_k = n_1 + \left(k - \frac{1}{2}\right) \cdot \Delta n, \qquad k = 1,2, \dots N$

where N is the total number increments in the range of (n_{low}, n_{up}).

Another method for creating rail track irregularity was inspired by Claus and Schiehlen [1997], Yang *et al*. [2004] and Dias *et al*. [2008]. Assume that PSD standard $G_{rr}(\Omega)$ is defined as a function of the spatial wavenumber (rad/m). The random track irregularity can be produced by implementing the trigonometric series, as expressed by:

$$r(x) = \sqrt{2} \sum_{n=0}^{N-1} A_n \cos(\Omega_n \cdot x + \theta_n) \tag{4.2}$$

where:

N = total number of discrete angular wavenumber considered

Ω_n = discrete angular wavenumber (rad/m), which defined as:

$$\Omega_n = n \cdot \Delta\Omega = n \cdot \frac{(\Omega_u - \Omega_l)}{N}, \qquad n = 1,2, \dots N-1$$

where: Ω_u and Ω_l are the upper and the lower limits considered.

θ_n = phase angle distributed between 0 and 2л randomly

A_n = the amplitude coefficient of random series, defined as:

$$A_0 = 0,$$

$$A_1 = \sqrt{\left(\frac{1}{2\pi} \cdot G_{rr}(\Delta\Omega) + \frac{4}{12\pi} \cdot G_{rr}(0)\right) \cdot \Delta\Omega},$$

$$A_2 = \sqrt{\left(\frac{1}{2\pi} \cdot G_{rr}(2\Delta\Omega) + \frac{1}{12\pi} \cdot G_{rr}(0)\right) \cdot \Delta\Omega},$$

$$A_n = \sqrt{\left(\frac{1}{2\pi} \cdot G_{rr}(\Omega_n)\right) \cdot \Delta\Omega}.$$

for $n = 3,4, \ldots N - 1$.

Checking Procedure

In order to use the spectrum standard for assessing track quality, the PSD function is transformed from the wavenumber-based domain to the solution in the spatial-based domain. The result, an artificial irregularity dependent of the travelled distance, is shown in Figure 4.5. Subsequently, to validate the proposed simulation approach, the reverse process is carried out by determining the power spectral density of the artificial track irregularity according to Equation 2.29 and comparing the result with the analytical curve of PSD standard. Figure 4.6 gives a good agreement between these two spectra, which indicates the appropriateness of the method in the rail irregularity simulation.

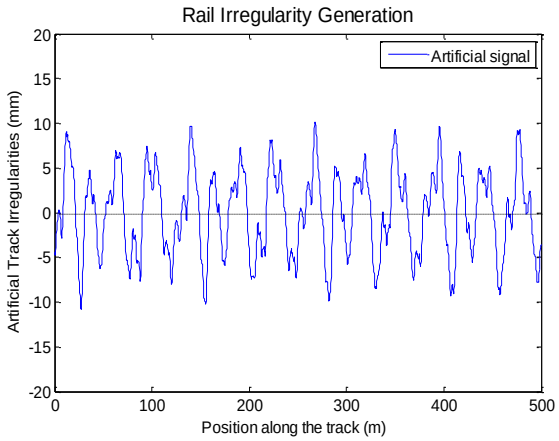

Figure 4.5 – Simulated track irregularities

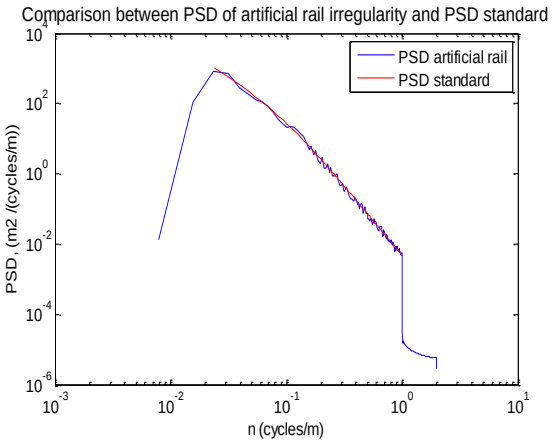

Figure 4.6 – Comparison of PSDs

4.4 FACTORS AFFECTING THE GENERATION OF TRACK IRREGULARITY

In order to provide an appropriate method in rail track generation, several factors that may influence to the magnitude of an artificial track irregularity should be clearly defined. For this purpose, some consideration factors such as the lines speed, the preference of wavelength interval (wave band) and the selection of PSD standard are investigated, and the results are given as follows.

A process for generating random track irregularity has been presented in the preceding section. Figures 4.7 to 4.9 present the examples of the track geometry simulation obtained from the Chinese power spectral density, corresponding to the line speeds of 120 km/h, 160 km/h and 200 km/h, respectively (see sec. 2.5.3). The simulation generated a longitudinal profile irregularity for general class spectrum with wavelength range between 3-25 m. The figures also show the threshold limits for isolated defect as defined in the European Standard (see sec. 2.5.2).

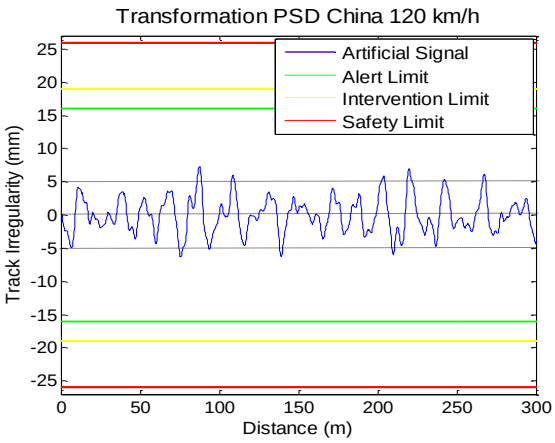

Figure 4.7 – Transformation PSD for China 120 km/h

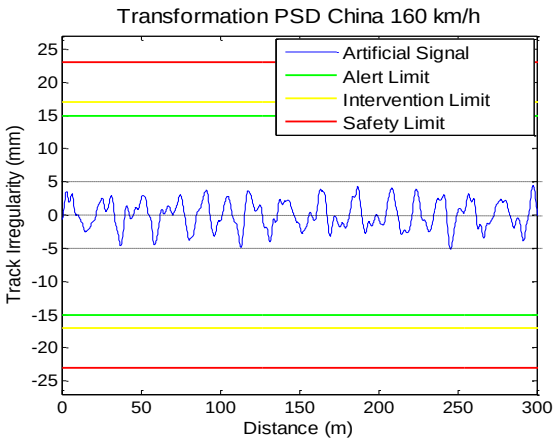

Figure 4.8 – Transformation PSD for China 160 km/h

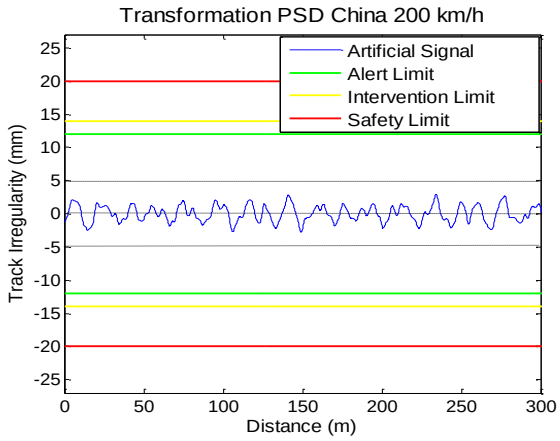

Figure 4.9 – Transformation PSD for China 200 km/h

Based on Figures 4.7 to 4.9, it can be observed that line speed has greatly contributed to the amplitude of the geometrical defect. The higher the line speed results, the lower the track irregularity obtained from PSD. As a matter of fact, all the rail generation produced from Chinese PSD are below those of European Standard limits.

The preference for the use of frequency bandwidths is another issue of interest. This fact is due to the limitation in the measurement equipment/track recording car that may not be able to detect the geometrical defects in some specific intervals. The spatial track irregularities have therefore been generated from various PSD functions, taking into

account different wavelength intervals as defined in the European Standard [prEN 13848-5].

- D1: wavelength of irregularities within the interval of $3 < \lambda \leq 25$ m
- D2: wavelength of irregularities within the interval of $25 < \lambda \leq 70$ m
- D3: wavelength of irregularities within the interval of $70 < \lambda \leq 200$ m

Figures 4.10 and 4.11 present the generations of rail track irregularity obtained from FRA 6 and German low disturbance spectra (best classes) using different wavelength ranges, respectively. The rail simulation follows the procedures as described in the Section 4.3.1, with an adjustment on the parameter of waveband (Δn) that is corresponding to the particular wave range in interest.

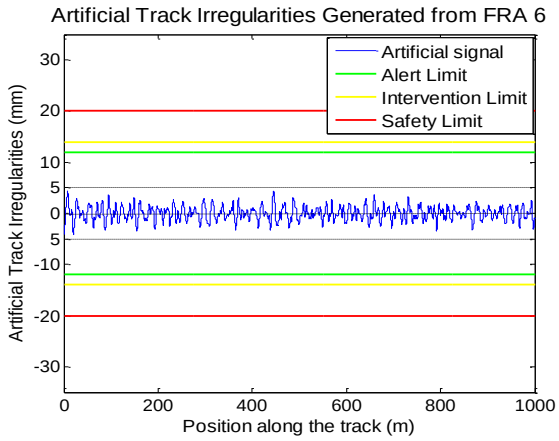

a) FRA 6 D1 ($3 < \lambda \leq 25$ m)

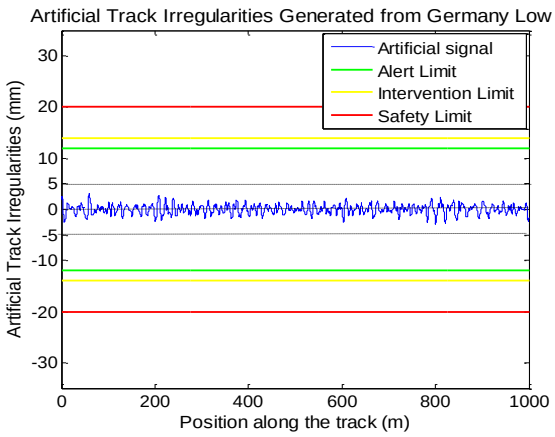

a) German Low D1 ($3 < \lambda \leq 25$ m)

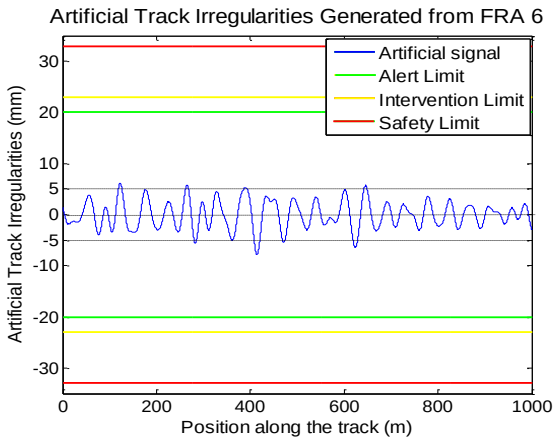

b) FRA 6 D2 (25 $< \lambda \leq$ 70 m)

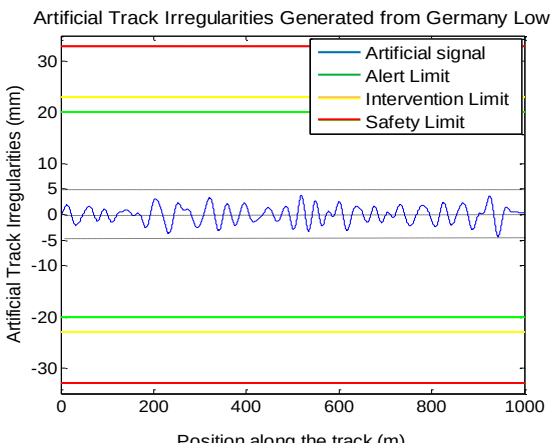

b) German Low D2 (25 $< \lambda \leq$ 70 m)

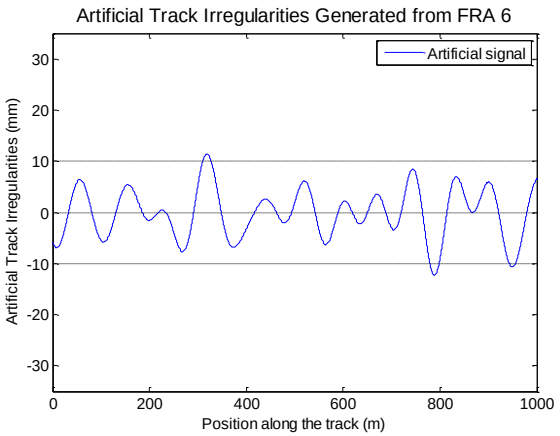

**No threshold limits defined for D3*

c) FRA 6 D3 (70 $< \lambda \leq$ 200 m)

Figure 4.10 – The Influence of Wavelength in the Artificial Longitudinal Profile Irregularity - FRA Class 6

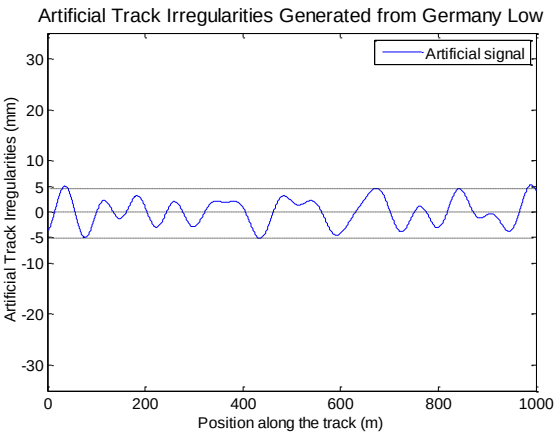

**No threshold limits defined for D3*

c) GermanyLow D3 (70 $< \lambda \leq$ 200 m)

Figure 4.11 – The Influence of Wavelength in the Artificial Longitudinal Profile Irregularity - German Low disturbance

As expected, the magnitude of track irregularities generated by "FRA 6" PSD appears to be greater than the one produced by "German low" track spectrum. This fact confirmed the finding in Figures 4.10a and 4.11a , which indicated the superior quality of the "German low disturbance" in relation to the "FRA 6" PSD.

Note that the magnitude of track defect grows as the wavelength of interest is becoming longer. For example, one can remark that the maximum irregularity of "German low D1" (Figure 4.11a) is around 2 mm, while the maximum defect of "German low D3" (Figure 4.11c) is about 5 mm.

4.5 THE APPLICATION OF PSD STANDARDS IN TRACK QUALITY ASSESSMENTS

The specimen used in this analysis was taken from a particular segment of the Portuguese Northern Railway Lines. The geometrical data was provided by the Track Recording Car (TRC), from successive inspections conducted on March 5, 2007 (before maintenance) and June 25, 2007 (after maintenance). Using an optical measurement system, this car is able to record various geometry parameters such as longitudinal profile, alignment, gauge, superelevation irregularity (cross level), and twist in points spaced by 0.25 m. Although the rail track in this study is only approximately 1 km long for a design speed of 120 km/h, this section mainly intends to show how the PSD method is put into practice in track quality assessments.

Rail Track Generation

Based on the proposed simulation method (see Chapter 4.3), the track irregularities are generated from German and FRA PSD standards. Each standard is comprised by two different track classes; one is the highest (best) track class of the standard and one is the same class with the real track data. In this case, FRA 6 and German low disturbance are classified in the first category while FRA 4 and German high disturbance are analyzed in the second category. Every rail simulation is generated with respect to a waveband between 3 m to 25 m. The track quality is then assessed by comparing the artificial track irregularity with the real track data.

Figure 4.12 gives a comparative sample of track longitudinal profile irregularities for a length of 250 m. Figures 4.13 and 4.14 show detailed comparisons of the artificial irregularities of the German and the FRA PSD, respectively.

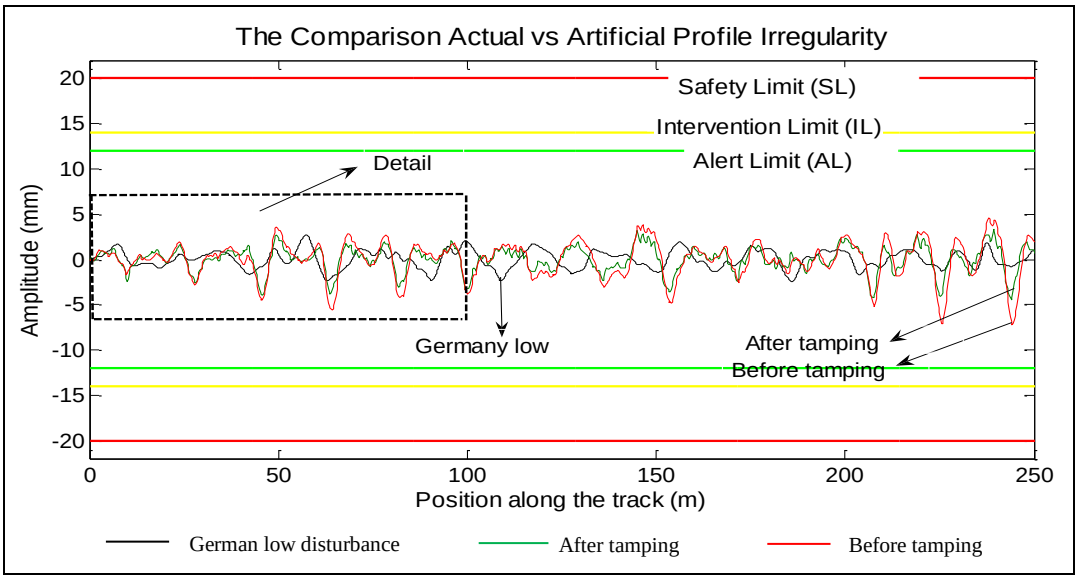

Figure 4.12 – Comparison between Actual and Artificial Longitudinal Profile Irregularities – German low PSD

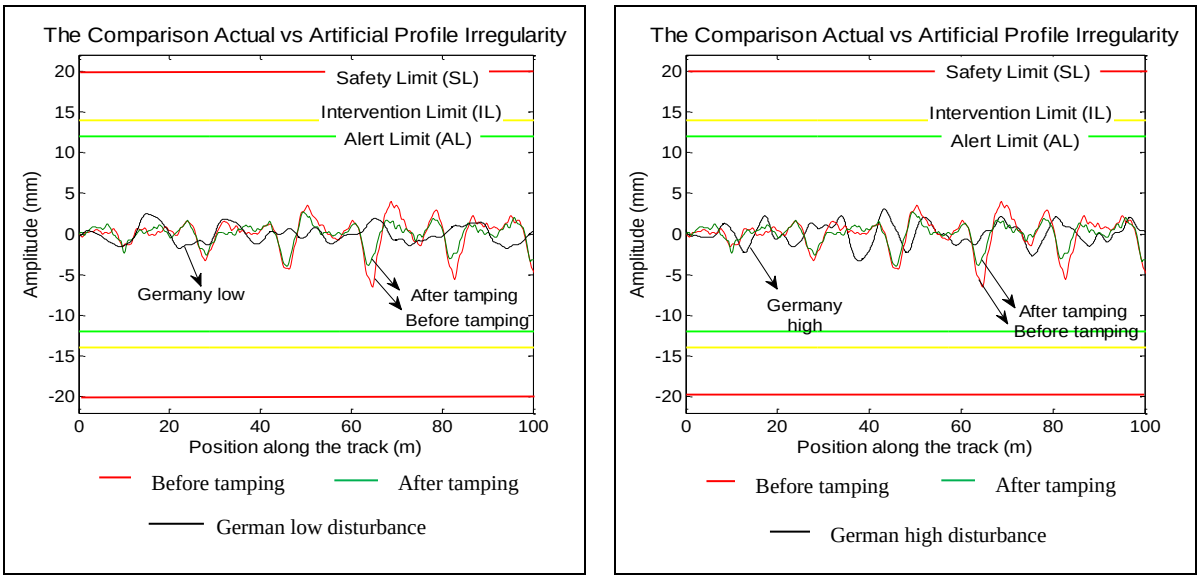

a) Actual and Artificial German low (best classes) b) Actual and Artificial German high (same classes)

Figure 4.13 – Comparison between Actual and Artificial Longitudinal Profile Irregularities– German PSD

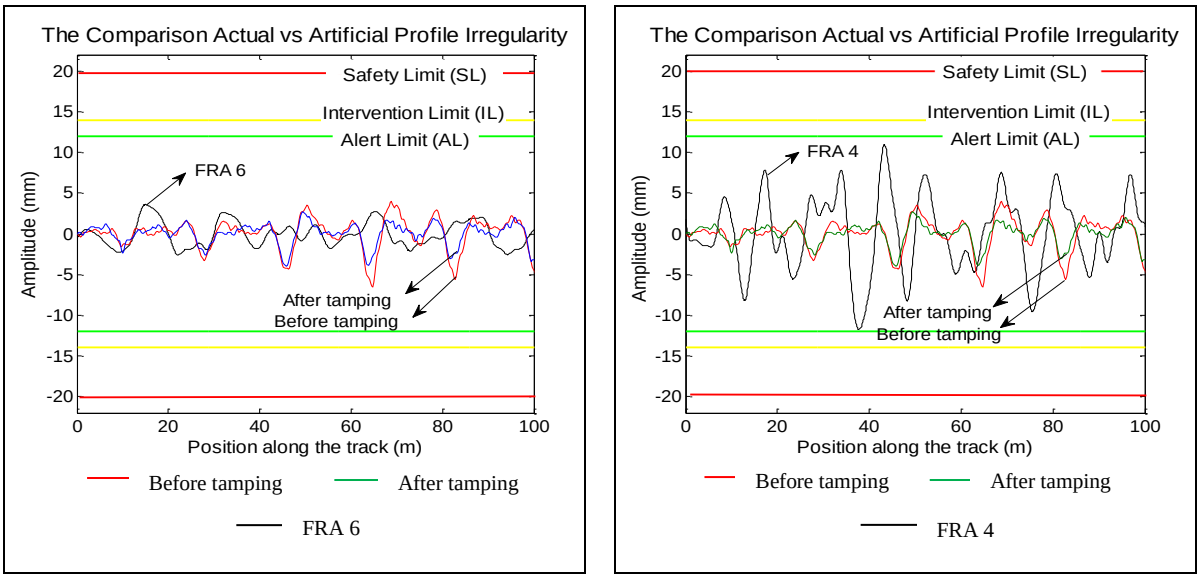

a) Actual and Artificial FRA 6 (best classes)

b) Actual and Artificial FRA 4 (same classes)

Figure 4.14 – Comparison between Actual and Artificial Longitudinal Profile Irregularities – FRA PSD

According to the figures, the magnitude of the defect of the actual track data after tamping is slightly higher than the German low disturbance, but close to the amplitude of the German high disturbance and the FRA PSD 6. For the track data before tamping, Figure 4.13a and 4.14a show the larger irregularities of real track data compared to the best PSD class standards. Although the measured track data can be categorized in the line speed of FRA class 4 (120 km/h), it can be seen that the amplitude of the actual track is even smaller than the irregularity generated by the FRA 4 spectrum. This fact thus confirmed the applicability of the sample lines for train services exceeding its predefined speed.

Table 4.1 gives the standard deviation values obtained from the above simulations and the predefined alert limits in the European Standard. German low disturbance generates a lower standard deviation of track irregularity than the one produced by FRA 6, and even lower than the European Standard limit for class $160 < V \leq 220$. However, German standard do not explicitly define the respective train speed for their spectra, which made it slightly more difficult to compare with the other standards.

In correspondence with the lower speed, FRA 4 shows a larger tolerance of standard deviation than European Standard, followed by German high disturbance. Note that all of the obtained results thus confirm the findings in Figures 4.13 and 4.14.

Table 4.1 – Comparison between Standard Deviations of Simulated Track Irregularities

PSD Standards		STD (mm)
German	low	0.98
	high	1.6
FRA	FRA 6 [≤ 177 km/h]	1.4
	FRA 4 [≤129 km/h]	5.6
European Standard	160 < V ≤ 220	1.2 – 1.9
	80 < V ≤120	1.8– 2.7

Fitting Curve Method

The other technique for measuring the state of the track condition can be accomplished by expressing the spectrum of a geometrical defect with a fitting curve function [Zhiping and Shouhua, 2009]. To obtain the best fit curve, an iterative non-linear least square optimization is applied to all the observation points. The result is then compared to the PSD standards. The results lying above the curve standards should be prioritized in the maintenance treatment, while those falling below the standard should be treated oppositely.

Figures 4.15 to 4.18 present the fitting curve samples of track irregularity spectrum and their inclusion in the Chinese PSD standard. Since the specimen used in this analysis is a geometry defect with wavelength between 3-25 m (D1), it can be seen that the power spectrum is decreasing considerably beyond this waveband.

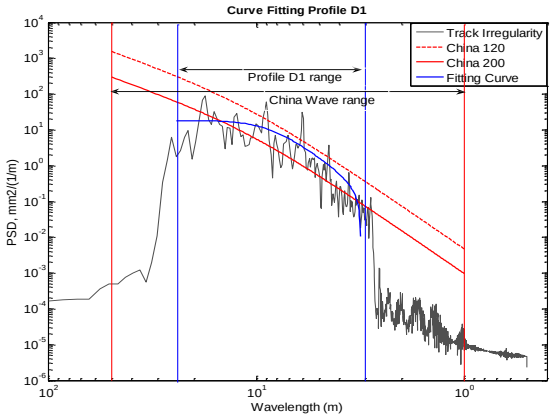

Figure 4.15 – Sample of fit. curve Longitudinal Profile D1

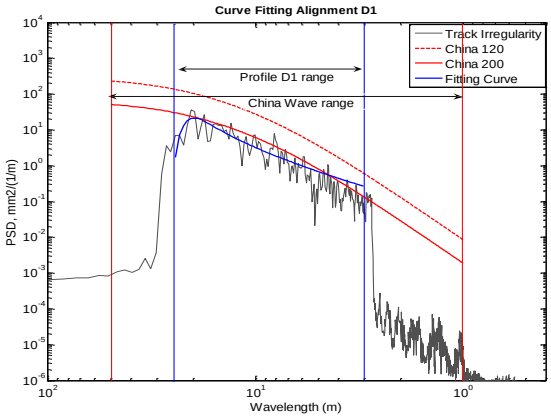

Figure 4.16 – Sample of fit. curve Alignment. D1

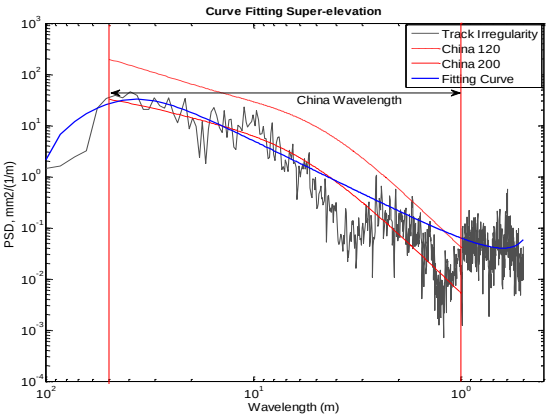

Figure 4.17 – Sample of fit. curve Super-elevation

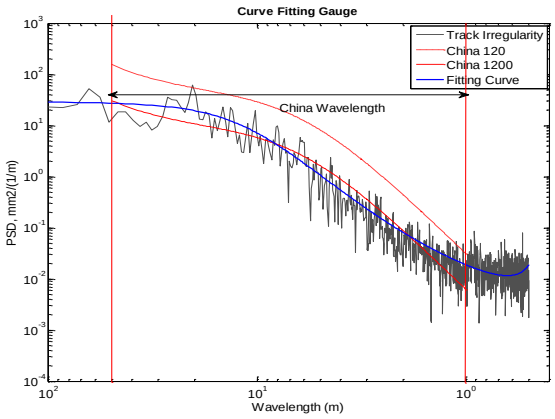

Figure 4.18 – Sample of fit. curve Gauge

The comparisons between the irregularity spectrum before and after maintenance with the PSD standard are given in Figures 4.19 to 4.22.

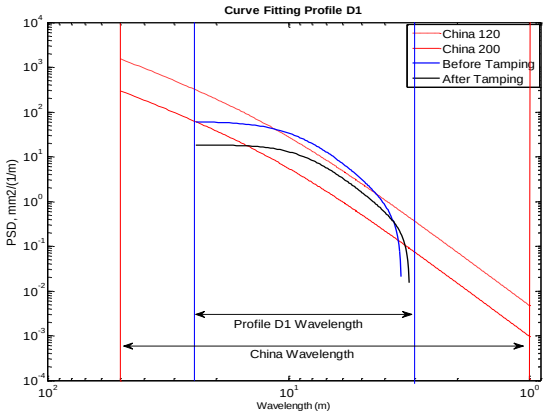

Figure 4.19 – Comparison of profile D1

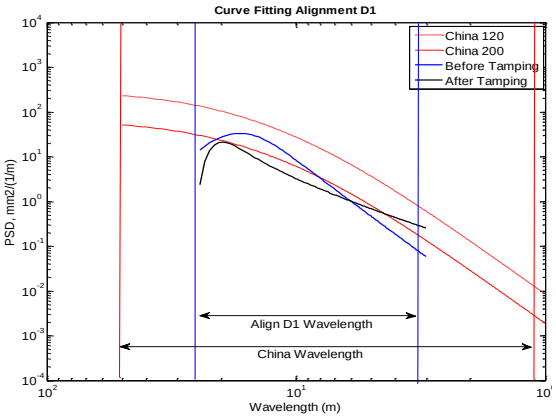

Figure 4.20 – Comparison of alignment D1

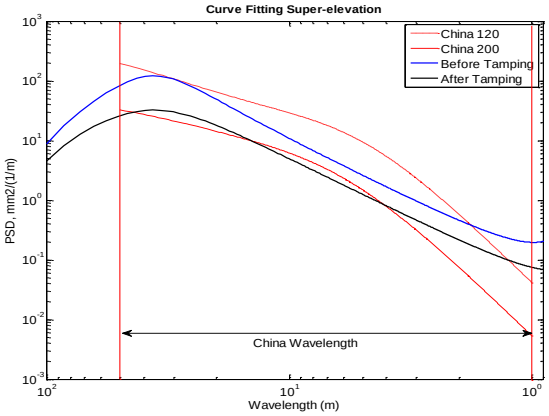

Figure 4.21 – Comparison of super-elevation

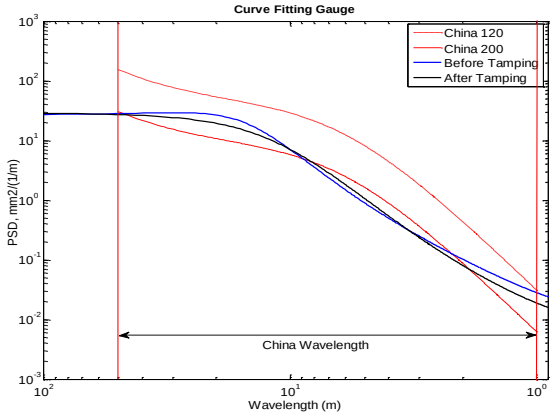

Figure 4.22 – Comparison of gauge

Figure 4.19 presents the track irregularity spectrum for the longitudinal profile before and after tamping. The spectrum of longitudinal profile after tamping is slightly higher than the Chinese 120 standard, particularly for the wavelength between 4.5 m and 11.5 m. However, when tamping is performed, the longitudinal profile experienced a gradual improvement, which moved the spectrum quality to the middle of the Chinese 120 and the Chinese 200 standards.

As indicated in Figure 4.20, the track alignment has revealed a superior quality compared to the Chinese PSD standard. Both irregularity curves, before and after tamping, are lower than the Chinese 200, especially for the wavelength below 8.1 m and

above 20.9 m. A better spectrum quality is also shown by the alignment curve after tamping, which validates the accomplishment of track maintenance in the improvement of the geometry quality.

Figure 4.21 presents a track irregularity spectrum corresponding with the super-elevation irregularity/ cross level. In general, the track qualities (before and after tamping) are adequate for train operation higher than 120 km/h and below 200 km/h. The maximum improvement is prominently visible for the track after tamping in the wavelength ranges from 4 m to 14 m, indicating the superiority of the segment compared to the PSD standards.

The irregularity of track gauge is inherently associated with the variation of the rail in horizontal alignment. As similar to the trend demonstrated for track alignment, the fitting curve of gauge shows a higher quality than the standards (Figure 4.22). The figure is also indicative of a well-treated gauge for short wavelength defects (2 m–8 m).

The quality assessment was conducted to various track geometry parameters. The results demonstrated the capability of the proposed method to identify the changing behaviour of track segment before and after intervention, as well as to detect particular wavelengths that need to be prioritized in future maintenance. The relation between the track quality level obtained before and after intervention is one of the most important indicators to assess the suitability of the maintenance strategy in order to obtain the established objective.

4.6 CONCLUSIONS

The PSD standards obtained from various countries have been briefly described. The comparisons among each of them as well as their application in practice were also reviewed. Several essential facts can be drawn as given in the following points.

- Power Spectral Density (PSD) has great advantages in the railway track quality assessment. It can describe a wide range of spectral characteristics of random wave irregularity, indicating peak and cyclic peak in each wave. The wavelength is strongly linked with problems; the short wavelength associates with train safety while the long wavelength corresponds to riding comfort.

- There are several functions and methods for transforming a particular PSD standard to the stochastic random series. The procedures are presented in detail in section 4.3. By comparing the inverse of the time series generated from the PSD function and the theoretical PSD, it was found that the applied methodology is concise and acceptable.

- In the simulation of rail geometry defect, the magnitude of track irregularity is considerably influenced by the preference of wavelength interval (waveband) and line speed. Longer wavelength intervals result in higher magnitude, whereas shorter wavelength intervals create the opposite. On the contrary, a higher line speed will give a smaller variability of the track defect while a lower line speed produces a larger magnitude.

- Based on the comparison among different PSD spectrums, it can be seen that the German PSD is generally stricter for the geometry errors of longitudinal profile, alignment and cross level or superelevation irregularity, which indicates a better quality control applied by the German railway standards. For the curves produced by Chinese and FRA spectrums, the analysis shows a comparable result in terms of

their magnitude and tendency especially for wave irregularities below 10 m. The detailed analysis on the comparison of various PSD standards is as follows.

A similar characteristic of the longitudinal profile is shown between Chinese 200 and German low disturbance at wavelengths shorter than 4 m, which is superior to the SNCF and FRA power spectral densities. As the wavelength increases, France spectrum (SNCF good) takes it into more consideration especially for the irregularities above 16 m. Note that in this particular wave, the SNCF PSD results correspond to a highest curve.

For the PSD comparison of track alignment, the magnitude of German low disturbance is lower than FRA and Chinese PSD at wavelengths lower than 38 m, indicating more restrictions to the allowable tolerance imposed by German high speed lines. At wavelengths below 10 m, the curves presented by Chinese 200, German high disturbance and FRA 6 are close and seem to be almost equal. A superiority of German PSD can also be found in the PSD comparison of cross level or superelevation irregularity at all the investigated wavelengths.

– The analysis reveals that the spectral quality of the track before and after tamping is considerably different. The spectra of the track after intervention shows a decrease in power compared with the track spectrum before intervention. This fact thus justifies the applicability of PSD to evaluate the performance indicators obtained from the maintenance work.

5

CORRELATION ANALYSIS OF RAILWAY TRACK GEOMETRY

5.1 INTRODUCTION

Track geometry is an important factor influencing journey quality and track performance. It consists of several geometry variables such as longitudinal profile, horizontal alignment, cross-level, twist and gauge, which are closely related. Combined track geometry irregularities may cause a severe vehicle-track interaction that affects train safety and derailment resistance.

Apart from that, the deterioration of certain track geometry parameters does not stand alone. Current research indicates that a degraded track geometry parameter can induce further degradation of the other parameters [Karttunen, 2012]. It is therefore necessary to understand the role and impact of each variable on the others and the type of relationship, if any, among track geometry parameters, to provide a base for developing a reasonably accurate model of track degradation. Such knowledge could also assist in modeling the input of rail excitation in vehicle-track dynamic simulation [Broeck, 2001].

The analysis has been conducted, using a typical track geometry data from the Northern line of the Portuguese Railways, to establish the actual relationship and statistical

correlation that may exist among track geometry variables. The relationship analyses were conducted in the wavelength domain using three different approaches: cross correlation, autocorrelation and coherence analysis. The analyses results will determine the appropriate method to construct the prediction model of deterioration used in the track maintenance optimization problem (Chapter 6). The following sections describe the methodology used and the results of these analyses.

5.2 THE CORRELATION OF TRACK GEOMETRY

The correlation among track geometry parameters is applied to quantify the degree of interdependency of one geometry variable to the other, or to establish the similarity between two different datasets. This concept enables to distinguish three correlation categories.

The first category is autocorrelation, which describes the general dependency of values of some observations at a certain distance (x) to the values of the same observations at another distance $(x + \tau)$. A symbol of τ is known as the lag distance between these observations. Equation 5.1 gives an autocorrelation formula for a random continuous track irregularity $[s(x)]$:

$$R_{ss}(\tau) = \lim_{L\to\infty} \frac{1}{L} \int_0^L s(x) \cdot s(x+\tau) dx \tag{5.1}$$

where L is the length of the track irregularity signal and τ represents the amount of lag that should be shifted in distance relative to the original signal $s(x)$.

For the sampled track irregularity signal, the autocorrelation function is given by the following equation:

$$R_{ss}(m) = \frac{1}{L} \sum_{n=0}^{L-1} s(n) \cdot s(n+m) \tag{5.2}$$

where space shift, m, is quantified by the number of lag samples and $s(n)$ is a space domain of track irregularity.

The autocorrelation of a random continuous track irregularity may exhibit a greater value at a smaller lag and probably a lower value at a larger lag. The highest peak of the function is identified at zero lag, $R_{ss}(0)$, which equals to the average power of the input waveform.

$$R_{ss}(0) = \frac{1}{L}\sum_{n=0}^{L-1} s^2(n) = S \tag{5.3}$$

$$R_{ss}(0) \geq |R_{ss}(m)| \; for \; m \neq 0 \tag{5.4}$$

where S is the average power of the input waveform and constitutes the maximum value of the autocorrelation function.

The autocorrelation function is particularly useful in identifying the presence of repetitive patterns or periodicities in a given dataset, which in turn can be beneficial to determine the condition of track geometry [Zhiping and Shouhua, 2009].

The second category is called cross-correlation. The concept is basically similar with autocorrelation. However, instead of correlating a waveform against itself, the cross correlation is performed by taking two different waveforms as a function of a space-lag applied to one of them. Considering two different waveforms $s(x)$ and $g(x)$, the cross correlation is given by:

$$R_{sg}(\tau) = \lim_{L\to\infty} \frac{1}{L}\int_0^L s(x) \cdot g(x+\tau)dx \tag{5.5}$$

or

$$R_{gs}(\tau) = \lim_{L\to\infty} \frac{1}{L} \int_0^L g(x) \cdot s(x+\tau) dx \tag{5.6}$$

where L is the length of the track irregularity signal and τ represents the amount of lag that should be shifted in distance relative to the original signal.

For a sampled signal of track irregularity, the cross correlation function is defined as:

$$R_{sg}(m) = \frac{1}{L} \sum_{n=0}^{L-1} s(n) \cdot g(n+m) \tag{5.7}$$

where m is the number of shifted distances or lags.

In practice, to determine the degree of similarity between two signals is not sufficient to simply compare the amplitude of the cross-correlation. Normalized cross-correlation is often used to quantitatively assess the quality of the correlation. This value is obtained by normalizing the magnitude $R_{sg}(m)$ by an amount depending on the energy content of the data, as given by:

$$p = \frac{R_{sg}(m)}{\frac{1}{L}\left[\sum_{n=0}^{L-1} s^2(n) \cdot \sum_{n=0}^{L-1} g^2(n)\right]^{1/2}} \tag{5.8}$$

The normalized quantity (p) will vary between -1 and 1. Zuo and Xiang [2006] have proposed a guideline for the interpretation of correlation coefficients:

a) When $|p| = 1$, the signals s(n) and g(n) are perfectly correlated, while a value of $|p| = 0$ shows that the signals are completely uncorrelated.

b) When $0 < |p| < 1$, a linear relationship exists between the two signals. A higher p value indicates a stronger correlation, while a lower p value means a weaker correlation. Further classifications of this category are:

- $0 < |p| \leq 0.3$, refers to a weak correlation
- $0.3 < |p| \leq 0.5$, refers to a low correlation
- $0.5 < |p| \leq 0.8$, refers to a significant correlation
- $0.8 < |p| < 1$, refers to a high correlation

c) When $|p| > 0$, the bond is identified as positive relationship while for $|p| < 0$, the bond is identified as negative correlation.

The last category is called coherence, which measures the linear dependence between two signals as a function of wavelength. The analysis of coherence is of particular importance, since it is able to identify at which wavelengths two stochastic waveforms are coherent and at which wavelengths they are not.

Given two sampled signals of track irregularity, $s(n)$ and $g(n)$, the coherence is based on the square of the absolute value of the cross-power spectrum divided by the power spectrum of the input signals, as defined by:

$$\gamma^2 = \frac{\left|P_{sg}(\lambda)\right|^2}{\left(P_{ss}(\lambda) \cdot P_{gg}(\lambda)\right)}, \quad 0 \leq \gamma^2 \leq 1 \tag{5.9}$$

where:

γ^2 = coherence

$P_{sg}(\lambda)$ = cross-power spectrum density between signal x and y, which is obtained by:

$$P_{sg}(\lambda) = \sum_{-\infty}^{\infty} R_{sg}(m) \cdot e^{-j2\pi\lambda m}$$

$P_{ss}(\lambda)$ = power spectrum of signal s, which is obtained by

$$P_{ss}(\lambda) = \sum_{-\infty}^{\infty} R_{ss}(m) \cdot e^{-j2\pi\lambda m}$$

$P_{gg}(\lambda)$ = power spectrum of signal g, which is obtained by

$$P_{gg}(\lambda) = \sum_{-\infty}^{\infty} R_{gg}(m) \cdot e^{-j2\pi\lambda m}$$

The magnitude of the coherence function γ^2 at any frequency has a range of values between 0 (zero) and 1 (one). The value of one indicates perfect coherence between two different datasets in a particular wavelength, while the value of zero indicates the opposite.

5.3 TEST DATA ANALYSIS

A comprehensive track geometry database was prepared to investigate the statistical correlation among rail geometry variables. The data was collected from the Track Recording Car (TRC) EM 120, which provided around 17 measurement surveys from October, 2003 to January, 2009 (1926 days). During the measurement process, the TRC EM 120 took samples once every 0.25 m and counted several geometry variables such as longitudinal profile, alignment, gauge, cross level or superelevation irregularity, curvature, altitude, etc.

Figure 5.1 gives the details of the track characteristics of the Portuguese Northern Line railway used in this analysis. The sampled line is located at the midpoint between two cities, Pampilhosa and Aveiro, with a total length of 34 km. In order to have a sufficient sample size for spectrum analysis, the track is partitioned into 34 equal sized sections that are averaged to obtain the value of correlation.

Analyses of track geometry irregularities in the vertical and horizontal planes were conducted for each rail separately. There are three types of the mentioned data used in these analyses: track irregularities based on the measurement of 10 m chord length (with no specified wavelength interval), track irregularities D1 (with wavelength range between 3-25 m) and track irregularities D2 (with wavelength range between 25-70 m).

Position	Start	End
	200+000.00	233+399.75
Length	33.4 km	
Period of Investigation	2003-2009 (17 Measurement Files)	
Design Speed	50 - 220 km /h	
Track Geometrical Characteristics	Mixed line [Straight and Curved]	

Figure 5.1 – Track Characteristics of Sample Track Segment

5.3.1 CROSS CORRELATION

Using the methods described in the preceding section, the computation of cross-correlation was conducted to seek the relationship among the track geometry variables, including:

- Left alignment
- Right alignment
- Left longitudinal profile
- Right longitudinal profile
- Gauge
- Super-elevation
- Twist
- Curvature

The samples of the typical track geometry irregularities are presented in Figure 5.2 and the curvature characteristic for overall segments is given in Figure 5.3. The sample data shows a historical record of each track geometry parameter for 1.5 km track section obtained in January, 2009.

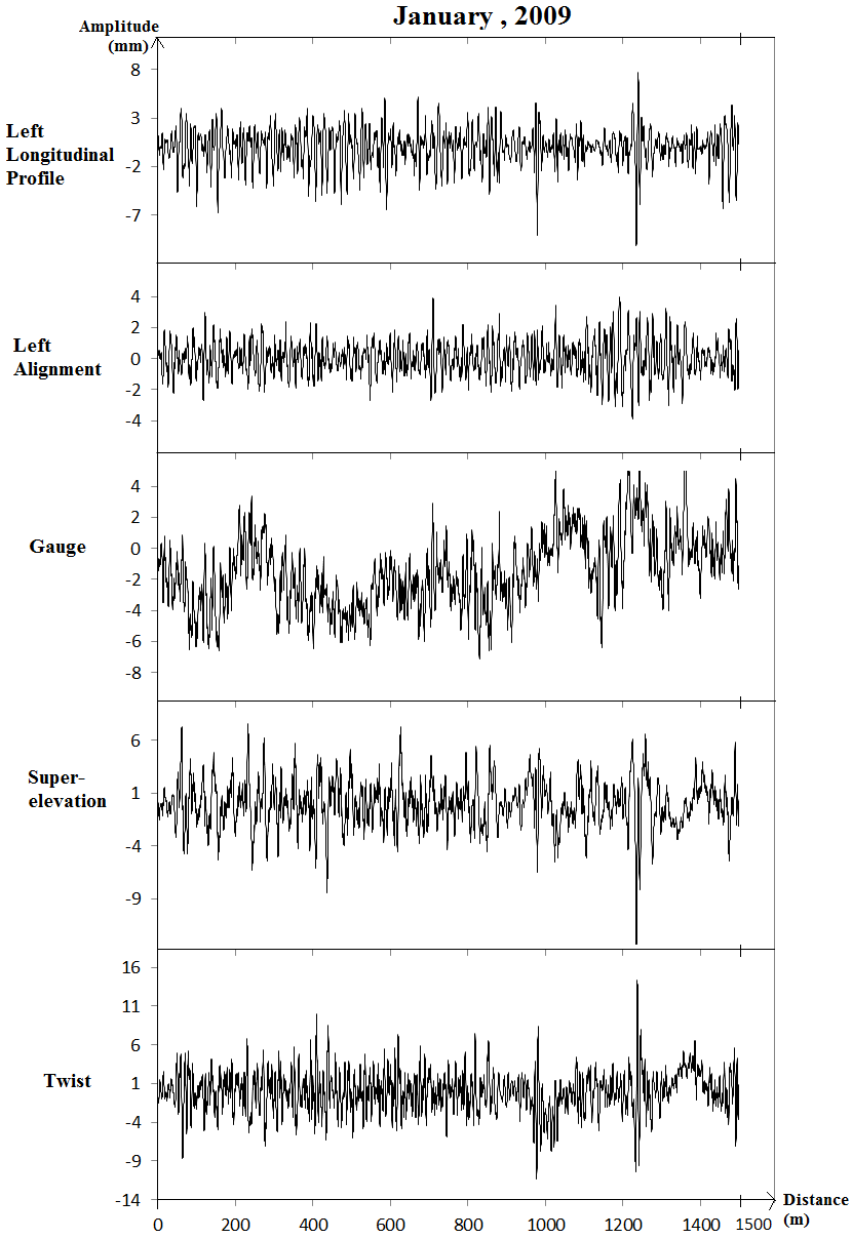

Figure 5.2 – Samples of Track Geometry (KM 200.00-201.50)

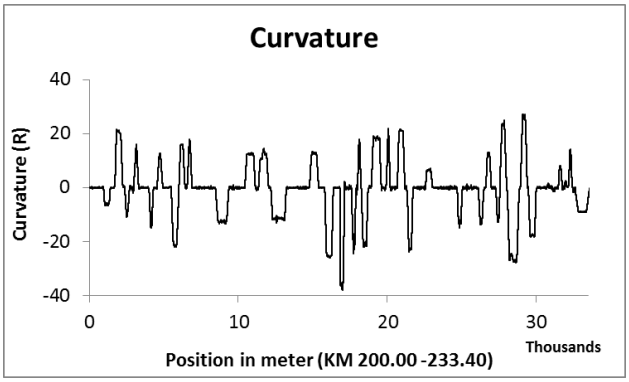

Figure 5.3 – Curvature Geometrical Characteristics (KM 200.00-233.40)

Analyses of cross correlation are summarized in the following figures. Figure 5.4 presents the averaged cross correlation between the left and the right rails of the 34 equal sized sections. It contains the evaluation in both longitudinal profile and alignment throughout the 17 measurement surveys. Figure 5.5 gives the averaged cross-correlation between longitudinal profile and alignment irregularities of each rail.

For the current analyses, the track irregularities in different wavelength ranges were used and their correlation results were compared. By doing so, the wavelengths at which the variables are correlated can be more clearly defined.

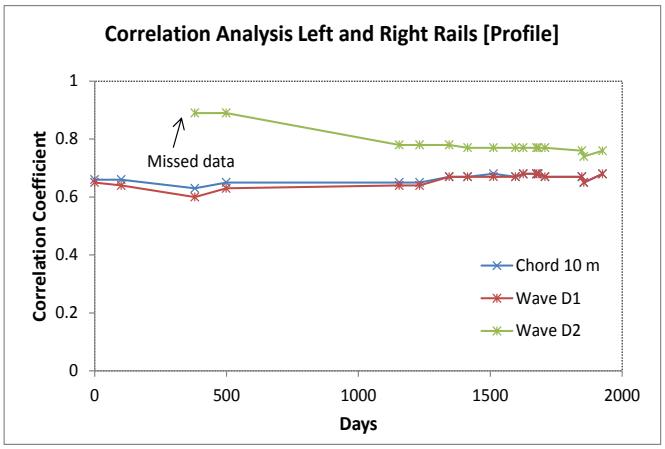

Wave Ranges	Average Profile (Left & Right)
10 m chord	0.66
D1	0.66
D2	0.78

a) Track Longitudinal Profile

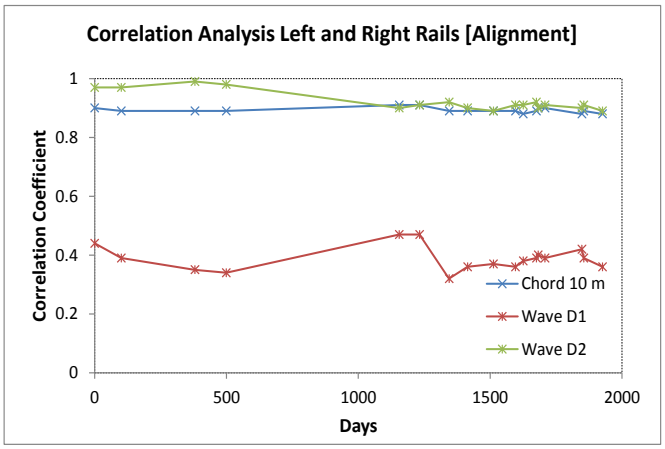

Wave Ranges	Average Alignment (Left & Right)
10 m chord	0.89
D1	0.39
D2	0.92

b) Track Alignment

Figure 5.4 – Cross-Correlation Analysis for Longitudinal Profile and Alignment

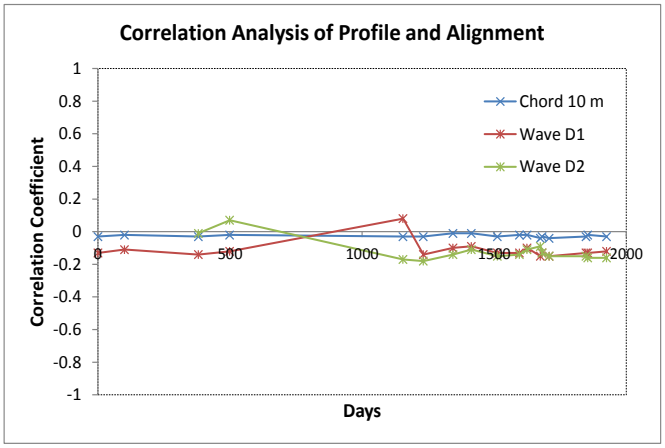

Wave Ranges	Average Left Rail (Profile & Alignment)
10 m chord	-0.02
D1	-0.11
D2	-0.12

a) Left Rail

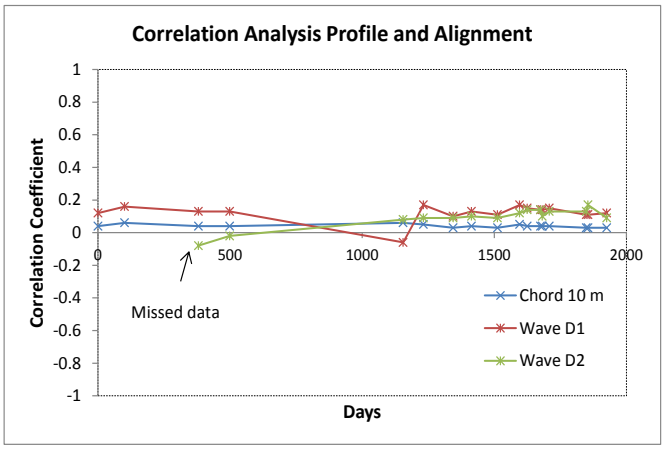

Wave Ranges	Average Right Rail (Profile & Alignment)
10 m chord	0.04
D1	0.12
D2	0.09

b) Right Rail

Figure 5.5 – Cross-Correlation Analysis for the Left and the Right Rails

Longitudinal profile irregularity is defined as the vertical deviation of the midpoint of the two rails from the nominal elevation of the track. On the other hand, alignment irregularity measures the deviation of the rails from the nominal centerline in the lateral direction. Since the track inspection car EM 120 inspected the left and the right rails separately, the correlation between the two variables can be examined.

As shown in Figure 5.4, the averaged cross-correlations of track longitudinal profile irregularity between the left and the right rails are 0.66 for the 10 m chord wave and wave D1, and 0.78 for wave D2, which are derived by averaging the correlation values of the 17 inspection dates. These values specify a significant correlation between the two rails within various wave ranges and indicate the influence of irregularity of one rail to the other rail.

Meanwhile, there exists a high correlation of track alignment irregularity between the left and the right rails in both the 10 m chord wave and D2, with the average values of 0.89 and 0.92, respectively. However, the track defects in D1 exposed a contrary result. The correlation of two rails is not considerably significant with an average value of 0.39. These facts indicate that the rails are similar and properly aligned especially in the

wavelength between 25-70 m instead of 3-25 m. It is also known that all the correlation values are positive, which means that if the irregularity in a certain rail increases, then the irregularity in the other rail will tend to increase as well.

Figure 5.5 shows a low correlation between longitudinal profile and alignment irregularities. The computation results demonstrate that these variables are uncorrelated and independent of each other, for example the averages of the correlation of the 10 m chord are -0.02 for the left rail and 0.04 for the right rail. These values suggest that the relationship should be classified in the "weak correlation" category.

Figure 5.6 presents the correlation analysis between super-elevation and the other geometry variables: twist, gauge, longitudinal profile and alignment. For the last two variables, the analysis of each rail was conducted separately.

It should be noted that, for the remaining analysis, the utilized track irregularities in the horizontal and vertical plane were based on the 10 m chord length measurement, as it provided the correlation results similar to the other two types of data (D1 and D2).

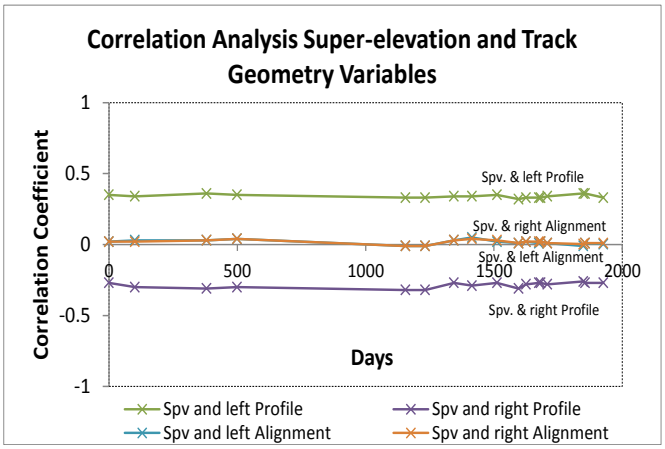

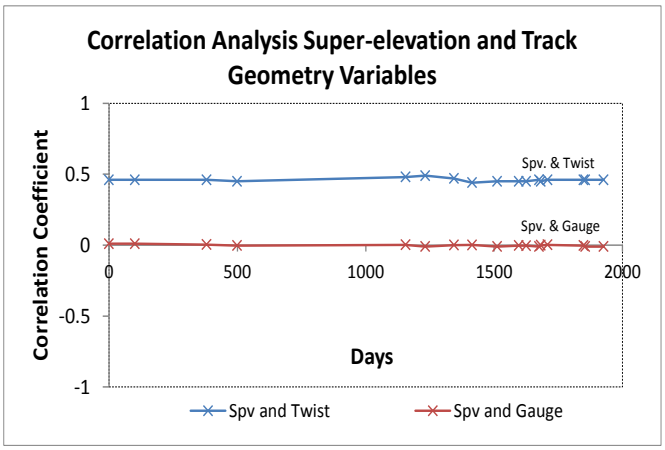

Correlation Variables	Average Coefficient
Superelevation & Twist	0.46
Superelevation & Gauge	-0.001
Superelevation & left Profile	0.34
Superelevation & right Profile	-0.3
Superelevation & left Alignment	0.02
Superelevation & right Alignment	0.02

Figure 5.6 – Cross-Correlation Analysis between Super-elevation and other Track Geometry Variables

Cross level or superelevation irregularity defines the amount of vertical deviations between the levels of two rails from a designated value. Twist, on the other hand, measures the difference in the super-elevation between two points taken at a separate fixed distance. Based on Figure 5.6, it can be stated that there exists a correlation between super-elevation and twist, although not statistically significant, with an average coefficient of 0.46. This experimental result thus compliments the logical judgment that super-elevation and twist are positively correlated due to the tie connection of the measurement.

Gauge specifies the inner distance between two rails measured at 16 mm below the top surface of the railhead. A very low value resulted from the correlation between super-

elevation and gauge, with an average of 17 time inspection dates is about -0.001. There is no apparent relationship, as one increases and the other one shows no effect.

Furthermore, there is also a correlation between super-elevation and longitudinal profile, even though the relationship is not so high. The coefficients are 0.34 and -0.30 for the left and the right rails, respectively. The positive and negative indicators are revealed since super-elevation takes into account the disparity between the two top level surfaces of the two rails. The positive symbol indicates that the longitudinal profile irregularity in the left rail is aligned with the super-elevation irregularity, while the negative represents the opposite.

Figure 5.6 also shows the independency of super-elevation irregularity with respect to alignment. The average coefficient is 0.02 for both the left and the right rails, which classifies the relationship in the “weak correlation” category.

Figure 5.7 presents the averaged correlation between twist and the other geometry variables: gauge, longitudinal profile and alignment, for the 17 inspection dates. For the last two variables, the analysis is conducted in each rail separately.

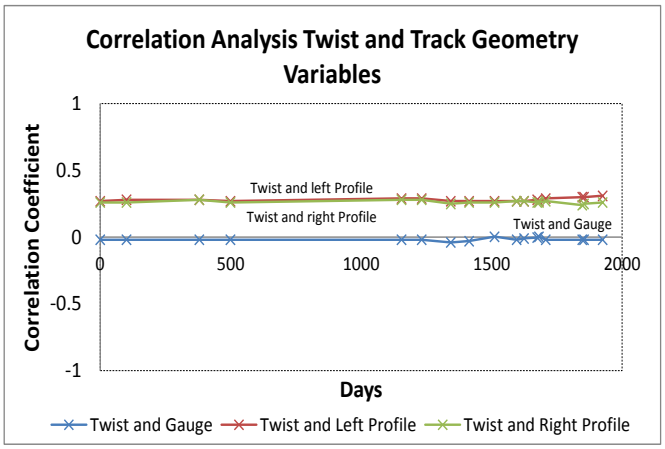

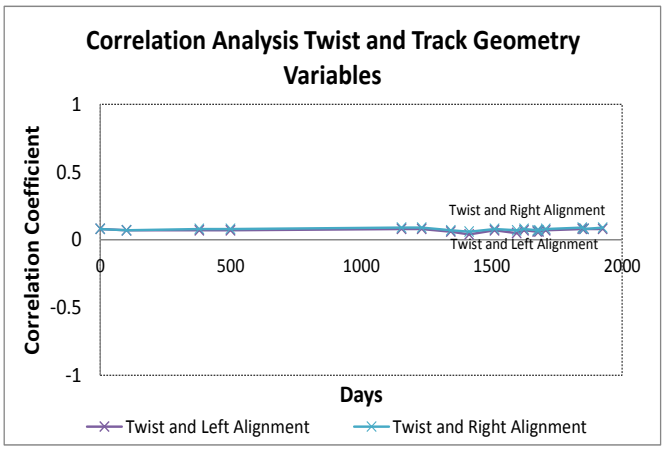

Correlation Variables	Average Coefficient
Twist & Gauge	-0.02
Twist & left Profile	0.28
Twist & right Profile	0.26
Twist & left Alignment	0.07
Twist & right Alignment	0.08

Figure 5.7 – Cross-Correlation Analysis between Twist and other track geometry variables

According to Figure 5.7, a very weak correlation exists between twist and gauge parameters. The averaged coefficient for the 17 inspection dates is about -0.02, which indicates the independency of the irregularity of one variable to the other.

With regard to the longitudinal profile irregularity, twist gives a very low correlation value with average coefficients of 0.28 and 0.26 for the left and the right rails, respectively. The same relationship is also observed when the cross-correlation is computed between twist and alignment. The average values are 0.07 and 0.08 for the left and the right rails, respectively, which places the relationship in the "weak correlation" category.

Figure 5.8 gives the analysis of cross-correlation between gauge and the other track geometry variables: longitudinal profile and alignment. Each analysis is conducted in each rail separately.

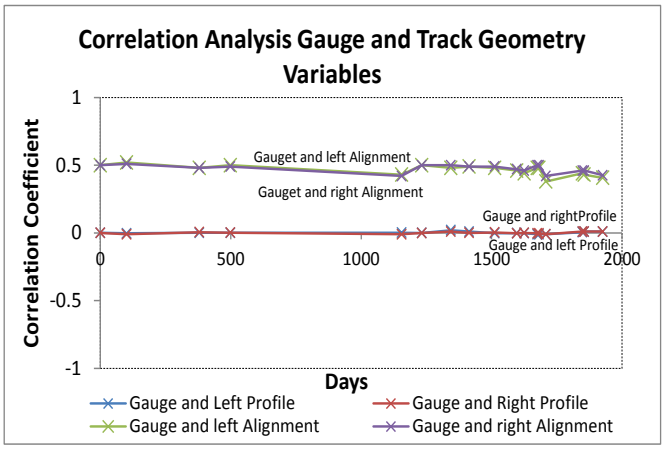

Correlation Variables	Average Coefficient
Gauge & left Profile	0.0002
Gauge & right Profile	0.0002
Gauge & left Alignment	0.47*
Gauge & right Alignment	0.48*

(*) correlation can be positive or negative

Figure 5.8 – Cross Correlation Analysis between Gauge and other track geometry variables

Based on Figure 5.8, a weak correlation is revealed between gauge and longitudinal profile. It accounts for an averaged coefficient of about 0.0002 for both the gauge and left longitudinal profile, and the gauge and right longitudinal profile. This means that the irregularity in one variable can remain constant although the other increases or decreases. On the contrary, there exists a relationship between gauge and alignment, although not statistically significant. The averaged coefficients are 0.47 for the correlation between gauge and left alignment and 0.48 for the correlation between gauge and right alignment. An asterisk symbol (*) indicates that the relationship can be either positive or negative and it can vary from low to high.

Figure 5.9 presents the averaged cross-correlation between curvature and various track geometry variables of 34 equal sized sections. It comprises the evaluation of 17 inspection dates.

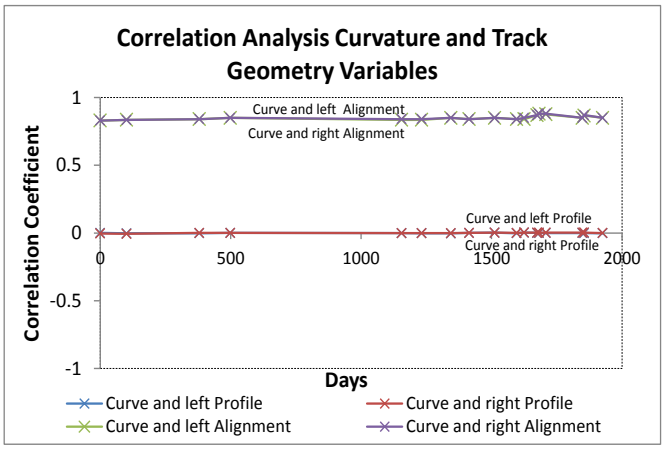

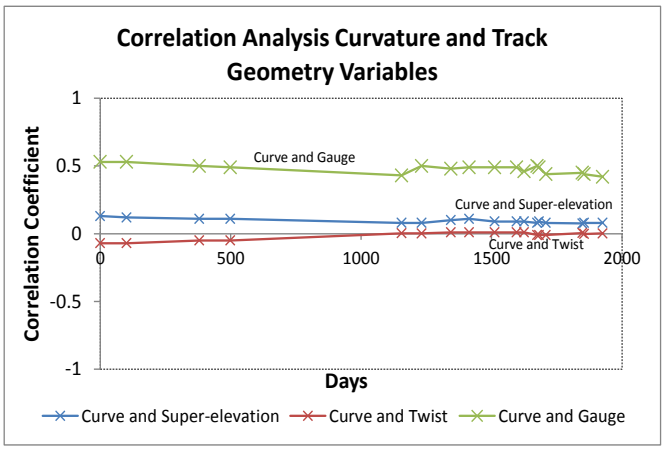

Correlation Variables	Average Coefficient
Curve & Super-elevation	0.09
Curve & Twist	-0.01
Curve & Gauge	0.48
Curve & left Profile	-0.001
Curve & right Profile	0.0004
Curve & left Alignment	0.85
Curve & right Alignment	0.85

Figure 5.9 – Cross-Correlation Analysis between Curvature and other track geometry variables

Curvature is defined as the spatial turning rate of the track. As presented in Figure 5.9, there exists a correlation between curvature and gauge variables, which magnitude varies depending on the track layout. The higher the curvature, the larger the correlation; conversely, the smaller the curvature, the lower the correlation. Note that the correlation between curvature and gauge can be either positive or negative. As it is the same, the strong positive correlations are shown between curvature and alignment for both of the left and the right rails, with the averaged correlation around 0.85. The correlation is quite high in the segment where the curvature is large and low where the curvature is small. For the correlation between curvature and the other geometry variables (super-elevation, twist and longitudinal profile), it is known that the influence of curvature is not considerably significant.

The experimental study that has been conducted is summarized in Table 5.1.

Table 5.1 – Summary of Cross-Correlation Analyses

Geometry Variables	Left Profile [a)]	Right Profile [a)]	Left Alignment [a)]	Right Alignment [a)]	Super-elevation	Twist	Gauge	Curvature
Left Profile [a)]	*	[+] Significant	[-] Weak	*	[+] Low	[+] Weak	[-] Weak	[-] Weak
Right Profile [a)]	[+] Significant	*	*	[-] Weak	[-] Low	[+] Weak	[+] Weak	[+] Weak
Left Alignment [a)]	[-] Weak	*	*	[+] High	[+] Weak	[+] Weak	[-/+] Low	[+] High
Right Alignment [a)]	*	[-] Weak	[+] High	*	[+] Weak	[+] Weak	[-/+] Low	[+] High
Super-elevation	[+] Low	[-] Low	[+] Weak	[+] Weak	*	[+] Low	[-] Weak	[-] Weak
Twist	[+] Weak	[+] Weak	[+] Weak	[+] Weak	[+] Low	*	[-] Weak	[-] Weak
Gauge	[+] Weak	[+] Weak	[-/+] Low	[-/+] Low	[-] Weak	[-] Weak	*	[-/+] Low
Curvature	[+] Weak	[+] Weak	[+] High	[+] High	[-] Weak	[-] Weak	[-/+] Low	*

[*)] Not applicable since the cross correlation is made between two different geometry variables

[a)] Track irregularities based on the measurement of 10 m chord length

5.3.2 COHERENCE ANALYSIS

This section describes the application of the coherence function to identify at which wavelengths the various track geometry variables are coherent and at which wavelengths these are not. The formula in Equation 5.9 was used to calculate the coherence between two different datasets.

The coherence is considered to be significant if the resulting value lies above the confidence level (CL) (Rosenberg *et al*, 1989). This level is used to indicate the reliability of an estimate of which coherence value can occur by chance. The commonly used confidence levels are 90, 95 and 99% corresponding to α=0.10, 0.05 and 0.01, respectively. The confidence level can be calculated by the following formula:

$$\gamma_{1-\alpha}^2 = 1 - \alpha^{[1/(EDOF-1)]} \tag{5.10}$$

where alpha, α, is the desired level of confidence and EDOF, the equivalent degrees of freedom, is determined by the smoothing parameter and the window function. For a normalized Hanning window, $edof = \left(\frac{8}{3}\right) \cdot \frac{N}{M}$, where *N* is the number of data points and *M* is the half width of the Hanning window.

Generally, the wavelengths occurring in the track can be classified into various regions or bands. Rao [1992] established three different waveband categories with correspondence to their respective causes.

- Short wavelengths with faults ranging between 50 mm to 2 m: The defect is associated with the rail shape such as hogged ends, alignment kinks, corrugation and imprecise welds.
- Medium wavelengths with faults between 2 m and 25 m: The defect is caused by various factors such as degradation of ballast, environment, traffic operations and joints in the rails.
- Long wavelengths with faults ranging between 25 m and 125 m: The defect is typically caused by the settlement of embankments, long-term ground movements and possibly due the inadequate original construction.

For the purpose of analysis, the utilized track irregularities in the horizontal and vertical plane are based on the 10 m chord length measurement (with no specified wavelength interval).

Figures 5.10 to 5.28 provide the results of the coherence analysis among various track geometry parameters with a 95% confidence limit.

The coherence between the left and the right longitudinal profile irregularity is given in Figure 5.10. A significant coherence is shown for wavelengths longer than 6 m, as the coherence curve is higher than the 95% confidence level. In the short wavelength irregularities, there are periodic waves appearing at 3 m, 2.5 m and 1.5 m, which confirm the similar evidences found by Li and Lian [2011]. Furthermore, they argued that these waves could be induced during the rail straightening process.

Figure 5.11 gives the coherence relationship between the left and the right alignment irregularity. The coherence for wavelengths longer than 66 m is close to one, which is indicative of a significant relationship between the two rails. As the wavelengths get shorter, the coherence becomes lower and the relationship of two rails is more independent. However, there is a noticeable peak at the 5 m wavelength. According to Rao [1992], traffic and environment could be the main sources of the fault in this particular wavelength.

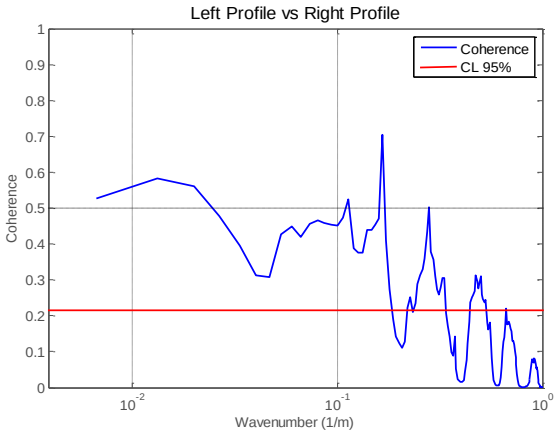

Figure 5.10 – Left and Right Longitudinal Profile

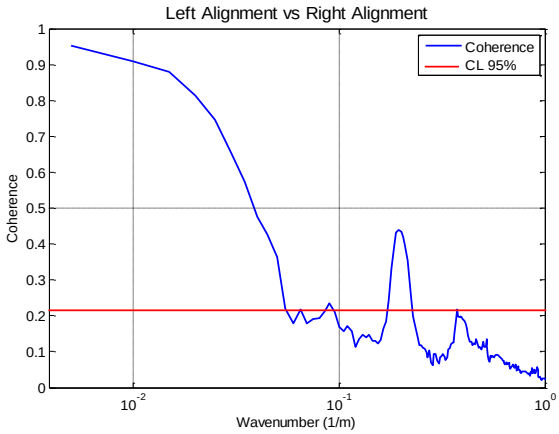

Figure 5.11 – Left and Right Alignment

Figures 5.12 and 5.13 present the coherence between track longitudinal profile and alignment for the left and the right rails, respectively. The coherence is close to zero at all wavelengths, with an average value lower than 0.2. Therefore, there is no evidence of a relationship between longitudinal profile and alignment irregularities. An increase in longitudinal profile variations will not bring an increase to the magnitude of alignment.

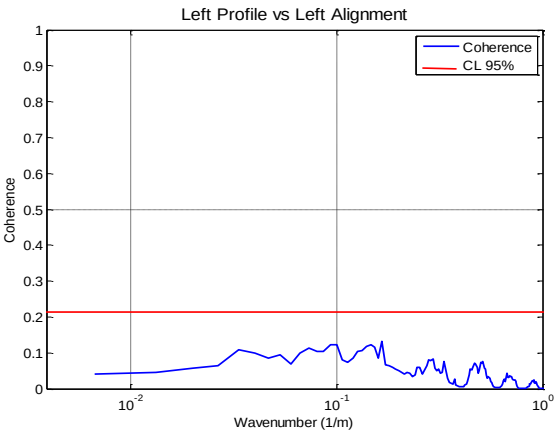

Figure 5.12 – Left Profile and Left Alignment

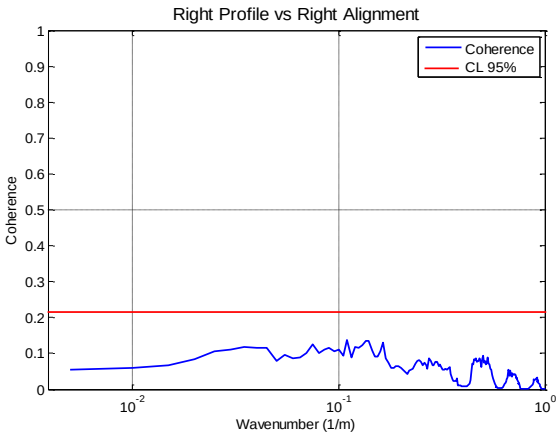

Figure 5.13 – Right Profile and Right Alignment

Figures 5.14 and 5.15 illustrate the coherence plot between gauge and single rail longitudinal profile of the left and the right rails, respectively. It can be seen that there is no significant coherence at all wavelengths since the curve is entirely below the 95% confidence limit. The lower value of coherence thus indicates the independency of longitudinal profile in relation to alignment irregularities and vice-versa.

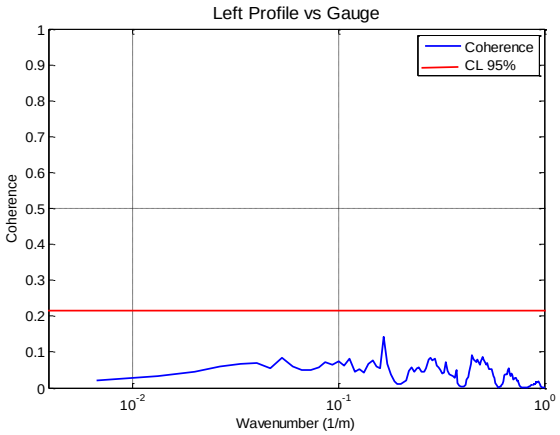

Figure 5.14 – Left Profile and Gauge

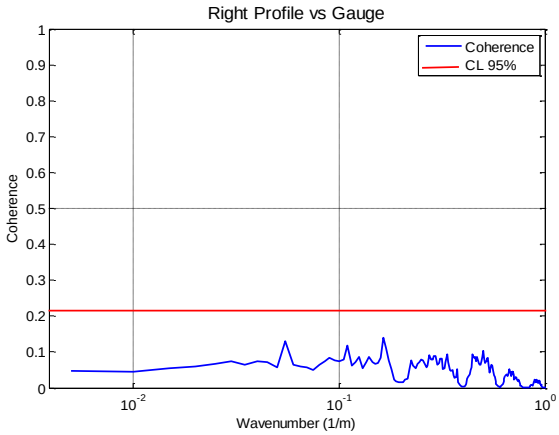

Figure 5.15 – Right Profile and Gauge

Figures 5.16 and 5.17 provide the coherence between super-elevation and single rail longitudinal profile. A slightly stronger relationship is found within the wavelength range between 6 and 30 m, with higher magnitude of coherence on the left rail than on the right. Rao [1992] argued that the faults in this waveband could result from traffic operation. It should be noted that there are also some periodicities at wavelengths of 2.7 m, 2 m, and 1.5 m that might have been induced during the rail straightening process.

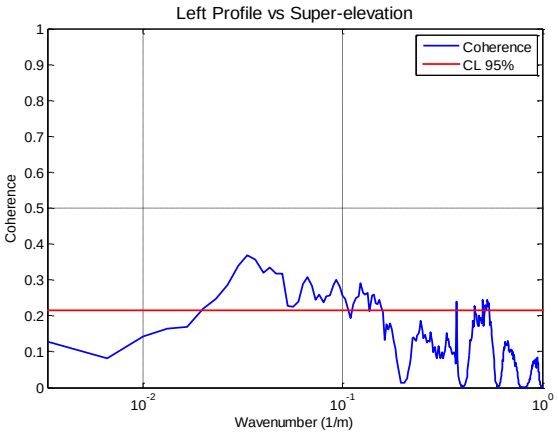

Figure 5.16 – Left Profile and Super-elevation

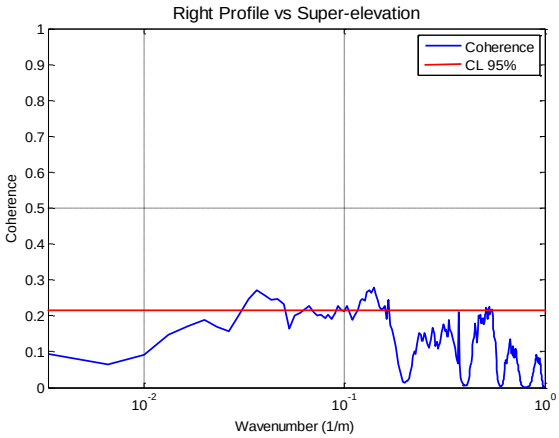

Figure 5.17 – Right Profile LD and Super-elevation

Figures 5.18 and 5.19 present the coherence between twist and longitudinal profile irregularities of the left and the right rails, respectively. A slightly stronger relationship is evident in the wavelength range between 6 and 30 m, similar to the wave found in the previous coherence plot of longitudinal profile and super-elevation. Periodicities can also be found at the wavelengths of 1.9 and 2.6 m, although not very significant.

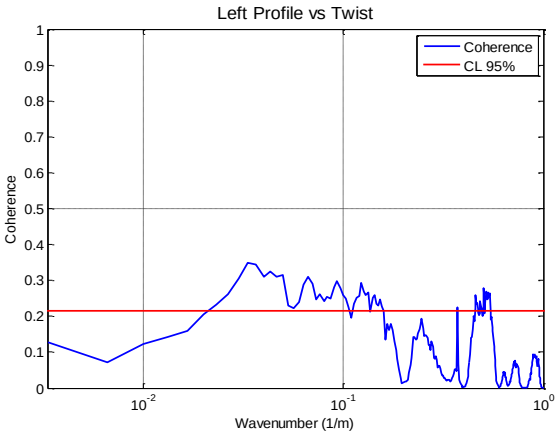

Figure 5.18 – Left Profile and Twist

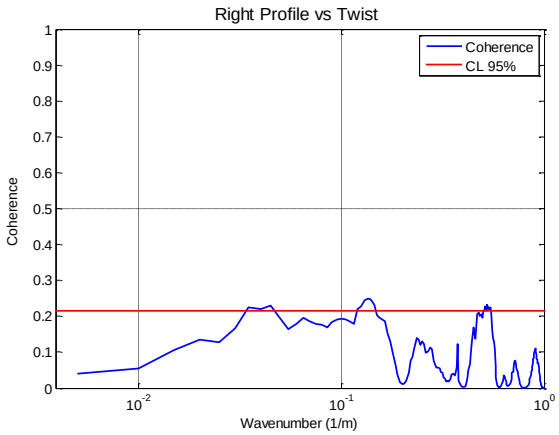

Figure 5.19 – Right Profile and Twist

The coherence relationships between super-elevation and single rail alignment, for both the left and the right rails, are given in Figures 5.20 and 5.21, respectively. Both figures indicate the similar trends in term of waveband and wave magnitude. At all wavelengths

shorter than 5.5 m, the coherence values are close to zero with general magnitudes lower than 0.1. A slightly stronger relationship is then observed at a waveband between 7.4 m and 10.5 m, which is possibly caused by traffic operations, joints in the rail or the environment.

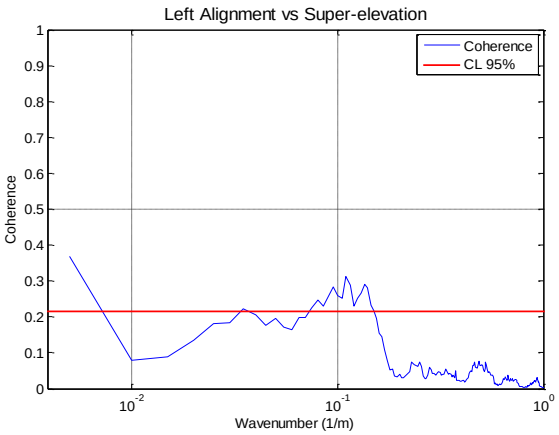

Figure 5.20 – Left Alignment and Super-elevation

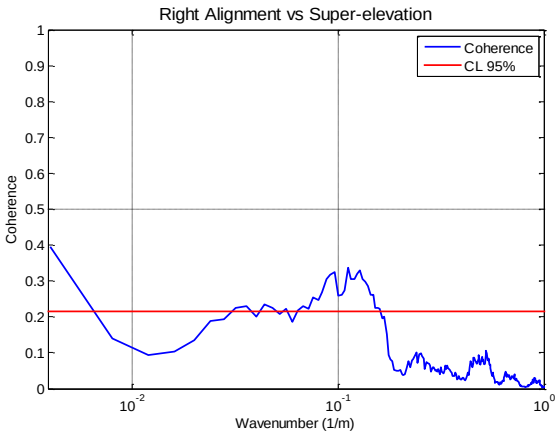

Figure 5.21 – Right Alignment and Super-elevation

Figures 5.22 and 5.23 present the coherence between single rail alignment and twist irregularities. Each figure consists of the investigation for the left and the right rails. The characteristic patterns of the coherence between alignment and twist are almost similar to those observed in the previous figures (alignment and super-elevation). At a certain wavelength range, from 7.4 to 10.5 m, the coherence exhibits a slightly stronger relationship in both the left and the right rails. For wave irregularities shorter than 5 m, no remarkable wavelengths could be found. The average of nominal value is also lower than 0.1.

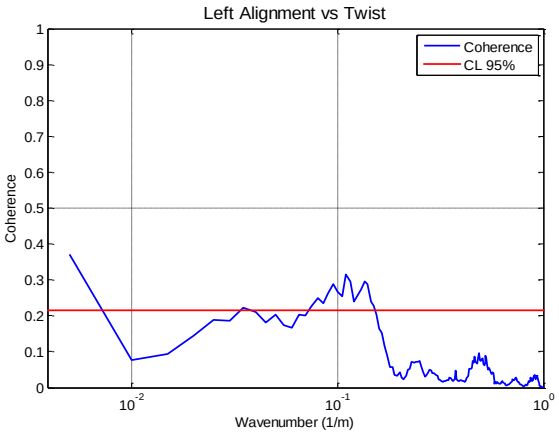

Figure 5.22 – Left Alignment and Twist

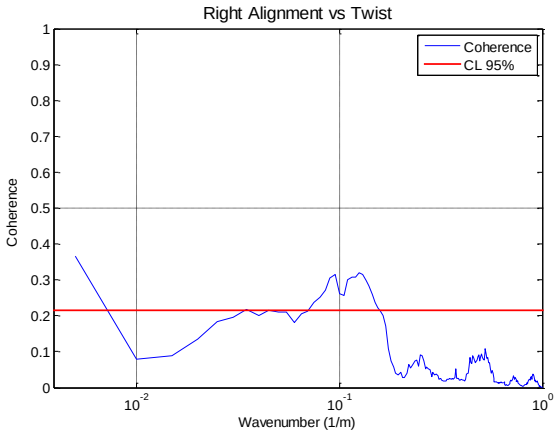

Figure 5.23 – Right Alignment and Twist

Figures 5.24 and 5.25 show the coherence between gauge and single rail alignment of the left and the right rails, respectively. A significant coherence is observed at the wavelength band between 6.2 and 15 m, as the coherence curve is higher than the 95% confidence level. Some noticeable periodicities are also detected at wavelengths of 3.6 m and 2 m, which could have been induced during the rail straightening process.

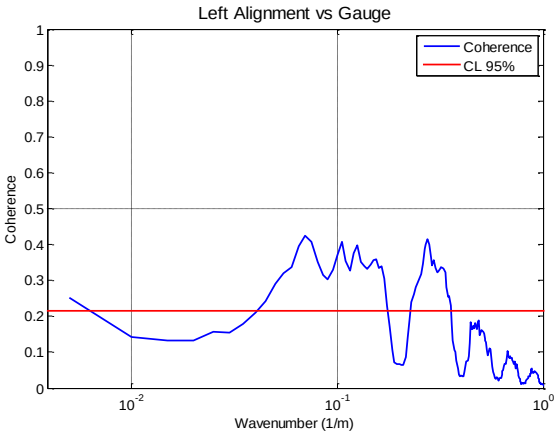

Figure 5.24 – Left Alignment and Gauge

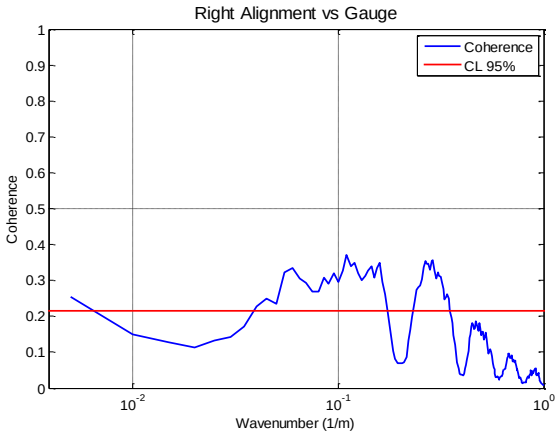

Figure 5.25 – Right Alignment and Gauge

Figure 5.26 gives the coherence between the irregularities of super-elevation and gauge variables. The coherence is significantly low over the wavelength range, as it yields magnitudes below 0.1. A similar result was also obtained in Figure 5.27, which presents the relationship between twist and gauge irregularities. Such results thus indicate the independency of irregularities among the investigated variables.

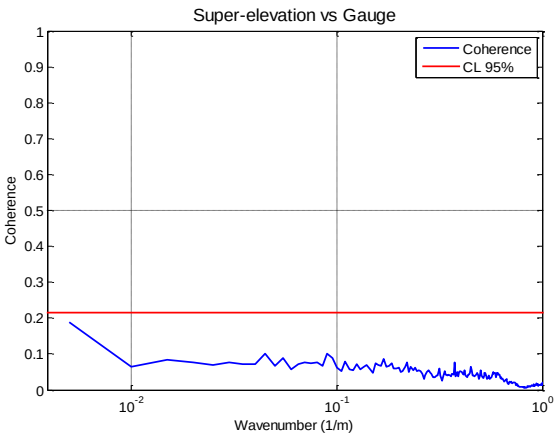

Figure 5.26 – Super-elevation and Gauge

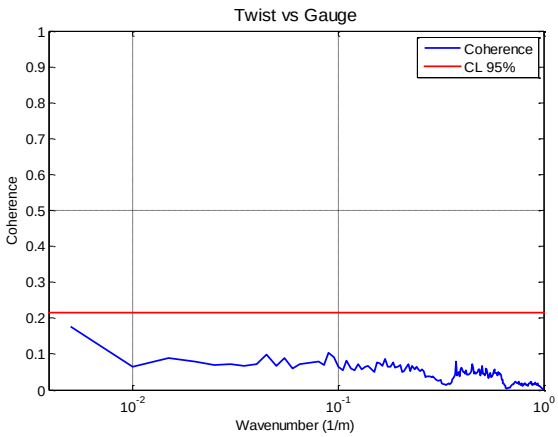

Figure 5.27 – Twist and Gauge

The coherence between super-elevation and twist variables is given in Figure 5.28. At the wavelengths longer than 6 m, the coherence values are close to one which is indicative of the dependency of the defects of one variable on the other. There is also a peak value identified above the 95% confidence level at a wavelength around 2.2 m. However, as the wavelengths decrease, the coherence between these two geometry variables is becoming more or less independent.

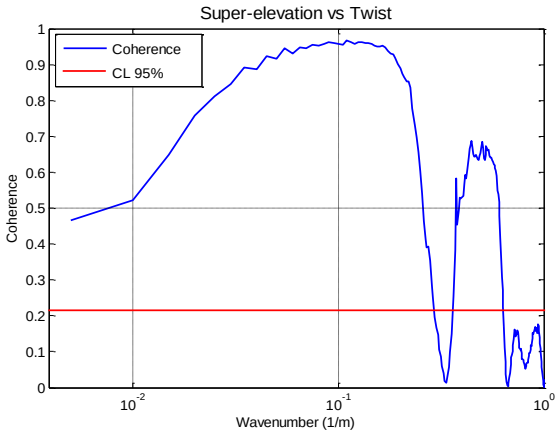

Figure 5.28 – Super-elevation and Twist

Table 5.2 presents the summary of the coherence analysis among track geometry parameters on the particular segment under investigation. It contains the typical prominent wavelengths shared between two geometry datasets. From the analysis, it can be noticed that the most detrimental wave of track geometries is found at a wavelength band between 6 and 30 m. Rao [1992] listed some possible factors that may contribute to defects in this particular waveband, such as traffic operation, environment, joints in the rail, etc.

Table 5.2 – Summary of the coherence analysis

Geometry Variables	Niv. LE	Niv. LD	Align E	Align D	Super-elevation	Twist	Gauge
Niv. LE	-	> 6 m	-	-	6– 30 m*	6– 30 m*	-
Niv. LD	> 6 m	-	-	-	6 – 27 m*	6– 30 m*	-
Align E	-	-	-	> 66 m	7– 10 m*	7– 10 m*	6 - 15 m[a]
Align D	-	-	> 66 m	-	7– 10 m*	7– 10 m*	6 - 15 m[a]
Super-elevation	6– 30 m*	6 – 27 m*	7– 10 m*	7– 10 m*	-	> 6 m	-
Twist	6– 30 m*	6– 30 m*	7– 10 m*	7– 10 m*	> 6 m	-	-
Gauge	-	-	6–15 m*	6–15 m*	-	`-	-

**) not significant*

5.3.3 AUTO-CORRELATION

Autocorrelation describes the general dependency of values of some observations at a certain distance (x) to the values of the same observations at another distance ($x + \tau$), where τ is defined as the lag distance between two observations (see Equation 5.2). This function can detect the presence of repetitive pattern or periodicity in a given dataset, which in turn is useful for determining the condition of railway track geometry [Zhiping and Shouhua, 2009].

In this current analysis, the autocorrelation has been applied on various track geometry parameters, such as longitudinal profile, alignment, super-elevation, twist and gauge. For the first two variables, autocorrelation was computed separately for the left and the right rails which corresponding to the wavelength irregularities between 3-25 m. The sample data was obtained from the inspection campaign in January, 2009 with the approximate length of 34 km track section. The autocorrelation is then imposed to the track segment based on the window size of 1024 data points and the results are averaged to obtain the final autocorrelation values. Taking a 100 m long segment as an example, the characteristics pattern of the autocorrelation curve for each track geometry parameter is given in the following figures.

Figures 5.29 and 5.30 show the auto correlations of track longitudinal profile and alignment irregularity, respectively.

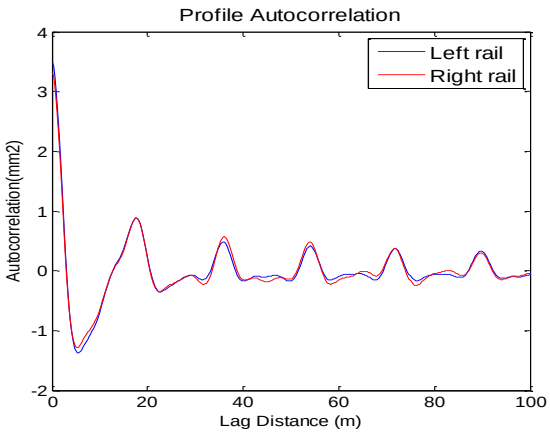

Figure 5.29 – Longitudinal Profile autocorrelation - January, 2009

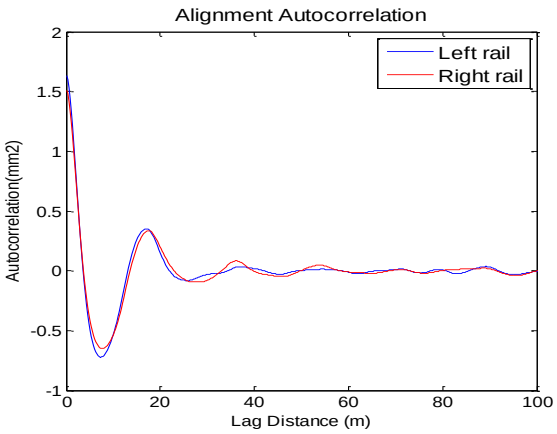

Figure 5.30 – Alignment autocorrelation - January, 2009

Based on Figure 5.29, the autocorrelation curves produced by the irregularity of the left and the right longitudinal profile are quite similar and close. Several spikes are remarkable and observed at the same lag distances, which informs that the track irregularity signals between the two rails are lined up and matched at some points. Both of the rails also have uniform defects with identical wave periodicities. Note that the magnitudes of periodicities are higher for the shorter lags and predominantly decrease as lags increase. The correlations of track irregularity are therefore higher for near track distances.

The autocorrelation of track alignment irregularities is given in Figure 5.30. It can be seen that both of the curves have the same peak and wave shape, indicating that the irregularities of the left and the right rails are fairly similar. A remarkable periodic wave is also observed at a lag distance of 18 m, which might be caused by various factors such as degradation of ballast, environment and traffic operations [Rao, 1992]. This finding also clearly shows the existence of a correlation of the left and the right rail at a certain wavelength.

Figures 5.31 and 5.32 present the autocorrelation curves of super-elevation and twist, respectively. Based on Figure 5.31, the only highest peak occurs at zero lag distance, and then decreases towards zero afterwards. This trend justifies the lack of correlation between super-elevation and the shifted distance of super-elevation (itself). On the other hand, twist shows similar characteristics with the autocorrelation of track longitudinal profile. Several spikes are identified in the middle of the graph, which points out that at some points, the signals are lined up and matched with each other.

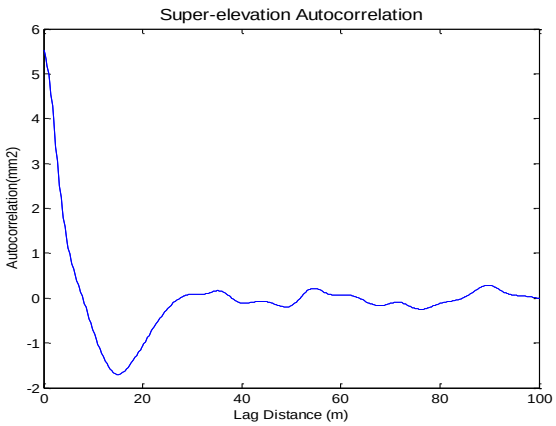

Figure 5.31 – Super-elevation Autocorrelation - January, 2009

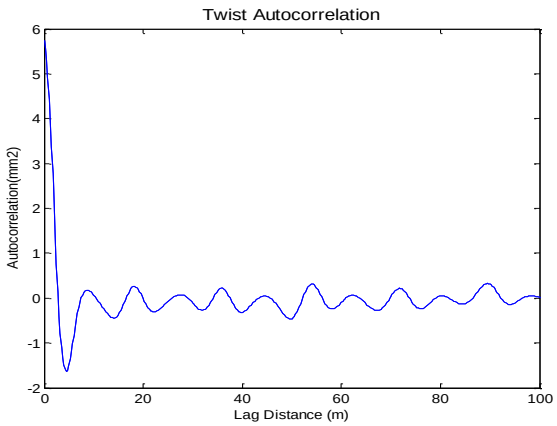

Figure 5.32 – Twist Autocorrelation - January, 2009

Figure 5.33 presents the autocorrelation of gauge irregularity. This autocorrelation has nearly zero memory, which means that the value at shifted distance x is independent of the value at other points. It is hard to find the similarity between the waveforms, since the peak is only observed at zero lag distance.

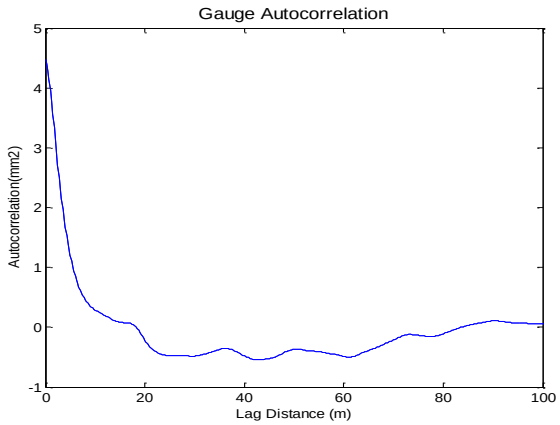

Figure 5.33 – Gauge autocorrelation - January, 2009

Different autocorrelation analysis has been conducted to the other inspection campaigns. As a matter of fact, the analysis was exposed the similar curve evidence, for example on the data in March, 2008. Figures 5.34 to 5.38 present the autocorrelation analysis for different track geometry parameters, taking a 100 m long segment as an example.

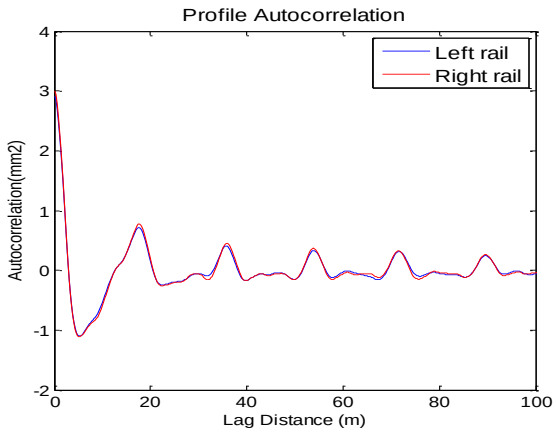

Figure 5.34 – Longitudinal Profile autocorrelation - March, 2008

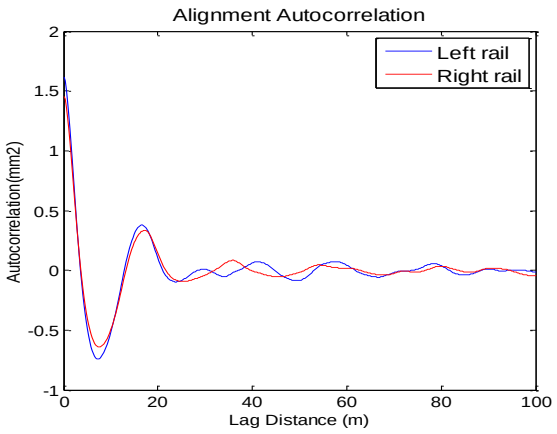

Figure 5.35 – Alignment autocorrelation - March, 2008

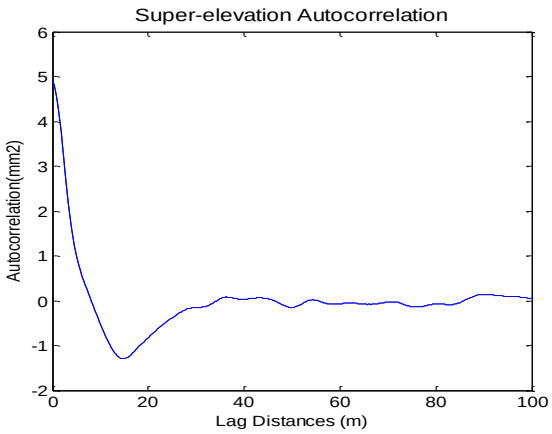

Figure 5.36 – Super-elevation Autocorrelation - March, 2008

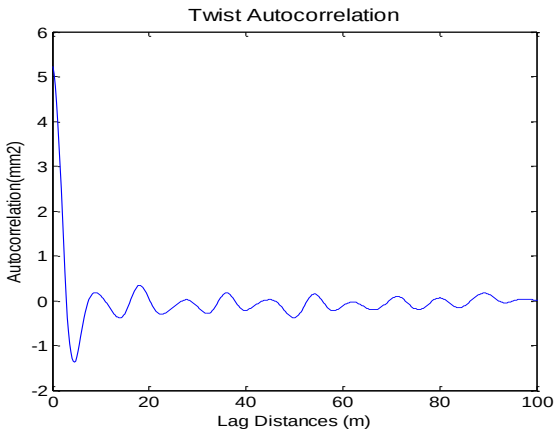

Figure 5.37 – Twist Autocorrelation - March, 2008

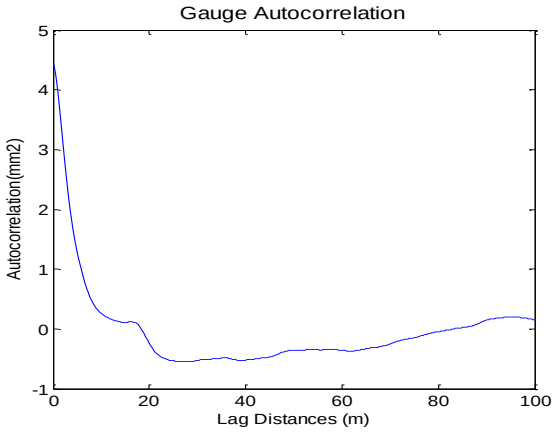

Figure 5.38 – Gauge autocorrelation - March, 2008

According to the figures, the autocorrelation curves produced by the irregularity of the left and the right rails are fairly similar, in both the track longitudinal profile and the alignment, which shows the existence of a correlation of both rails at a certain wavelength. In the autocorrelation of super-elevation and gauge, the peak is only observed at zero lag distance and is decreased towards zero as the number of lags increases. Twist exposes several spikes in the middle of the graph, which indicates a good sign of track quality.

5.4 CONCLUSIONS

The relationship analyses were conducted to quantify the degree of interdependency and to establish the statistical correlation among various track geometry variables. A typical track section in Portugal with the approximate length of 34 km has been used and the degree of association between variables has been calculated. The analyses were performed in the wavelength domain using three different approaches: cross-correlation, autocorrelation and coherence analysis.

From the three methodologies used in the analyses, the relationship of various track geometries can be best described by cross-correlation and coherence functions. The autocorrelation was found to be useful to assess the rail track quality by identifying the periodicity and pattern of the irregularity signals. However, the three methods generally provided similar relationship tendencies. For example, a very good and strong coherence between two sets of geometry will yield a higher value of cross-correlation.

From the analysis results, it shows that some track geometry variables are closely related. A defect on a particular track geometry variable may strongly impact, either positively or negatively, the others. A typical wavelength is also outlined especially at a waveband between 6 and 30 m. A detailed analysis for each variable will be subsequently discussed.

The strongest positive relationship is observed between the left and the right rails, for both longitudinal profile and alignment. The cross-correlation of the longitudinal profile of both rails is 0.66 while for the alignment is 0.89, which indicates that if one variable decreases, the other variable also decreases and vice-versa. According to Table 5.7 (coherence table), the variations in the left and the right longitudinal profile are similar for wavelengths above 6 m, as the coherence curve is higher than the 95% confidence level. For shorter wavelengths, there are periodic waves appearing at 3 m, 2.5 m and 1.5 m that might have been induced during the rail straightening process. Meanwhile, the alignment exhibits a strong relationship for wavelengths longer than 66 m and decreases

for shorter wavelengths. A noticeable periodic peak is also observed especially at the 5 m wavelength.

Medium correlations are further revealed between super-elevation and twist, and between track alignment and gauge. The average coefficients for each of these are 0.46 and 0.47, respectively. Cross level or superelevation irregularity defines the amount of vertical deviations between the levels of two rails from their design value. Twist, on the other hand, measures the difference in the super-elevation between two points taken at a separate fixed distance. The existing correlation between these two parameters is possibly due to the tie connection on the measurements as described above. According to the coherence table, the most detrimental waves between twist and super-elevation can be found at wavelengths longer than 6 m with values close to one. This means that, at these particular waves, an increase on twist irregularity may imply an increase on the magnitude of super-elevation. Similarly, the coherence analysis between single rail alignment and gauge shows stronger relationships at some discrete wavelengths typically between 6.2 and 15 m. Although the correlation values are not sufficiently significant, it can be attested that there is some level of relationship between these track geometry parameters.

There are low correlations between the irregularities of track longitudinal profile and twist, and track longitudinal profile and super-elevation, which can be perceived in both methods: cross-correlation and coherence. Analyses also show the independency of variations between longitudinal profile and alignment, super–elevation and gauge, twist and gauge, and longitudinal profile and gauge.

In correspondence with curvature, there exists a correlation between curvature and gauge variables, which magnitude varies depending on the track layout. The higher the curvature, the larger the correlation will be and vice-versa. Note that the correlation between curvature and gauge can be either positive or negative and it can vary from low to high. The strongest positive correlations are shown between curvature and alignment for both the left and the right rails, with an average correlation around 0.85. The

correlation is quite high in the segment where the curvature is large and lowers where the curvature is small. For the correlation between curvature and the other track geometry variables (super-elevation, twist and longitudinal profile), it is known that the influence of curvature is not significant.

Further analyses show that the autocorrelation curves produced by the irregularity of the left and the right rails are quite similar, in both the track longitudinal profile and the alignment. Several spikes are clearly observed at the same lag distances, which is indicative that the track irregularity signals between the two rails are lined up and matched at some points. Both of the rails also have uniform defects with identical wave periodicities. Note that the magnitude of periodicities is higher for the smaller lags and tends to decrease as lags increase. The correlations of track irregularity are therefore higher for near track distances. A similar pattern of periodicities can also be found in the autocorrelation of twist.

On the other hand, the opposite result is observed for the autocorrelation of the gauge and the super-elevation. It is hard to find the similarity between the waveforms, since the peak is only observed at zero lag distance. Afterwards, the autocorrelation curve decreases towards zero as the number of lags increases.

6

THE APPLICATION OF AN OPTIMIZATION MODEL FOR TRACK MAINTENANCE

6.1 INTRODUCTION

In order to ensure the safety and continued operation of a railway network system, Infrastructure Managers (IMs) are responsible for planning and organizing all the rail maintenance actions. The implementation of these tasks can be achieved by applying a specific method and appropriate instruments of project control, which may reduce the maintenance cost in a finite time horizon.

This chapter outlines the fundamental concept of the optimization model designed to achieve the stated objectives. It consists of the analysis of track quality evolution on a stretch of a Portuguese railway section, supplemented by assessments of quality improvement due to the maintenance actions. The results are applied to solve the maintenance scheduling problem in a given track with respect to certain constraints. Finally, the model is validated with some evaluation criteria to test how effective and accurate the prediction compares to the actual data.

As this research sees the degradation of track geometry through two different perspectives, TQI and PSD, the relationship between these two methods is therefore

investigated. Such relation may facilitate a deterioration model based on the assessment of statistical analyses (TQI) and PSD.

6.2 THE RELATIONSHIP BETWEEN POWER SPECTRAL DENSITY (PSD) AND TRACK QUALITY INDEX (TQI)

In the previous section, it was described how TQI and PSD may assess the actual change in track geometry behavior. TQI can provide the characterization of track quality by calculating the standard deviation for each geometry variable while PSD carries more information concerning the frequency content of the track geometry defect. Both of these approaches, in fact, do not stand independently. The square root of the area under PSD is recognized to be equal to the standard deviation of stationary random irregularity [Jianbin and Songliang, 2009]. Detailed analysis concerning the relationship between TQI in terms of standard deviation and PSD was carried out to verify this theory.

The track quality index developed by the European Standard deals with the utilization of several track geometry variables as the main performance criteria. This index relies on the implementation of standard deviation over a 200 m segment. Moreover, the specification of geometry irregularities with wavelength domain in the range of 3 m < λ $\leq$ 25 m is another required parameter to be calculated in the standard deviation.

The European Standard TQI formula is given by:

$$\sigma_i = \sqrt{\frac{1}{N_i}\sum_{k=1}^{N_i}\left(x_{k,i} - \mu_i\right)^2} \tag{6.1}$$

where:

σ_i = standard deviation of the track geometry variable (mm)

i = track geometry of longitudinal profile or alignment (-)

N_i = the number of measurements of profile or alignment in the track section

$x_{k,i}$ = value of longitudinal profile or alignment parameter at point k (mm)

μ_i = average value of signal of longitudinal profile or alignment (mm)

k = point of measurement (mm)

On the other hand, to derive the power spectrum graph, the geometry irregularity should be transformed from the spatial-based domain to the wavenumber-based domain using a corresponding algorithm, called Fourier Transform. Then, by multiplying the Fourier transform of the wavenumber by its conjugate, the PSD is obtained [Naser and Toledano, 2011]. The unit of the PSD is $G^2 \,/\, Hz$ in the frequency-based domain or $[mm]^2 \,/\, k$ in the wavenumber-based domain, where $k = {}^1/_{\lambda}$. It represents the squared value of the Fourier Transform or FFT.

A bilateral spectrum of PSD is given by following formula:

$$S_x = FFT(k) \cdot FFT(k)^* \qquad S_x = \int_{-\infty}^{\infty} |F(k)|^2 \, dk \tag{6.2}$$

where $F(k)$ represents the Fourier transform of a continuous waveform registered in the segment. A bilateral power spectrum displays half the energy at the positive wavenumber and the other half at the negative frequency. To convert a bilateral spectrum to a unilateral or single-sided spectrum, the second half of the array should be disregarded and all the wavenumber points must be multiplied by a factor of 2 except for zero (DC) and the Nyquist. Equation 6.3 gives indication on how to compute the single sided power spectrum.

$$G_{kk}\begin{cases} 2S_x(k) & \Leftarrow \quad 0 < k \leq k_c - 1 \\ S_x(k) & \Leftarrow \quad k = 0 \; and \; k = k_c \\ S_x(k) & \Leftarrow \quad k = 0 \; and \; k = k_c \end{cases} \tag{6.3}$$

where S_x is defined as a bilateral spectrum and k_c expresses a cutoff wavenumber.

6.2.1 THE CORRELATION BETWEEN POWER SPECTRAL DENSITY (PSD) AND TRACK QUALITY INDEX (TQI)

The spatial and wavenumber domains are related in two different ways. First, the relationship can be represented through the use of Fourier Transform, which refers to the process to transforming one function into the other.

Provided that $f(x)$ is a continuous waveform in the spatial domain, the transformation from spatial-based to wavenumber-based domain is given by:

$$F(k) = \int_{-\infty}^{\infty} f(x) \cdot e^{-j2\pi kx} dx \tag{6.4}$$

And the inverse of the Fourier transforms is:

$$f(x) = \int_{-\infty}^{\infty} F(k) \cdot e^{j2\pi kx} dk \tag{6.5}$$

where:

$F(k)$ = continuous Fourier transform

$f(x)$ = continuous spatial-domain waveform

k = analysis wavenumber, where $k = {}^{1}/_{\lambda}$ and λ is wavelength

x = distance

The second relationship is obtained through the implementation of Parseval theorem, which states that the sum (or integral) of the square of a function is equal to the sum (or integral) of the square of its transform [Henriksson, 2003]. This statement is clearly described by:

$$\int_{-\infty}^{\infty} |f(x)|^2 \, dx = \int_{-\infty}^{\infty} |F(k)|^2 \, dk \tag{6.6}$$

which can also be given by:

$$\int_{-\infty}^{\infty} f_1(x) \cdot f_2(x) \, dx = \int_{-\infty}^{\infty} F_1(k) \cdot F_2(k) \, dk \tag{6.7}$$

If $F_1(k)$ is defined as the Fourier transform of $f_1(x)$, thus:

$$\int_{-\infty}^{\infty} f_1(x) \cdot f_2(x) \, dx = \int_{-\infty}^{\infty} \left[\int_{\infty}^{\infty} F_1(k) \cdot e^{j2\pi kx} dk \right] f_2(x) \, dx \tag{6.8}$$

$$\int_{-\infty}^{\infty} f_1(x) \cdot f_2(x) \, dx = \int_{-\infty}^{\infty} \left[F_1(k) \cdot \int_{-\infty}^{\infty} e^{j2\pi kx} dk \right] f_2(x) \, dx \tag{6.9}$$

$$\int_{-\infty}^{\infty} f_1(x) \cdot f_2(x) \, dx = \int_{-\infty}^{\infty} F_1(k) \left[\int_{-\infty}^{\infty} f_2(x) \cdot e^{j2\pi kx} dx \right] \, dk \tag{6.10}$$

The factor in the bracket is defined as Fourier transform, $F_2(-k)$, and corresponds to the conjugate of function $F(k)$. Since $f_1(x) = f_2(x)$ and $F(-k) = F^*(k)$ thus:

$$\int_{-\infty}^{\infty} f^2(x) \, dx = \int_{-\infty}^{\infty} F_1(k) \cdot F^*(k) \; dk \tag{6.11}$$

$$= \int_{-\infty}^{\infty} |F(k)|^2 \; dk \tag{6.12}$$

The square of the magnitude of the Fourier transforms is also known as Power Spectral Density (PSD), containing the signal energy density within a given wavenumber band. The unit of PSD is energy per wavenumber.

The variance of a continuous spatial domain gains from the squared value of the variations around the mean, which is given by:

$$Variance = \int_{-\infty}^{\infty} |f(x) - f_{mean}|^2 \, dx \tag{6.13}$$

thus, for a spatial waveform with zero mean, the variance will be equal to the power in the time domain, and hence will also be equal to power spectral density. By defining variance as the square of standard deviation, the relationship between SD and PSD can be described by the following equation:

$$TQI_{Europ\ Std} = \sigma = \sqrt{\left(\int_{-\infty}^{\infty} |F(k)|^2 \, dk \right)} \tag{6.14}$$

Therefore, the standard deviation of a stationary random waveform is equal to the square root of the area under the power spectral density. The implementation of the trapezoidal formula should then be used for solving the integration within this area.

Figure 6.1 provides a side by side comparison between the square root of the total area under PSD curve and the standard deviation of track geometry data for both track longitudinal profile and alignment variables. It contains results from 17 measurement surveys within 1926 consecutive days.

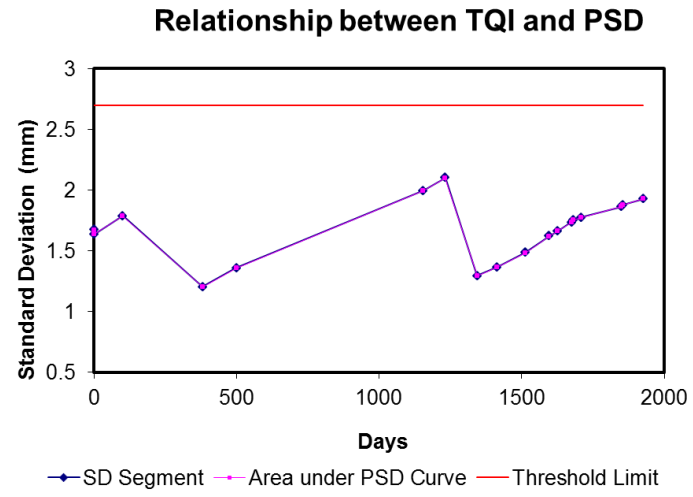

a) Track longitudinal Profile

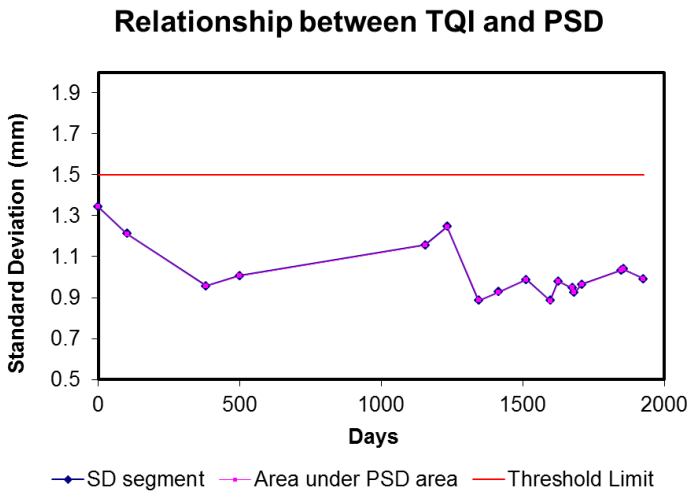

b) Track Alignment

Figure 6.1 – Relationship Analysis Between PSD and TQI

According to Figure 6.1, the standard deviation values of track irregularity are extremely close to the square root of the area under the PSD curve. This evidence is thus validating the existence of a relationship between PSD and track quality index, and confirming the applicability of the area under the frequency spectrum as an indicator of railway track quality.

6.2.2 IMPLEMENTATION OF TRAPEZOIDAL FORMULA TO PSD STANDARDS

Using the method as described in the preceding section, the areas under the curve of various PSD standards were calculated. This PSD should be associated with short wavelength defects (3-25 meters), in order to comply with the pre-requisite wavelengths in prEN 13848-5.

Tables 6.1 to 6.3 present the estimation results for US FRA, German and Chinese PSD respectively. Each table provides the area under the spectrum for both longitudinal profile and alignment.

Table 6.1 – Areas under spectrum for PSD FRA

PSD FRA	PSD Trapz	
	Longitudinal Profile	Alignment
1	8.54	14.23
2	7.83	8.54
3	6.40	4.98
4	5.69	4.27
5	3.55	2.14
6	1.42	1.42

Table 6.2 – Areas under spectrum for PSD Germany

PSD German	PSD Trapz	
	Longitudinal Profile	Alignment
Low Disturbance	0.98	0.71
High Disturbance	1.60	1.21

Table 6.3 – Areas under spectrum for PSD China

PSD China	PSD Trapz					
	Longitudinal Profile			Alignment		
	Upper	General	Lower	Upper	General	Lower
200 km/h	2.35	1.22	0.84	2.07	1.09	0.77
160 km/h	4.07	2.12	1.14	3.27	1.72	0.94
120 km/h	4.73	2.75	1.63	4.01	2.31	1.37

As a matter of fact, different PSD standards specify the track quality under different conditions. PSD FRA and PSD China consider line speed as the main indicator for track quality, while PSD German distinguishes track quality based on two levels of disturbance.

Track classes 1 to 6 in PSD FRA are designed for line speeds from 24 km/h up to 177 km/h. In Table 6.2, although the speed line is not cited in the PSD German, it is recognized that the German railway network serves for train speeds up to 300 km/h, either in upgraded or newly constructed lines. Furthermore, the lower and upper bound in PSD China define the range of track quality commonly observed.

6.3 Optimization Model for Track Maintenance

This section describes the selected optimization method to minimize the number of maintenance operations required in a given track segment. For this purpose, the quality limit defined in the European Standard and the proposed PSD limits are utilized as the main prerequisite to demand tamping. The preference for the use of these limits may allow us to determine the suitability of track quality in terms of either Track Quality Index or Power Spectral Density.

6.3.1 CHARACTERISTICS OF THE PORTUGUESE RAILWAY TRACK SAMPLE

The sample analysed in this study belongs to the Portuguese Northern Line, which connects the two biggest cities of Portugal, from the central city of Lisbon to Porto. The network has a total length of about 337 km and is subjected to mixed traffic, with passenger trains running at a maximum speed of 220 km/h and freight trains at a maximum speed of 80 km/h. This line has experimented reconstruction in the last few years, with the replacement of the track-bed, to increase its bearing capacity, and track superstructure: new mono-block concrete sleepers spaced at 600 mm, rail UIC 60, vossloh fastening system, and plastic rail pad zw 687 (stiffness 450 kN/mm) [Andrade and Teixeira, 2011]. Figure 6.2 and Table 6.4 present a description of the sample segment in detail.

Figure 6.2 – Location of the Sample Track Segment in Portugal

Table 6.4 – Characteristics data of Sample Track Segment

Track Data Position	Start	End
	200+000.00	233+399.75
Length	33.4 km	
Design Speed	50 - 220km/h	
Track Geometrical Characteristics	Mixed line [Straight and Curve]	
Period of Investigation	2003-2009 (17 Measurement Files)	

In this analysis, the track data were collected from the Track Recording Car EM 120, which sampled the geometry variables once every 0.25 m. It provided up to 17 inspection campaigns, from October 2003 until January 2009.

Afterwards, the track segment was evaluated based on the following steps:

1. Synchronization of the measurement readings among numerous track inspection dates.
2. Discretization of railway lines to be 200 m long segments (recommended by prEN13848).
3. Analysis of the track quality of each segment.

6.3.2 SYNCHRONIZATION OF MEASUREMENT READINGS

Due to irregular rotation of the car wheel, the measurement files generated by the track recording car may change slightly in the actual position of sampling location. In such case, the only way to check the correctness and to correct the possible location error is by comparing the plots of the track rails in the surveys.

Thus, in order to synchronize the individual measurement readings, the data from two track geometry measurement surveys was used: one served as a reference, while the other was treated as a dataset to be shifted. Both data are then plotted in MATLAB and by performing a cross-correlation for the specified segment, the disparity on the distance between the two datasets is identified and then the adjustment process is carried out automatically. In order to ensure the appropriateness of the method and to examine the existence of any dead spots, the MATLAB DSP toolbox was also utilized during the process.

The formula of the coefficient correlation is expressed as follows:

$$r_k = \frac{\sum_{x=1}^{N-k}(s_x - \bar{s}) \cdot (s_{x+k} - \bar{s})}{\sum_{x=1}^{N}(s_x - \bar{s})^2} \tag{6.15}$$

where s_x is the data value at distance x, N is the number of measurements, k is the lag and the overall mean $\bar{s}$ is given by

$$\bar{s} = \frac{\sum_{x=1}^{N} s_x}{N} \tag{6.16}$$

After the synchronization, the start and end points of each track are identified and processed for further analysis. Figure 6.3 provides the sample results of the track adjustment between the two datasets, where January 2009 was taken as reference and April 2008 as shifted data. Figure 6.4 gives indications of the dead spots observed along the segment.

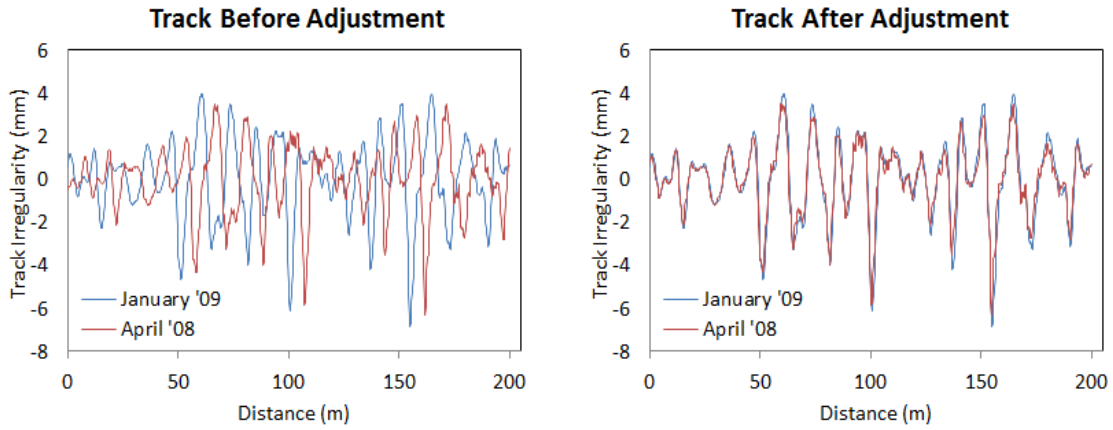

a) Before Adjustment b) After Adjustment

Figure 6.3 – Sample Before and After Track Adjustment at KM 200.00 – 200.200

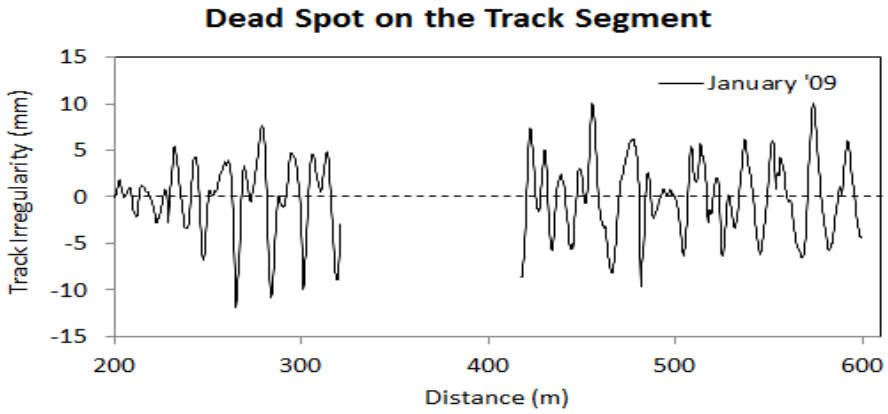

Figure 6.4 – Dead spots on track segment at KM 217.200 – 217.600

6.3.3 General Evolution of Track Geometrical Quality

A set of 167 track sections of 200 meter in length each and a series of 17 measurement records were examined to identify the quality evolution of each track segment over time. With a point spacing of 0.25 m, the analysis contained about 133,600 numbers of geometrical data values for each rail in each inspection campaign. Figures 6.5 and 6.6 give the standard deviation at the initial time instant for longitudinal profile and alignment, respectively. In each figure is incorporated the threshold values defined by the European Standard.

Since the square root area under PSD curve is identical to the standard deviation of the random signals, it can be assumed that the quality values obtained from STD are also appropriate to represent the track in terms of PSD. The comparison of track quality with the proposed PSD limit is given in Figures 6.7 and 6.8. The change in line speed throughout the entire segments is specified in Figure 6.9.

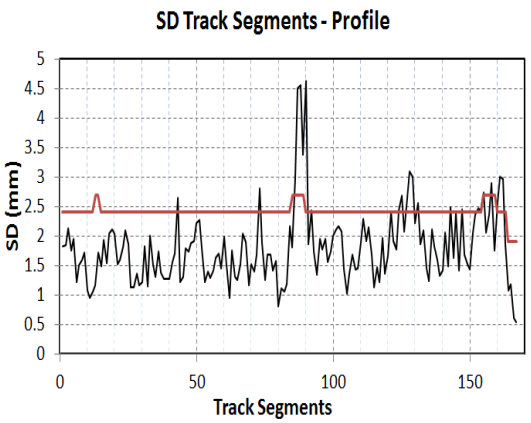

Figure 6.5 – SD of Longitudinal Profile at the initial time instant and European Standard limit – January 2009

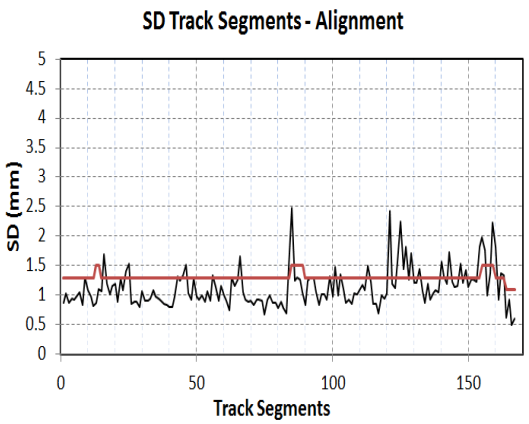

Figure 6.6 – SD of Alignment at the initial time instant and European Standard limit – January 2009

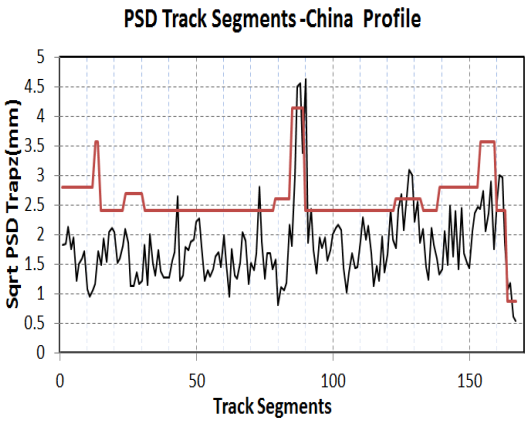

Figure 6.7 – PSD China of Longitudinal Level and PSD Chinese limit – January 2009

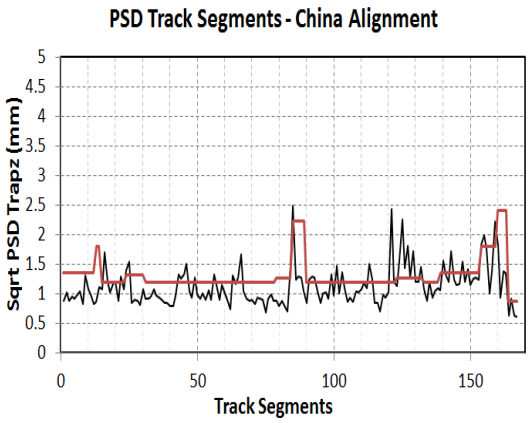

Figure 6.8 – PSD China of Alignment and PSD Chinese limit – January 2009

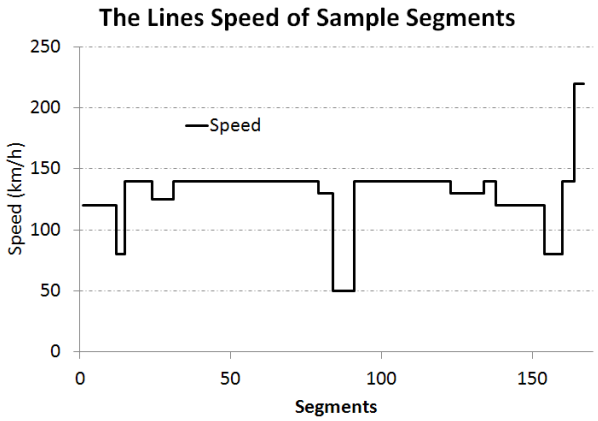

Figure 6.9 – Line speed of Track Segments

The identification of the line speed in the sample segments is as follows:

- Line speed of 50 km/h to 80 km/h: Segment 13-14, 85-89 and 155-159
- Line speed of 120 km/h to 140 km/h: Segments 1-12, 15-84, 90-154 and 160-163
- Line speed of 220 km/h: Segment 164-167

According to Figures 6.5 and 6.6, the SD for track longitudinal profile ranges from the lowest value of 0.55 mm up to the highest value of 4.6 mm, while the SD for alignments lies between 0.6 mm and 4.3 mm. The segments with the poorest quality were segments 85-89, with a line speed below 100 km/h.

Figures 6.7 and 6.8 present the track quality of segments compared to the Chinese PSD limits for longitudinal profile and alignment, respectively. In order to be comparable with the European Standard, a regression line is employed to PSD China limit values. Afterwards, the proposed new thresholds for other speed lines, which may not considered in PSD China, were obtained from extrapolation. The accuracy of the estimated value is measured by squared regression, which resulted in more than 95% in both the longitudinal profile and the alignment.

As mentioned before, the span in PSD China is ranging from lower, general and upper spectra, and its utilization may depend on the characteristics of the sample segments in use (see Table 6.3). In this analysis, it is decided to employ the allowable limits from the general spectrum of PSD China for the track longitudinal profile and the lower spectrum of PSD China for the alignment variable.

6.3.4 DEGRADATION RATE

Track geometry degradation is a complex process occurring under the influence of dynamic load. It is normally calculated as a function of traffic in mm/MGT or of time in mm/day [Esveld, 2001]. In terms of the time needed to deteriorate, the rate of track degradation varies from one section to the other even in the same line. Therefore, to clarify this situation, the change in quality of each track segments over time was analyzed, and then the degradation rate was calculated for each of them.

The present study attempts to define an equation describing the deterioration rate as a function of time, assuming that all other variables affecting the degradation remain unchanged. Figure 6.10 illustrates an example of quality evolution for longitudinal profile for the left and the right rails. The samples of track geometry data are obtained from the historical records from 2003 until 2009 (1926 days of measurements), which provided up to 17 inspection campaigns (see Table 6.4).

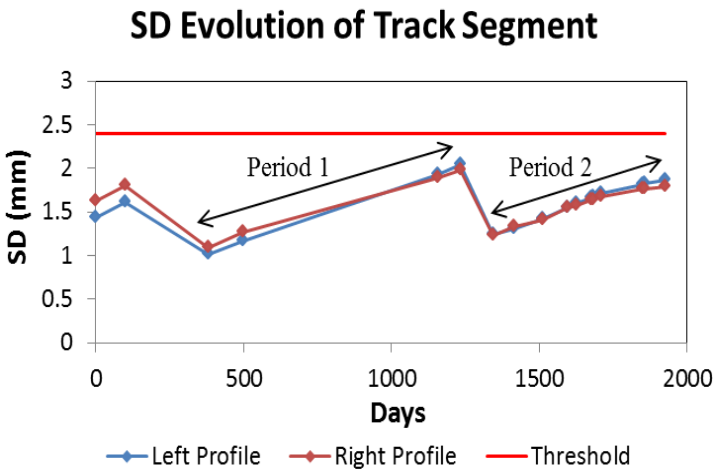

Figure 6.10 – The evolution of SD of track longitudinal profile for Segment 1 (KM 200.00-200.199)

Since the information concerning any maintenance and the exact time for renewal are not sufficient, the difference between inspection times was decided by identifying the discrepancy of index magnitude within the sequence of measurements. As a result, the first time interval is identified from the inspection of day 380 to day 1232, containing 4 inspection campaigns, while the second interval is started from day 1344 to day 1926, containing 11 inspection campaigns.

In fact, it is apparent that a linear relationship is generally good to capture the progress of defect in almost all track segments under study. The measure of the fit of the linear regression in period 2, using R^2, resulted on an average value of about 0.86 for the longitudinal profile (Table 6.5) and 0.67 for the alignment variable (Table 6.6), which are considerably high. The limitation in the number of inspection records is also one of the considerations for using this method.

The formula of linear regression is expressed as follows:

$$y = ax + \beta \tag{6.17}$$

where :

y = predicted value (mm)

a = degradation coefficient (mm/days)

x = independent variable (days)

β = constant parameter

The sample results of calculation are given in the following tables (see Appendix A and B):

n = number of measurements

R^2 = regression square

Table 6.5 – Degradation Rates of Track longitudinal Profile

Segments	Period 2 [Days 1344 - 1926]								Average Degrad. Rate
	Left longitudinal profile				Right longitudinal profile				
	a	β	n	R^2	a	β	n	R^2	
1	0.0011	-0.27	11	0.98	0.0010	-0.07	11	0.97	0.0011
2	0.0009	0.02	11	0.97	0.0012	-0.41	11	0.97	0.0011
…	…	…	…	…	…	…	…	…	
…	…	…	…	…	…	…	…	…	
166	0.0002	0.21	8	0.89	0.0001	0.36	8	0.49	0.0002
167	0.0001	0.30	5	0.98	0.0001	0.42	5	0.82	0.0001
Average				0.86	Average			0.85	0.001

Table 6.6 – Degradation Rates of Track Alignment

Segments	Period 2 [Days 1344 - 1926]								Average Degrad. Rate
	Left alignment				Right alignment				
	a	β	n	R^2	a	β	n	R^2	
1	0.0002	0.59	6	0.41	0.0003	0.20	9	0.70	0.0003
2	0.0008	-0.42	8	0.47	0.0007	-0.07	11	0.86	0.0007
…	…	…	…	…	…	…	…	…	
…	…	…	…	…	…	…	…	…	
166	0.0001	0.26	6	0.58	0.0001	0.22	8	0.34	0.0001
167	0.0002	0.27	5	0.84	0.0002	0.19	5	0.89	0.0002
Average				0.67	Average			0.67	0.0005

For the purpose of this study, the analysis will be focused on the second period due to the higher number of inspections dates (11 inspection campaigns). Figures 6.11 and 6.12 give the distribution of the degradation rate among the track segments for longitudinal profile and alignment, respectively.

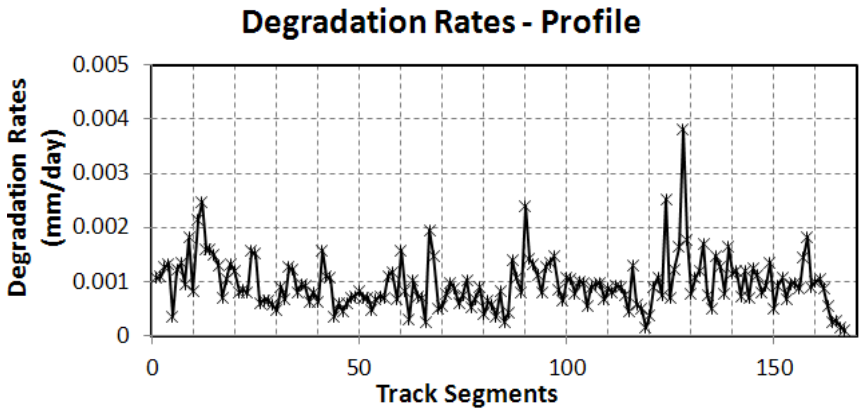

Figure 6.11 – Degradation Rate of longitudinal Profile

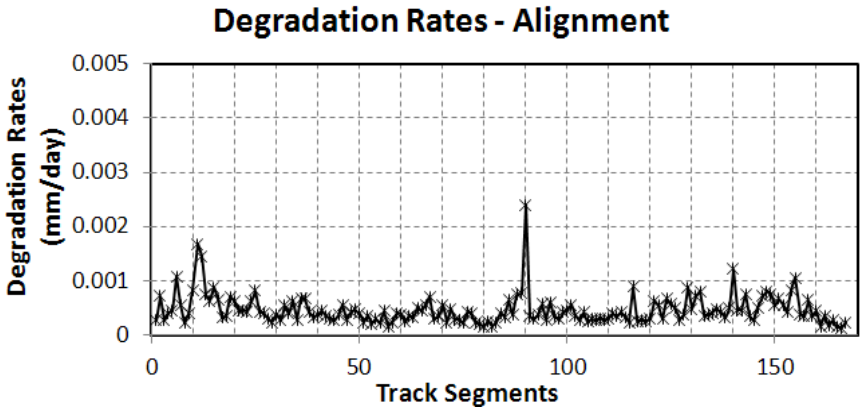

Figure 6.12 – Degradation Rate of Alignment

6.3.5 TRACK RECOVERY

Track recovery is defined as the quality improvement (absolute value) due to renewal or maintenance activities imposed on the track. This quality enhancement varies from segment to segment and depends on the track quality at the moment when the maintenance action is performed.

In order to obtain the quantity of improvement, it was decided to take as many recovery values observed in the data as possible. The gained recoveries for period 1 and 2 of the 167 track sections were thus taken, and the recovery function was calculated by the least square method.

Figures 6.13 and 6.14 illustrate the relationship between the track response before and after tamping maintenance for the longitudinal profile and alignment variables, respectively.

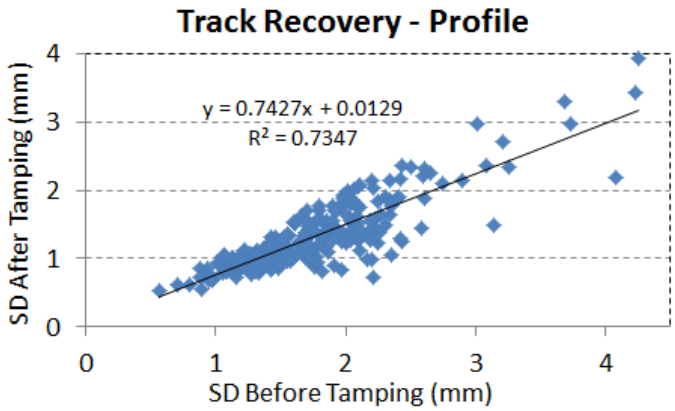

Figure 6.13 – Track Recovery - Longitudinal Profile

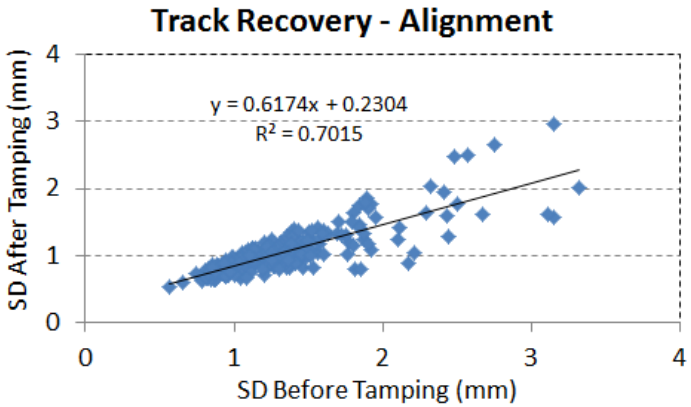

Figure 6.14 – Track Recovery - Alignment

Figures 6.13 and 6.14 demonstrate that the segments with lower quality have greater improvement after tamping, than those with high quality. This is reasonable because if the quality of a segment is low, there is much larger room for improvement.

The change of track quality in terms of standard deviation can thus be represented by the following expressions:

- Longitudinal Profile : $y = 0.7427 \cdot x + 0.0129\ ;\ R^2 = 0.735$ (6.17)
- Alignment: $y = 0.6174 \cdot x + 0.2304\ ;\ R^2 = 0.702$ (6.18)

Concerning the values of the squared regression coefficient (R^2), the fitting of the linear regression is greater than 0.7. Although there is no absolute standard for what is a "good" R^2 value, the application of squared regression could then be used as the option to predict the development of track degradation.

6.3.6 MATHEMATICAL MODELS FOR OPTIMIZING TRACK MAINTENANCE

A mathematical program, called Mixed Integer Linear Programming (MILP), is proposed to find the best alternative solutions from a given maintenance scheduling problem. The mathematical model consists of minimizing a linear function (the number of maintenance actions) in binary variables on a set of linear constraints.

The basis of this optimization model was taken initially from Vale [2010], and then modified so thus it complied with the other track maintenance approaches. For instance, the existing model seeks to minimize the total number of tamping operations during a predefined time (preventive maintenance), while in the new model, different approaches on the track maintenance strategy are introduced, such as delay maintenance and the combination of regular and corrective maintenance. In the delay maintenance strategy, the track quality is allowed to fall beyond the threshold limits, which is opposite with the existing model policy. The intervention thus would be generated exactly after the track quality reached in this condition (passed the limits). In the combination of regular and corrective maintenance, the intervention is planned to perform at the beginning of the period. Then, an additional tamping is calculated for the remaining time. The application of the proposed strategy may also determine the maintenance schedule not only based on the degradation of the longitudinal profile, but also on the degradation of the alignment, so that the functionality model may cope with the reality as much as possible.

As identified in Chapter 2.6, there are various types of maintenance that may be used to correct the railway ballast geometry. One of those activities is tamping, and it is identified as the main cost driver in the track life cycle cost (LCC) during its service life. In this study, the optimization model is devoted to find the optimum schedule for track maintenance by means of tamping.

The mathematical models described by integer linear programming, are presented below. The model is complied with the preventive maintenance strategy.

1. Decision Variables

   a) Segment-assigned tamping

$$m_{ij} = binary\ variables;\ \ i \in S\ and\ j \in T \tag{6.19}$$

   where:

   $S = \{1,2,3,4, \ldots\ n_s\}, n_s$ specifies the total number of segments considered

   $T = \{1,2,3,4, \ldots\ n_t\}, n_t$ indicates the total number of times considered

   b) Segment quality evolution

$$A_{aij} = A_{aij-1} + d_{ai} - m_{ij} r_{aij};\ \ a \in G, i \in S\ and\ j \in T \tag{6.20}$$

   where:

   $G = \{1,2\}$; $G\{1\}$ indicates longitudinal profile and $G\{2\}$ indicates alignment parameter

   A_{aij} corresponds to the railway track degradation, d_{ai} is the degradation rate of track geometry and r_{aij} is the quantity of improvement. The evolution of track segment is characterized by the progressive development of longitudinal profile and alignment.

c) Quality improvement

$$r_{aij} = \alpha(A_{aij-1} + d_{ai}) + b \tag{6.21}$$

This variable gives the quantity of improvement of track geometry after tamping. From the analysis, it is clear that this value depends considerably on the track quality at the moment of the maintenance action. The changes in track quality defined for longitudinal profile and alignment are shown in Equations 6.22 and 6.23.

$$\text{Longitudinal Profile : } y = 0.2573 \cdot x - 0.0129, \quad \text{so that } \alpha = 0.2573 \text{ and } b = -0.0129 \tag{6.22}$$

$$\text{Alignment : } y = 0.3834 \cdot x - 0.2304, \quad \text{so that } \alpha = 0.3834 \text{ and } b = -0.2304 \tag{6.23}$$

2. Constraints

a) Threshold limit

$$0 \leq A_{aij} \leq A_{ai\,limit} \tag{6.24}$$

where $A_{ai\,limit}$ is the threshold for preventive maintenance, which limits the track condition under the state defined by prEN 13848-5 and PSD limits proposed in Chapter 6.2.2.

b) Recovery limit

$$0 \leq r_{aij} \leq r_{ai\,limit} \tag{6.25}$$

This constraint gives the upper bound of improvement each track segment can reach after tamping. The upper bound corresponds to the maximum limit of track quality for a unit segment. For instance, the unit segment with maximum quality of 2.4 (longitudinal profile threshold for line speed of 120 km/h) will have maximum recovery of:

$$r_{ai\ limit} = (0.257 \cdot 2.4) - 0.0129 = 0.604 \tag{6.26}$$

3. Objective function

$$T = min \sum_{i=1}^{n_t} \sum_{j=1}^{n_p} m_{ij} \tag{6.27}$$

The maintenance model tries to seek an optimal number of tamping operations required in a given track section within a predefined time horizon. This model takes into account the degradation of two geometry variables: longitudinal profile and alignment.

Linear Relaxation

The existence of the multiplication product of a binary variable (m_{aij}) and a continuous variable (r_{aij}) in equation (6.20) limits the use of utilization software in solving mixed integer problems. In order to overcome this limitation, the product should be linearized using several steps:

1. Introduce a new variable t_{aij}, where: $t_{aij} =$

$$t_{aij} = m_{aij} r_{aij} \tag{6.28}$$

2. As r_{aij} is considered to be limited, $0 \leq r_{aij} \leq r_{ai\ limit}$, add the following four constraints that iteratively modify the solution in a manner that will eventually satisfy the inequalities.

$$t_{aij} \geq 0 \tag{6.29}$$

$$t_{aij} \leq m_{aij} r_{ai\ limit} \tag{6.30}$$

$$t_{aij} \geq r_{aij} - r_{aij\,limit}\left(1 - m_{aij}\right) \tag{6.31}$$

$$t_{aij} \leq r_{aij} \tag{6.32}$$

$t_{aij} \leq$

$t_{aij} \geq$

$t_{aij} \leq$

Consider if $m_{aij} = 0$, then the product $t_{aij} = m_{aij} r_{aij}$ will be equal to 0. The first pair of inequalities will be $0 \leq t_{aij} \leq 0$, so that $t_{aij} = 0$. The second pair of inequalities will be $r_{aij} - r_{aij\,limit}\left(1 - m_{aij}\right) \leq t_{aij} \leq r_{aij}$, and $t_{aij} = 0$ satisfies the inequalities.

If $m_{aij} = 1$, then the product $t_{aij} = r_{aij}$. The first pair of inequalities becomes $0 \leq t_{aij} \leq r_{ai\,limit}$, and the second pair of inequalities will be $r_{aij} \leq t_{aij} \leq r_{aij}$. The product of $t_{aij} = r_{aij}$ is therefore satisfied the inequalities.

6.3.7 THE APPLICATION OF THE MAINTENANCE MODEL

The general description of the maintenance model for scheduling the tamping operations has already been presented in Chapter 6.3.6. The model considers the degradation rate of mm per day.

As a summary, the mathematical model consists of several variables, i.e.:

- Track degradation rates obtained from 167 equal-length segments of longitudinal profile and alignment.
- Initial standard deviation of each track segment. For frequency spectrum assessments, the defect of track geometry is measured by the square root of the area under the PSD curve.

- Recovery function due to tamping, which is defined by actual on-site measurements.
- Limit values for generating track maintenance, which are derived from the European Standard and the proposed PSD limits.
- Time horizon of investigations. The selection of a time horizon determines the time taken by the software to perform the analysis. The longer the time horizon applied to obtain the optimal track maintenance schedule, the longer the software will take to finish the calculation. Therefore, it was decided to consider a 2-year time horizon in the analysis (8 x 90 days).

Furthermore, it is assumed that tamping actions may reduce the geometric fault below the intervention limits. Therefore, the segment with extreme value of initial track quality is expected to be repaired in the first tamping operation, although the rate of degradation remains the same. This is a reasonable assumption since no maintenance will be taken two consecutive times for correcting a particular geometry defect.

To develop a mathematical model and the associated constraints, CPLEX solver of the AMPL software and visual basic were utilized. Afterwards, the results were analyzed and compared to find the best practice for scheduling maintenance within the given constraints. Chapter 2.7.1 detailed how this software may solve an optimization problem using a technique called branch and bound.

For analyzing the influence of different criteria of track quality assessments as well as various geometry parameters to tamping, several scenarios are assumed, i.e.:

- Consideration of one geometry variable; either longitudinal profile or alignment, with TQI limit
- Consideration of two geometry variables; both longitudinal profile and alignment, with TQI limit

- Consideration of one geometry variable; either longitudinal profile or alignment, with PSD limit
- Consideration of two geometry variables; both longitudinal profile and alignment, with PSD limit

For analyzing the influence of various maintenance strategies to tamping, the assumed scenarios are as follows:

- RM+CM : consideration of one geometry parameter; either longitudinal profile or alignment, with TQI limit
- PM : consideration of one geometry parameter; either longitudinal profile or alignment, with TQI limit
- DM : consideration of one geometry parameter; either longitudinal profile or alignment, with TQI limit
- RM+CM : consideration of two geometry parameter; both longitudinal profile and alignment, with TQI limit
- PM : consideration of two geometry parameter; both longitudinal profile and alignment, with TQI limit
- DM : consideration of two geometry parameter; both longitudinal profile and alignment, with TQI limit

Note:

1. Regular maintenance (RM) + Corrective Maintenance (CM)

   Maintenance is conducted at a regular basis, once every two years. It is determined that all segments are maintained at the beginning of the period. Then, an additional tamping is calculated for the remaining time.

2. Preventive maintenance (PM)

   Maintenance is conducted with respect to minimizing the total number of tamping operations needed.

3. Delayed Maintenance (DM)

   Maintenance is performed immediately after the track quality falls beyond the threshold limits. The estimation of track tamping is determined one period before execution.

The mathematical problems used to analyze Preventive Maintenance (PM) and the combination of Regular Maintenance and Corrective Maintenance (RM+CM) were performed using AMPL and IBM ILOG CPLEX optimization software, while the Delayed Maintenance (DM) strategy was assessed using Visual Basic algorithms.

Tables 6.7 and 6.8 present the optimal solution for the total number of maintenance operations required in the given track sections. This solution considers various scenarios, as described above.

Table 6.7 – Influence of the Track Quality Assessment Criteria and the Consideration of Track Geometry Parameters

Geometry Parameters	Power Spectral Density (PSD)	Track Quality Limit (TQI)
Longitudinal Profile	94	124
Alignment	199	158
Longitudinal Profile + Alignment	222	206

Table 6.8 – Influence of Various Track Maintenance Strategies

Geometry Parameters	Delayed Maintenance	Preventive Maintenance	Regular & Corrective Maintenance
Longitudinal Profile	117	124	209
Alignment	150	158	234
Longitudinal Profile + Alignment	193	206	256

The influence of the track quality criteria to the tamping decision is presented in Table 6.7. In the first part, the maintenance is required by the limit defined in the European Standard which ranges from 1.9 to 2.7 for longitudinal profile and from 1.1 to 1.5 for alignment, depending on the line speed. The second part optimizes the number of track maintenance with respect to the limit values proposed in the PSD China standard.

The preference to use the aforementioned PSD is due to the similarity of the spectrum characteristics with the frequency spectrum shown by the sample segments. The Chinese PSD may also facilitate obtaining the threshold limit with respect to line speed, which is comparable with the European Standard.

Based on Table 6.7, it appears that longitudinal profile defect resulted in a lower number of required tamping operations than the alignment defect. The declination ranges up to 52% for PSD criteria and 22% for TQI criteria. If the combination of these two geometry defects is used, the tamping quantity increases considerably, 12% for PSD and 30% for TQI. These results show that alignment takes a greater part on maintenance consideration in railway.

In correspondence with the quality criteria used in the assessment, PSD gives a larger tamping quantity than TQI. It accounts for up to 7% higher for the combination of the

defects. The same result is obtained for alignment, but the contrary for longitudinal profile. The PSD China appears to put more awareness towards the alignment irregularity than TQI.

Table 6.8 presents various maintenance strategies and their influence to the maintenance decision. Delayed maintenance was revealed as the most efficient strategy. However, it should be noted that this approach does not restrict the track quality from the predefined threshold limit. Tamping may be precisely decided after the track quality reaches the threshold limit. The second most efficient strategy is preventive maintenance. It accounts for 7% larger number of actions than delayed maintenance and 19% lower than the combination of regular and corrective maintenance. The third efficient strategy is the combination of regular and corrective maintenance, which is the common strategy adopted by many railway infrastructure managers around the world. However, this approach is considered less efficient when compared to the other two strategies.

Figures 6.15 and 6.16 show the distribution of track tamping over time in correspondence with TQI and PSD limits, respectively. A higher tamping is identified in the first time interval due to an initial bad quality of some track segments. As time went by, the required tamping declined considerably by about 60% according to the TQI limit and by 78% according to the PSD limit, with respect to the combination defects. Furthermore, it is noticed that only a small percentage of tamping is required in the last time period.

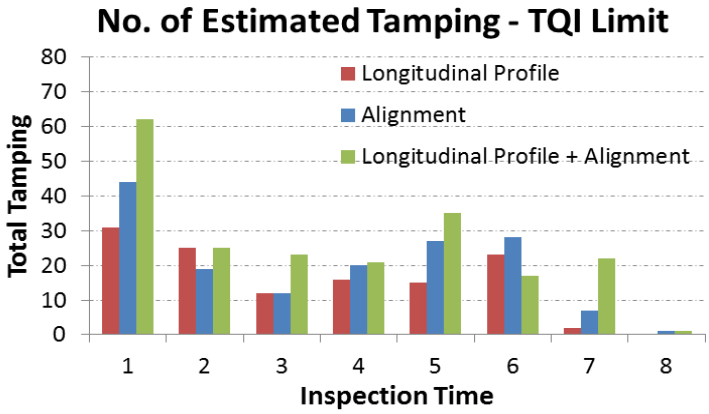

Figure 6.15 – Distribution of Total Tamping over time based on TQI limit

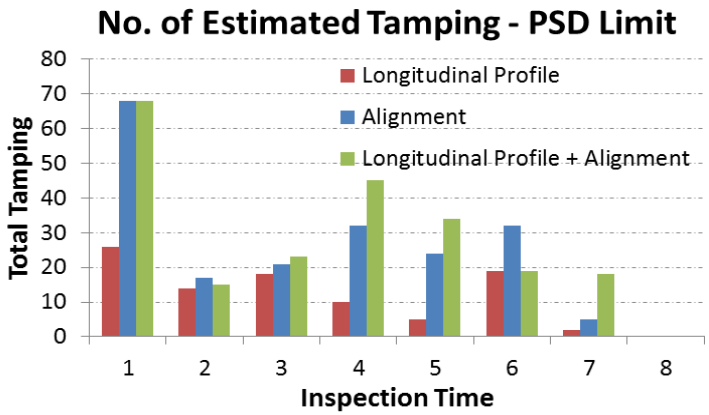

Figure 6.16 – Distribution of Total Tamping over time based on PSD limit

Figure 6.17 explores the distribution of the total number of tamping operations according to the various maintenance strategies. It can be seen that the combination of regular and corrective maintenance has the highest tamping quantity in the beginning of the time horizon. This is justified by the fact that the policy for tamping comprises the whole track, that is, all segments once a year in the initial period, hence the total maintenance is considerably high. However, the required maintenance decreased afterwards. Compared with the other two maintenance approaches, this particular strategy is the least efficient.

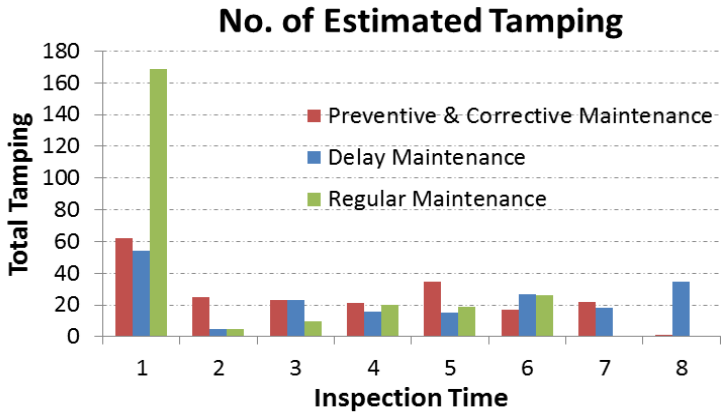

Figure 6.17 – Distribution of Total Tamping over time based on various maintenance strategies

Figures 6.18 to 6.21 present the sample of track quality evolution for the geometrical parameters on segment 2 and on segment 12. The analysis of the figures in detail allows identifying the influence of the type of geometry variables to the amount of tamping.

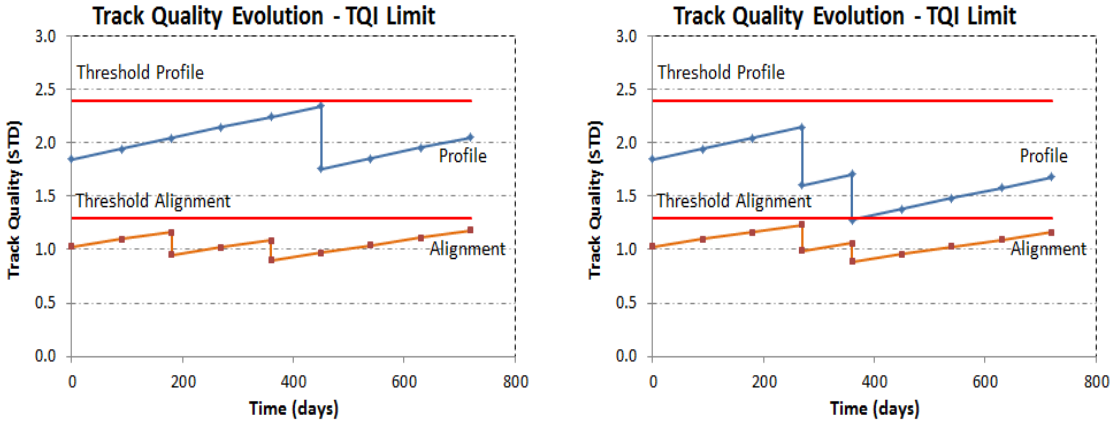

a) Single Parameter Defect

b) Combination Defect

Figure 6.18 – Evolution of Track Quality for Segment 2 with Preventive Maintenance strategy, based on TQI limit

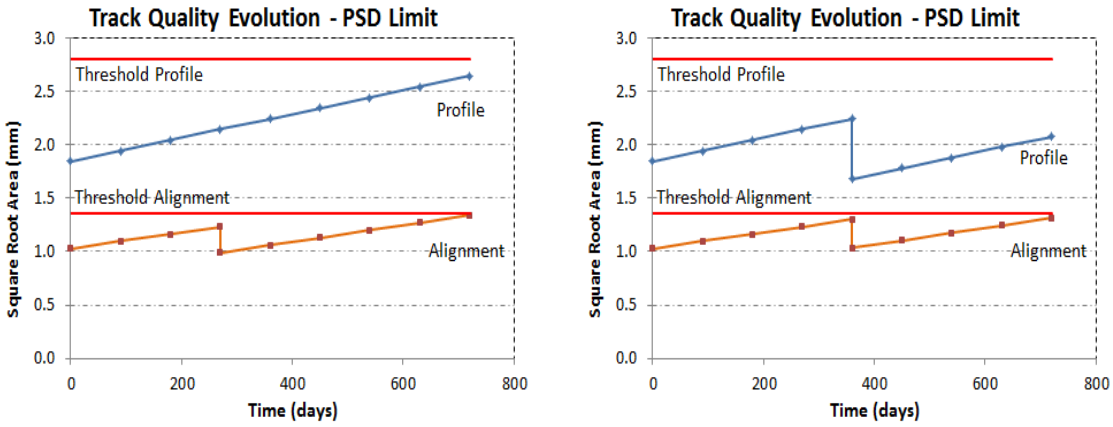

a) Single Parameter Defect

b) Combination Defect

Figure 6.19 – Evolution of Track Quality for Segment 2 with Preventive Maintenance strategy, based on PSD limit

The change in quality for either longitudinal profile or alignment corresponding to the TQI limit is given in Figure 6.18a, and the combination of those two geometrical defects is shown in Figure 6.18b. In this segment, the alignment defects cause the maintenance actions to double in relation to those of the longitudinal profile. It also acted as the influencing factor in the tamping decision when longitudinal profile and alignment defects were considered at the same time. This fact is also revealed in Figure 6.19, which exposes the required maintenance based on the PSD limit. Again, tamping decision was determined by the alignment, though it was considered unnecessary in terms of the longitudinal profile defects until the end of the time period.

Another sample segment is given in Figures 6.20 and 6.21, which show the number of tamping actions required in segment 12 according to the TQI and PSD limits, respectively. The tamping quantity required for the alignment defects is times higher than that for longitudinal profile with respect to the TQI limit and two times higher than longitudinal profile with respect to the PSD limit. Considering the quantity of tamping generated by the combination of these geometrical defects, alignment is acknowledged as the influencing factor in the tamping decision. Most of the planned tamping is generated because of the need for maintenance of the alignment.

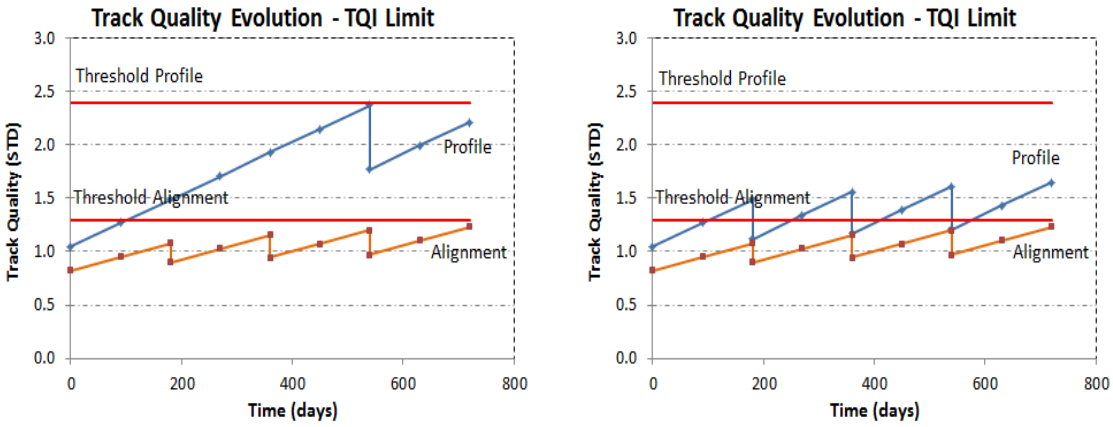

a) Single Parameter Defect b) Combination Defect

Figure 6.20 – Evolution of Track Quality for Segment 12 with Preventive Maintenance strategy, based on TQI limit

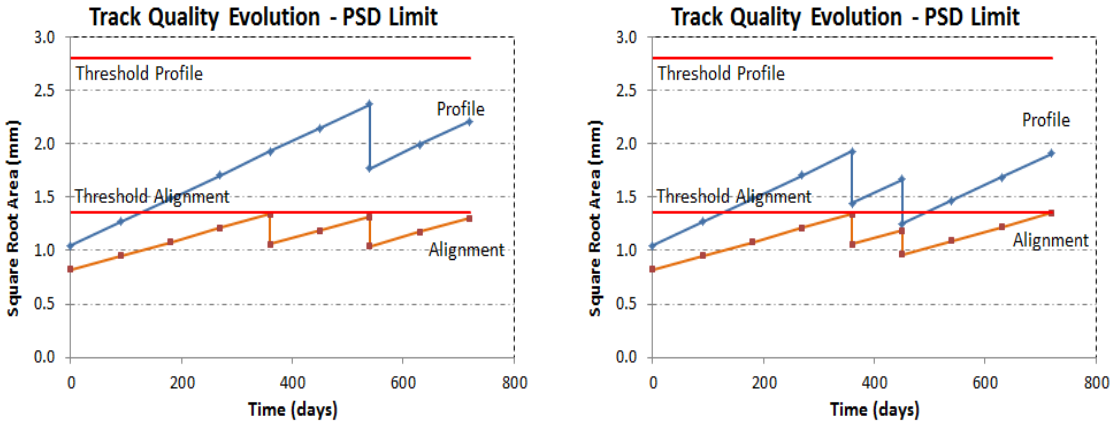

a) Single Parameter Defect b) Combination Defect

Figure 6.21 – Evolution of Track Quality for Segment 12 with Preventive Maintenance strategy, based on PSD limit

There are also some segments which tamping decision is driven by longitudinal profile, for example in the segment 145. Figure 6.22 portrays the evolution of the standard deviation of track geometry variables and the distribution of tamping actions in this segment. The quantity of tamping scheduled for the longitudinal profile is two times higher than for the alignment variable. The first tamping operation is planned at the beginning of the time period, followed by the second tamping at the middle of the period of time. It should be noted that the segments in this case are usually characterized

by a higher standard deviation at the initial time instant and larger deterioration rate. Another sample on this case can also be seen in segment 67, as given by Figure 6.23. According to the results, the initial standard deviation and the deterioration rate of the longitudinal profile in this segment are larger in comparison with the other segments.

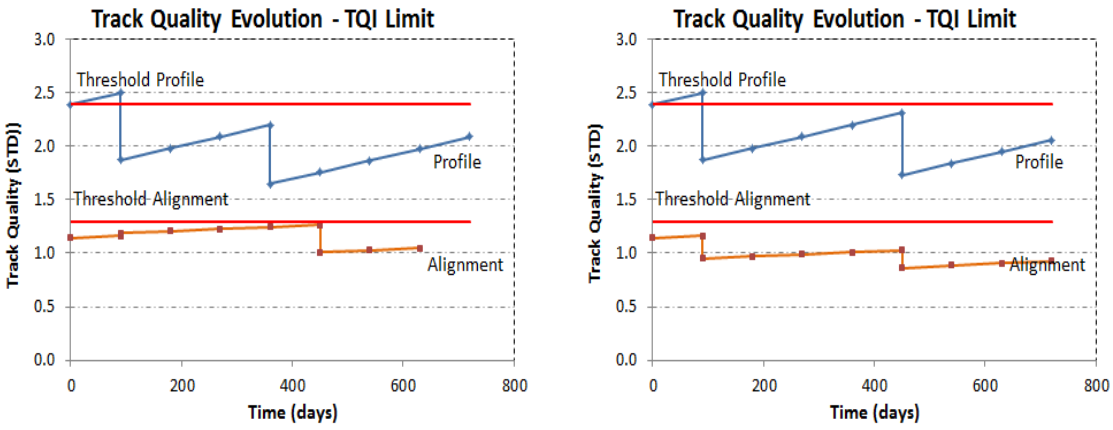

a) Single Parameter Defect b) Combination Defect

Figure 6.22 – Evolution of Track Quality for Segment 145 with Preventive Maintenance strategy, based on TQI limit

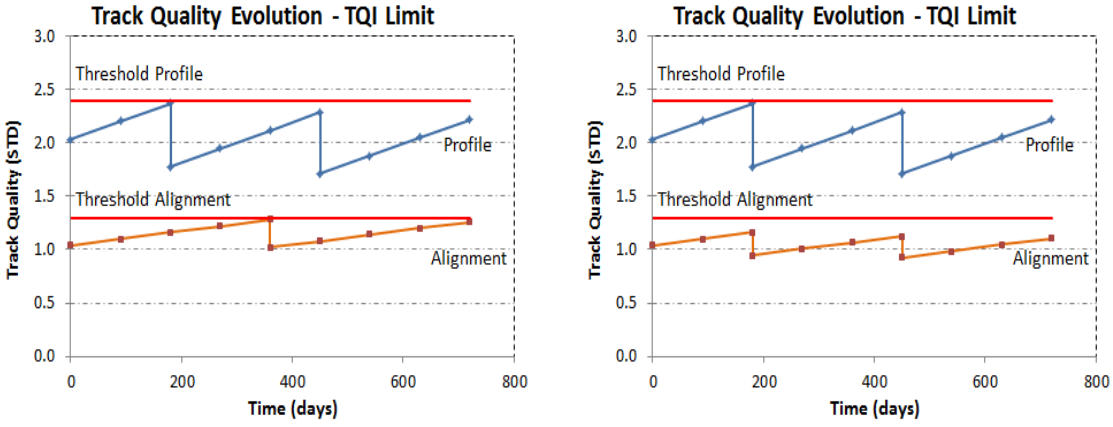

a) Single Parameter Defect b) Combination Defect

Figure 6.23 – Evolution of Track Quality for Segment 67 with Preventive Maintenance strategy, based on TQI limit

Figure 6.24 shows the evolution of standard deviation for track segment 121. At the initial time instant, the values are considered higher than the limit for all geometrical variables. These values are not predicted by the model, but they correspond to the real standard deviation measured in that segment. It has been assumed that the tamping intervention should be able to bring the track back to order. Thus, in this case, the improvement obtained by the segment is in between the threshold and the real value plus the possible maximum recovery.

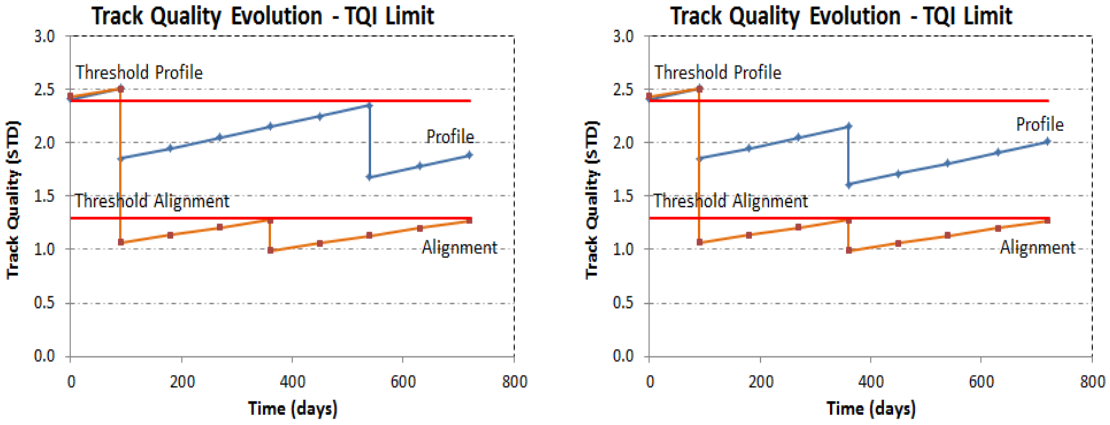

a) Single Parameter Defect

b) Combination Defect

Figure 6.24 – Evolution of Track Quality for Segment 121 with Preventive Maintenance strategy, based on TQI limit

In order to analyze the effectiveness of the maintenance strategies, Figures 6.25 a, b, and c present the results of tamping for three different scenarios, which correspond to the combination defect. The combination of regular and corrective maintenance is revealed as the least efficient approach compared to the other two strategies. It has scheduled three times of tamping, mainly caused by alignment defects. The number of tamping in preventive and delayed maintenance is less one time. However, it should be mentioned that in the latter technique, the mathematical model allows tamping to be generated when the track quality is slightly higher than the threshold limit.

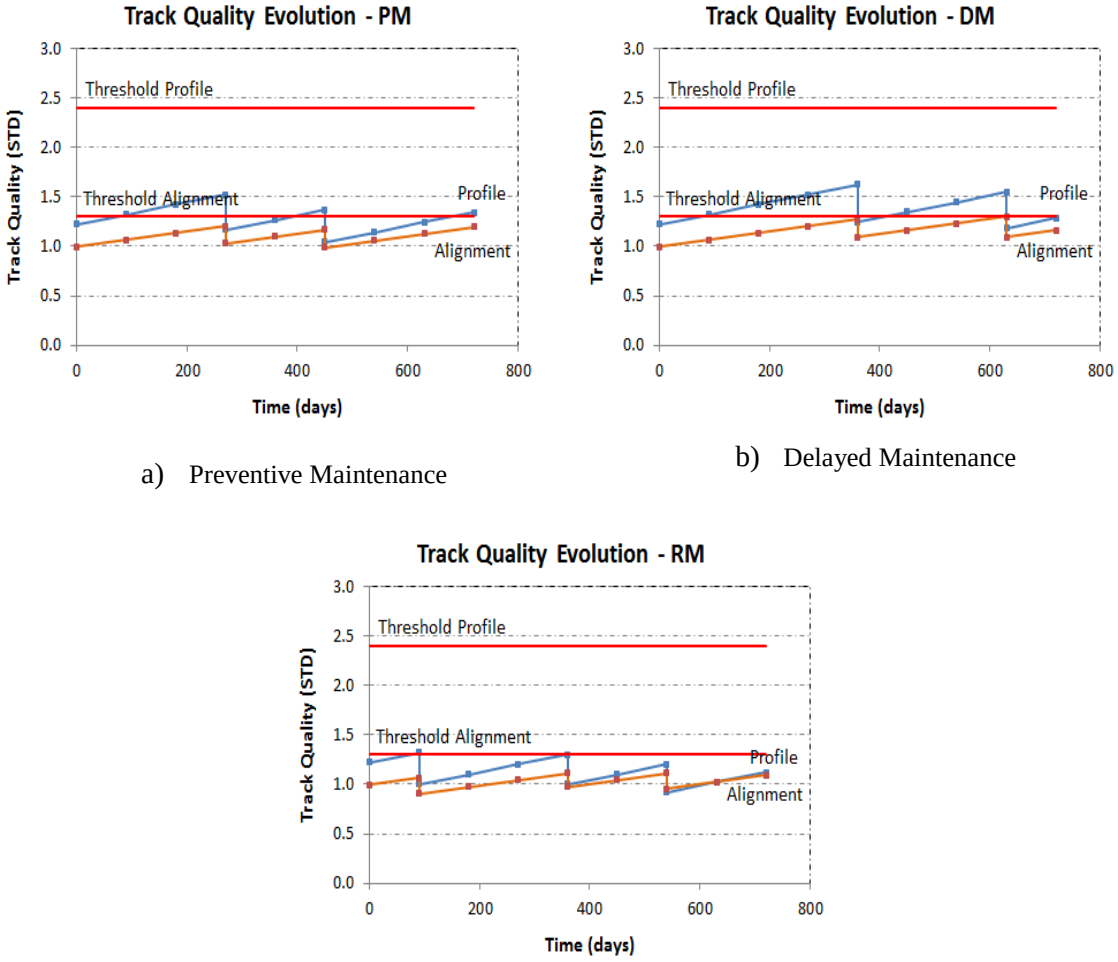

a) Preventive Maintenance

b) Delayed Maintenance

c) Regular and Corrective Maintenance

Figure 6.25 – Analysis of maintenance strategies to tamping decision for segment, based on TQI limit

6.3.8 VALIDATION OF THE MODEL

The model validations are needed to provide the confidence associated with the accuracy and reliability of the output predictions. The evaluation criteria, namely Root Mean Squared Error (RMSE) and Mean Absolute Error (MAE), are the common standards used for evaluating the model performance. The analysis results of these two methods are given in Table 6.9, considering the prediction of both longitudinal profile and alignment.

Table 6.9 – Prediction Performance

Prediction Performance	MAE	RMSE	Estimation Error below 5 %
Forecast Longitudinal Profile	0.065	0.159	87%
Forecast Alignment	0.045	0.079	78%

The evaluation formula and the methodologies used to validate the model are given in Chapter 3.5. A prediction of the future values should be conducted in the early stages, using the degradation rates and necessary variables that form the model. The analysis takes an initial value from the beginning of the inspections, which is used to construct the model and to make the projection of the forecast value, which corresponds to the sequence of observations in the time period ahead. The accuracy between actual and predicted values is measured by the forecast error.

Based on Table 6.9, the calculation of the Mean Absolute Error (MAE) and the Root Mean Square Error (RMSE) gives good results of the performance of the indicators. The track geometry variables in either longitudinal profile or alignment have low MAE and RMSE, with slightly higher values for the former than for the latter variable. In correspondence with the estimation error below 5%, the forecasting accuracy of the longitudinal profile variable is of about 87%, while for the alignment 78% of accuracy was obtained. Again, this serves to show that the prediction model provides a good forecasting performance.

6.4 CONCLUSIONS

This chapter presented the relationship between power spectral density and track quality index in terms of standard deviation. It is recognized that both methods are correlated as follows. The standard deviation of a random track irregularity is in fact equal to the square root of the area under the power spectral density curve. A higher geometry defect will result in a larger area under the PSD curve, and a smaller geometry defect means the opposite. The dimension of the total area under the power spectrum can thus be used as an indicator of the track quality index.

Furthermore, this chapter also showed a model development for track degradation as well as a recovery model due to tamping. The first model attempts to clarify the degradation process of track geometry irregularity: longitudinal profile and alignment, for each unit segment of track (200 m in length). The latter model tries to predict the quantity of improvement obtained from a tamping action. These two models are then used as input to derive the optimization model for scheduling maintenance in a given time period. Afterwards, several scenarios of maintenance strategies are proposed and compared to each other.

For analyzing the influence of different criteria of track quality assessment to the number of tamping operations, the proposed PSD limit and the European Standard limit were used. From the analysis, PSD generated a larger number of tamping than TQI. PSD accounted for up to 7% more tamping operations for the combination of geometrical defects. The same result is obtained for the alignment but the contrary for the longitudinal profile variable. PSD China seems to provide more awareness for the alignment irregularity than TQI.

In correspondence with the influence of the consideration of geometrical defects to the tamping decision, longitudinal profile defects have resulted in a lower number of tamping actions than alignment. The declination ranges up to 52% for PSD criteria and 22% for TQI criteria. If the combination of these two geometry defects is considered,

the tamping quantity increases considerably, 12% for PSD and 30% for TQI. These results indirectly show that alignment takes a greater part on maintenance consideration in the railway.

Regarding the influence of various maintenance strategies to the maintenance decision, delayed maintenance reveals as the most efficient strategy than the other two. However, it should be noted that this approach does not restrict the track quality always under the predefined threshold limit. Tamping may be precisely decided after the track quality reaches the threshold limit. The second most efficient strategy is preventive maintenance. It accounts for 7% larger number of actions than delayed maintenance and 19% lower than the combination of regular and corrective maintenance. The third efficient strategy is the combination of regular and corrective maintenance, which is the common strategy adopted by many railway infrastructure managers around the world. However, this approach is considered less efficient compared to the other two strategies.

For validating the prediction model, some performance criteria; such as Mean Absolute Error (MAE) and Root Mean Square Error (RMSE), were selected. The results show that these two values are considerably low, thus providing a good indication of the prediction performance. In correspondence with the estimation error of less than 5%, the forecasting accuracy of the longitudinal profile is of about 87%, while alignment obtained 78% of accuracy.

7

RESULTS AND DISCUSSIONS

7.1 INTRODUCTION

The purpose of this final chapter is to summarize the key conclusions of the research. This chapter clarifies the original contribution of this thesis to the body of knowledge, particularly on track quality assessments and maintenance for railway ballasted tracks. A number of recommendations for further research are also presented in this chapter.

This research primarily sought to develop an optimization model for scheduling track maintenance with respect to safety and reliability issues. The Power Spectral Density (PSD) forms a core focus of the studies since it involves a systematic technique for evaluating track quality condition. To achieve the underlying objective, the research was divided into two major phases. The first phase attempted to examine the application of power spectral density in track quality assessments. The investigation was then further continued by evaluating the existing relationship between various types of track geometry parameters. This phase is of particular importance towards establishing a reasonably accurate model of track degradation, which takes into account the interactions among various geometry variables. The second phase was conducted by developing a predictive degradation model which may capture the evolution of track quality in terms of statistical index and frequency spectrum. The results obtained from this model together with a track recovery model were then applied to analyze different maintenance scenarios.

7.2 RESEARCH GOALS AND OBJECTIVES

The primary goals of this research are:

1. To investigate the application of Power Spectral Density in the assessment of railway track quality. For this purpose, PSD standards developed in various countries have been analyzed and the implementation of those methods in real field assessments was conducted.
2. To quantify the degree of interdependency and to establish the similarity of one track geometry variable to another. For evaluating the existing relationship between each of them, correlation analyses were employed in this research.
3. To develop an optimization model for scheduling track maintenance in ballasted tracks. The proposed model consists of two parts: the predictive degradation model, able to capture the evolution of track quality in terms of statistical index and frequency spectrum, and the track recovery model due to tamping operation. The results obtained from the optimization model were then applied to analyze different maintenance scenarios.

The first objective was addressed in "The Application of Power Spectral Density (PSD) in track quality assessments" chapter. This chapter provided theoretical PSD standards developed in many countries. A comparison review is then carried out to define the characteristic features contained in each particular standard. The comfort-ability and the suitability of the standard with the sample segment were also examined through a case study.

The second objective was addressed in the "correlation analysis of railway track geometry" chapter. The analyses were conducted in the frequency domain through three different approaches: cross-correlation, autocorrelation and coherence analyses.

The third objective is the core of the research. It was addressed in the "Development of an optimization model for track maintenance" chapter. The optimization model was

built based on the predictive degradation model and the track recovery model due to tamping operation. Several analyses were carried out in this chapter, such as the identification of relationship between track quality index and power spectral density, and the establishment of an alternative criteria of threshold limit based on power spectral density. The results were used to solve the maintenance scheduling problem, and then followed by validation with some performance criteria.

7.3 SUMMARY AND CONCLUSIONS

This research was started by the discussion on the lack of use of Power Spectral Density (PSD) to assess railway track geometry condition. The expertise and knowledge required to process and to interpret information regarding the Power Spectral Density is the main drawback in the development of this method.

The first objective of this research is addressed in chapter 4. The application of PSD has several advantages when compared with the TQI technique, for example, PSD can identify the particular wavelength of track geometry irregularity. This wavelength is strongly linked with problems; the short wavelength associated with train safety, while the long wavelength corresponds to riding comfort. In order to use the spectrum standard in the track quality assessment, several techniques can be used. First, the PSD standard is transformed from the wavenumber-based domain to the solution in the spatial-based domain. The artificial solution in the spatial domain is then compared to the actual data of track geometry irregularity. For obtaining a valid result, some factors which may affect the amplitude of geometry roughness are carefully considered, such as the preference on the use of wavelength interval (waveband) and the line speed. From the analysis, it is reckoned that the longer the considered wavelength interval, the higher the variation of the track geometry defect, while for lines speed the opposite was observed. The higher the line speed, the lower the track roughness obtained from PSD.

The second technique for measuring the state of the track condition is accomplished by expressing the spectrum of geometrical defect with a fitting curve function. The result is

then compared to the theoretical PSD standards. An analysis from the sample segment revealed a considerable difference between track quality before and after intervention. This difference is one of the most important indicators to assess the appropriateness of maintenance works.

A study was also conducted to evaluate the characteristic features of various PSD standards. From this research stage, it was found that the German PSD is generally stricter in terms of the geometry errors of longitudinal profile, alignment, and cross level or superelevation irregularity, thus indicating a better quality control applied by the German railway standards. For the curves produced by Chinese and FRA spectra, the analysis shows a comparable result in terms of their magnitude and tendency, especially for wave irregularities shorter than 10 m. The detailed analysis on the comparison of various PSD standards is as follows.

A similar characteristic of the longitudinal profile is shown between Chinese 200 and German low disturbance at wavelengths shorter than 4 m, which is superior to the SNCF and FRA power spectral densities. As the wavelength increases, France spectrum (SNCF good) takes it into consideration especially for the irregularities laid above 16 m. Note that in this particular wave, the SNCF PSD results corresponds to the highest curve.

For the PSD comparison of track alignment, the magnitude of German low disturbance is lower than FRA and Chinese PSD at wavelengths below 38 m, indicating more restrictions to the allowable tolerance imposed by German high speed lines. At wavelengths below 10 m, the curves presented by Chinese 200, German high disturbance and FRA 6 are close and seem to be almost equal. A superiority of German PSD can also be found in the PSD comparison of cross level (superelevation irregularity) at all the investigated wavelengths.

The second objective of the research is presented in Chapter 5, consisting of the relationship analysis between various track geometry parameters. From the three methodologies of correlation, the relationship of various track geometries can be best described by cross-correlation and coherence functions. The autocorrelation was found to be useful to assess the rail track quality by identifying the periodicity and pattern of the irregularity signals. However, the three methods generally provided similar relationship tendencies. For example, a very good and strong coherence between two sets of geometry variables will yield a higher value of cross-correlation.

From the analysis results, it shows that some track geometry variables are closely related. A defect on a particular track geometry variable may strongly impact, either positively or negatively, the others. A common typical of wavelength is also outlined especially at a wave band between 6 and 30 m. The detailed analysis for each variable is subsequently discussed.

The strongest positive relationship is observed between the left and the right rails, for both longitudinal profile and alignment. The cross-correlation of the longitudinal profile of both rails is 0.66 while for the alignment is 0.89, which indicates that if one variable decreases, the other variable also decreases and vice versa. According to Table 5.7 (coherence table), the variations in the left and the right longitudinal profile are similar for wavelengths longer than 6 m, as the coherence curve is higher than the 95% confidence level. For shorter wavelengths, there are periodic waves appearing at 3 m, 2.5 m and 1.5 m that might have been induced during the rail straightening process. Meanwhile, the alignment exhibits a strong relationship for wavelengths longer than 66 m and decreases for shorter wavelengths. A noticeable periodic peak is also observed especially at the 5 m wavelength.

Medium correlations are further revealed between super-elevation and twist, and between track alignment and gauge. The average coefficients for each of these are 0.46 and 0.47, respectively. Cross level or or superelevation irregularity defines the amount of vertical deviations between the levels of two rails from their design value. Twist, on

the other hand, measures the difference in the super-elevation between two points taken at a separate fixed distance. The existing correlation between these two parameters is possibly due to the tie connection on the measurements as described above. According to the coherence table, the most detrimental waves between twist and super-elevation can be found at wavelengths longer than 6 m with values close to one. This means that at these particular waves, an increase on twist irregularity may imply an increase on the magnitude of super-elevation. Similarly, the coherence analysis between single rail alignment and gauge shows stronger relationships at some discrete wavelengths typically between 6.2 and 15 m. Although the correlation values are not sufficiently significant, it can be attested that there is some level of relationship between these track geometry parameters.

There are low correlations between the irregularities of track longitudinal profile and twist, and track longitudinal profile and super-elevation, which can be perceived in both methods: cross-correlation and coherence. Analyses also show the independency of variations between longitudinal profile and alignment, super–elevation and gauge, twist and gauge, and longitudinal profile and gauge.

In correspondence with curvature, there exists a correlation between curvature and gauge variables, which magnitude varies depending on the track layout. The higher the curvature, the larger the correlation will be, while the smaller the curvature means the opposite. Note that the correlation between curvature and gauge can be either positive or negative and it can vary from low to high. The strongest positive correlations are shown between curvature and alignment for both the left and the right rails, with an average correlation around 0.85. The correlation is quite high in the segment where the curvature is large and lowers where the curvature is small. For the correlation between curvature and the other track geometry variables (super-elevation, twist and longitudinal profile), it is known that the influence of curvature is not significant.

Further analyses show that the autocorrelation curves produced by the irregularity of the left and the right rails are quite similar, in both the track longitudinal profile and the

alignment. Several spikes are clearly observed at the same lag distances, which show that the track irregularity signals between the two rails are lined up and matched at some points. Both of the rails also have uniform defects with identical wave periodicities. Note that the magnitude of periodicities is higher for the smaller lags and predominantly decreases as lags increase. The correlations of track irregularity are therefore higher for near track distances. A similar pattern of periodicities can also be found in autocorrelation of twist. On the other hand, the opposite result is observed for the autocorrelation of gauge or super-elevation. It is hard to find the similarity between the waveforms, since the peak is only observed at zero lag distance.

The third objective, as the core of this research, is presented in chapter 6. This chapter started by discussing the relationship between PSD and TQI method. As it is recognized, both methods are correlated through the use of the trapezoidal function, which represents the sum of the square root area under the power spectral density curve, equal to the standard deviation of a random track irregularity. This method is then implemented in various PSD standards, and the proposed threshold limits are derived for track defects with span between 3 and 25 m.

Furthermore, this chapter also shows a model development for track degradation as well as a recovery model due to tamping operation. The first model attempts to describe the quality evolution of track geometry parameters: longitudinal profile and alignment, in terms of statistical index and frequency spectrum. The latter model tries to predict the quantity of improvement obtained from the tamping action. These two models are then used as input to derive the optimization model for scheduling maintenance in a given period of time. Afterwards, several scenarios of maintenance strategies are proposed and compared to each other.

For analyzing the influence of different criteria of track quality assessment to the quantity of tamping, the proposed PSD limit and European Standard limit were used. From the analysis, PSD gives larger number of tamping operations than TQI. PSD accounts for up to 7% higher for the combination of geometrical defects. The same

result is obtained for alignment but the contrary for longitudinal profile. The Chinese PSD seems to provide more awareness for the alignment irregularity than TQI.

In correspondence with the influence of the consideration of geometrical defect to the tamping decision, longitudinal profile defects resulted in a lower number of tamping operations than alignment. The declination ranges up to 52% for PSD criteria and 22% for TQI criteria. If the combination of these two geometry defects is used, the tamping quantity increases considerably, 12% for PSD and 30% for TQI. These results indirectly show that alignment takes a greater part on maintenance consideration in the railway.

Regarding the influence of various maintenance strategies to the maintenance decision, delayed maintenance was revealed as the most efficient strategy. However, it should be noted that this approach does not restrict the track quality always under the predefined threshold limit. Tamping may be precisely decided after the track quality reaches the threshold limit. The second most efficient strategy is preventive maintenance. It accounts for 7% larger number of actions than delayed maintenance and 19% lower than the combination of regular and corrective maintenance. The third efficient strategy is the combination of regular and corrective maintenance, which is the common strategy adopted by many railway infrastructure managers around the world. However, this approach is considered less efficient compared to the other two strategies.

For validating the prediction model, some performance criteria, such as Mean Absolute Error (MAE) and Root Mean Square Error (RMSE), were selected. The results show that these two values are considerably low, thus providing a good indication of the prediction performance. In correspondence with the estimation error of less than 5%, the forecasting accuracy of the longitudinal profile is of about 87%, while alignment accounts for 78% of accuracy.

7.4. CONTRIBUTION TO KNOWLEDGE

The contribution to knowledge made by this thesis is associated with the improvement of the track maintenance decision, by evaluating various maintenance strategies commonly used in practice. The research findings also show that longitudinal profile and alignment, two variables considered in the maintenance model, stand independently. Any defect that occurs in one of these particular variables would not impact the other variable. The maintenance decision thus should be performed individually with different criteria limits for each. Alignment is also reckoned to require more maintenance than longitudinal profile.

Secondly, this thesis proposes alternative criteria for track quality limits according to the PSD standard. The proposed limit is obtained by identifying the square root area under the power spectral density curve corresponding to the irregularity wave between 3 to 25 m. This method allows identifying the suitability of the railway track quality according to the preference criteria.

7.5. RECOMMENDATIONS FOR FURTHER RESEARCH

It is important that research continues in the area of maintenance optimization studies. Whilst this thesis was performed to improve the effectiveness of a maintenance decision, there is a considerable amount of work that can be conducted in the future. The following recommendations are suggested for future works:

1. The limitation on the number of maintenance operations caused the researcher to model the degradation and recovery models using a linear regression technique. Although this model is considered accurate according to the validation analysis, sometimes the prediction may not effective particularly if a long period of horizon time is considered. Further research could gather more information concerning track irregularity data and use different methods for modeling track degradation.

2. In addition, the proposed model in this thesis did not yet take into account some relevant parameters, such as traffic load, maintenance cost, penalty cost, and environmental strategy. The consideration of these parameters would further enhance the effectiveness of the maintenance decisions.

REFERENCES

1. Alp, A., Erdemir, A., & Kumar, S. (1996). Energy and wear analysis in lubricated sliding contact. *Wear*, vol. 191, pp. 261–264.
2. Anderson, M. (2002). *Strategic planning of track maintenance*. Department of Infrastructure, Borlange.
3. Andrade, A. R. and Teixeira, P. F. (2011). Uncertainty in Rail-Track Geometry Degradation: Lisbon - Oporto Line case study. *Journal of Transportation. Engineering*, vol. 137(3), pp. 193–200.
4. Andren, P. (2006). Power Spectral Density approximations of longitudinal road profiles. *International Journal of Vehicle Design*, vol. 40, No.1/2/3.
5. Archard, J. F. (1953). Contact and Rubbing of Flat Surfaces. *Journal of Applied Physics*, vol. 24, no. 8, pp. 981–988.
6. Bazaraa, M. S., Sherali, H. D. and Jarvis, J. J. (1990). *Linear Programming and Network Flows.* 2nd edition, John Wiley and Sons, New York.
7. Berggren, E. (2005). *Dynamic track stiffness measurement: a new tool for condition monitoring of track substructure.* KTH Engineering Science, Stockholm, Sweden.
8. Bing, A. J. and Gross, A. (1983). Development of railway track degradation models. *Transportation Research Record*, vol. 939, pp. 27-31.
9. Bouma, G. D. and Atkinson, G. B. (1995). *A Handbook of Social Science Research*. Oxford: Oxford University Press.
10. Broeck, V. P. (2001). *A prediction model for ground-borne vibrations due to railway traffic*. PhD Thesis. Katholieke Universiteit Leuven.
11. Budai, G., Dekker, R. and Nicolai, R. (2008). Maintenance and production: a review of planning models. *Complex systems maintenance handbook, part D, series in reliability engineering*, vol. 13, pp. 321–344. Berlin: Springer.
12. Cacho, M. (2009). *Manutencao e conservacao em fias –ferreas:o caso da via alfarelos–figuera da foz*. Licienciatura thesis. Civil Engineering Department, University of Coimbra.

13. Cai, W. F. (2008). *A study on statistical regularities of ballastless track irregularity in Sui-Yu railway line*. Master Thesis. Civil Engineering Department, Southwest Jiaotong University.
14. Chrismer, S. and Selig, E. T. (1993). Computer model for ballast maintenance planning. *Proceedings of 5th international heavy haul railway conference*, Beijing.
15. Clauss, H. and Schiehlen, W. (1997). Modeling and Simulation of railways bogie structural vibrations. *Vehicle System Dynamics*, vol. 29, pp. 538–552.
16. Comboios.org (2007). *EM 120 - veículo de inspecção geométrica de via*. Available: http://www.comboios.org/forum/viewtopic.php?t=10923&view=previous [Accessed 20 December 2012].
17. Cope, H. (1993). *British railway track, Design, construction and maintenance*. The Permanent Way Institution, Echo Press. England.
18. Creswell, J. W. (1994). *Research design: Qualitative & quantitative approaches*. Thousand Oaks, CA.
19. Dahlberg, T. (2003). Railway track settlements – a literature review. *Report for the EU project SUPERTRACK*. Division of Solid Mechanics, IKP, Linköping University.
20. Demharter, K. (1982). *Setzungsverhalten des Gleisrostes unter vertikaler Lasteinwirkung. Mitteilungen des Prüfamtes für Bau von Landverkehrswegen der Technischen Universität München*, Heft 36.
21. Dias, R., Goicolea, M., Gabaldon, F., Cuadrado, M., Nasarre, J., Gonzalez, P. (2008). A study of the lateral dynamic behavior of high speed railway viaducts and its effect on vehicle ride comfort and stability. *Bridge Maintenance, safety, management, health monitoring and Informatics*. Koh & Frangopol (eds) Taylor & Francis Group, London.
22. El-Sibaie, M. and Zhang, Y. J. (2004). Objective Track Quality Indices. *83rd TRB Annual Meeting*, Washington, D.C.
23. Esveld, C. (2001). *Modern Railway Track*. 2nd edition, MTR-productions, Zaltbommel, The Netherlands. ISBN 90-800324-3-3.
24. Ferreira, L. and Murray, M. (1997). Modelling rail track deterioration and maintenance current practices and future needs. *Transport Reviews*, vol. 17, pp. 207-221.

25. Frýba, L. (1996*). Dynamics of railway bridges*. T. Telford, London, UK.
26. Gines, R. (2008). *The economic effects of high speed rail investment*. Discussion paper, no. 2008-16. International Transport Forum.
27. Grabe, P. and Maree, J. (1997). *Use of a dynamic track stabilizer to improve track maintenance and optimization of track tamping*. RTR Railway Technical review.
28. Greene, J.C., and Caracelli, V.J. (1997). Defining and describing the paradigm issue in mixed method evaluation. *Advances in mixed-method evaluation: The challenges and benefits of integrating diverse paradigms. New Directions for Evaluation*, no. 74, pp. 5-17. San Francisco: Jossey-Bass.
29. Grimes, C. A. (1995). Application of genetic techniques to the planning of railway track maintenance work. *1st International Conference on Genetic Algorithms in Engineering Systems: Innovations and Applications*, vol. 414, pp. 467-472. Galesia.
30. Gupta, S., Liu, W., Degrande, G., Lombaert, G. and Liu, W. (2008). Prediction of vibrations induced by underground railway traffic in Beijing. *Journal of Sound and Vibration*, vol. 310 (3), pp. 608-630.
31. Hamdy T. (1997). *Operations Research: An Introduction*. 6th Edition. Prentice Hall, Inc.
32. Heij, C., Boer, Franses, P., Kloek, T. and Dijk H.K. (2004). *Econometric Methods with Application in Business and Economics*. Oxford: Oxford University Press.
33. Henriksson, U. (2003). *Power Spectrum and Bandwidth*. Available: http://www.commsys.isy.liu.se/TSDT45/Material/UlfsSpectrum2003.pdf [Accessed 12 December 2013].
34. Hokstad, P., Langseth, H., Lindqvist, B. and Vatn, P. (2005). Failure modeling and maintenance optimization for a railway line. *International Journal of Performability Engineering*, vol. 1(1), pp. 51–64.
35. Holmgren, M. (2005). Maintenance-related losses at the Swedish Rail. *Journal of Quality in Maintenance Engineering*, vol. 11, no. 1, pp. 5-18.
36. Hummitszch, R. (2005). *Calculation Schemes for MDZ and "Modified Standard Deviation".* Technical University of Graz.
37. Iwnicki, S., Grassie, and Kik, W. (1999). Track settlement prediction using computer simulation tools. *Vehicle System Dynamics Supplement* pp. 37–46.

38. Jendel, T. (1999). Prediction of wheel and rail wear. *TRITA-FKT Report 20002:22*. Royal Institute of technology, Railway technology. Sweden. ISSN 1103-470X.
39. Jianbin, L. and Songliang L. (2008). Study on the Relationship between Track Irregularity Spectrum Area and Track Quality Index. *Journal of Shijiazhuang Railway Institute (Natural Science)*. ISSN: 1674-0300.
40. Jianmin, Z. (2007). *Modelling and optimizing track maintenance and renewal*. Phd Thesis, Civil Engineering Department, University of Birmingham.
41. Johansson, A., Nielsen, J., Bolmsvik, R. and Karlström, A. (2008). Under sleeper pads - Influence on dynamic train track interaction. *Wear*, vol. 265, pp. 1479-1487.
42. Jovanovic, S. (2004). Railway track quality assessment and related decision making. *Systems, Man and Cybernetics. IEEE International Conference*, vol. 6, pp. 5038-5043.
43. Ju, S., Liao, R., Ye, Y. (2010). Behavior of ground vibrations induced by trains moving on embankments with rail roughness. *Soil Dynamics and Earthquake Engineering*, vol. 30, pp. 1237-1249.
44. Judge, T. (2002). To grind, or not to grind?. *Railway Age*, vol. 203(11), pp. 33.
45. Karttunen, K. (2012). *Mechanical track deterioration due to lateral geometry irregularities.* Licentiate thesis. Applied Mechanics Department, Chalmer University of Technology.
46. Kumar, S. (2006) *A Study of the Rail Degradation Process to Predict Rail Breaks*. Licentiate Thesis. Division of Operation and Maintenance Engineering, Lulea University of Technology, Lulea, Sweden. ISSN: 1402-1757.
47. Larsson, D. (2004*). A study of the track degradation process related to changes in railway traffic*. Division of Operation and Maintenance Engineering, Luleå University of Technology, Luleå, Sweden. ISSN: 1402-1757.
48. Lei, X, and Noda, N. A. (2002). Analysis of Dynamic Response of Vehicle and Track Coupling System with Random Irregularity of Track Vertical Profile. *Journal of Sound and Vibration*, vol. 258(1), pp. 147-165.
49. Lichtberger, B. (2005). *Track Compendium: Formation, Permanent way, maintenance, economics*. 1st Edition, ISBN 3-7771-0320-9. Hamburg, Germany.
50. Lichtberger, B. (2001). *Track maintenance strategies for ballasted track- a selection*. Rail engineering international ed., no. 2.

51. Lin, J., Chen, J., and Su, Y. (2004) Theory Analysis and Test Research of Chinese Main Track Irregularities PSD [J]. *Chinese Journal of Mechanical Engineering*, vol. 40(1), pp. 174-178.
52. Lindner, D. (1999). *Introduction to Signal and System*. Mc-Graw Hill International Edition.
53. Liu, L., Wang, J. and Rui (2011). Finite Element Analysis of Ballastless Track Rail-Floating Slab's Dynamic Characteristics. *Applied Mechanics and Material Journal*, vol. 44-47, pp. 3907-3911.
54. Lofsten, H. (1999). Management of industrial maintenance – economic evaluation of maintenance policies. International Journal of Operations & Production Management, vol. 19, Iss: 7, pp. 716-737.
55. Lundqvist, A. and Dahlberg, T. (2005). Railway track stiffness variations – consequences and countermeasures. *Proceedings of the 19th IAVSD symposium on dynamics of vehicles on roads and on tracks*. Milan, Italy.
56. Lyngby, N. (2009). Railway Track Degradation: Shape and Influencing factors. *International Journal of Performability Engineering*, vol. 5(2), pp. 177-186.
57. Lyngby, N., Hokstad, P., and Vatn, J. (2008). *RAMS Management of Railway Tracks*. Handbook of Performability Engineering, pp. 1123-1145. Springer Verlag. ISBN 9781848001305.
58. Madejski, J. and Grabczyk, J. (2002). Continuous geometry measurement for diagnostics of tracks and switches. *Proceedings of the International Conference on Switches Delft University of Technology*. Delft, Netherlands.
59. Magel, E. and Kalousek, J. (2002). The application of contact mechanics to rail profile design and rail grinding. *Wear*, vol. 253(1-2), pp. 308-316.
60. Martland, C. D., Hargrove, M.B. and Auzmendi, A.R. (1994). TRACS: A tool for managing change. *Railway Track and Structures*, vol. 90, pp. 27-29.
61. Memolub (2013). *Rail Lubrication*. Available: http://www.memolub.com/index.cfm?fuseaction=applications.casestudy&caseID=22 [Accessed 20 December 2013].
62. Naser, J., M. and Toledano, F., S. (2010). *Analysis of vibration-induced fatigue cracking on steel bridges*. Master Thesis. Civil and Environmental Engineering Department, Chalmers University of Technology.

63. Oyama, T. and Miwa, M. (2006). Mathematical modeling analysis for obtaining an optimal railway track maintenance. *Japan Journal of Industrial and applied mathematics*, vol. 23, no. 2, pp. 207-224.

64. Pita, A. L., Teixeira, P. F. and Robusté, F. (2004). High Speed and track deterioration: the role of vertical stiffness of the track. *Part F: Journal of Rail and Rapid Transit*. Proceedings of the Institution of Mechanical Engineering, vol. 218, pp. 31-40.

65. Plasser and Theurer (2013). *Machines and Systems*. Available: http://www.plassertheurer.com/en/machines-systems/tamping-109-4x-dynamic.html [Accessed 20 December 2013].

66. prEN 13848-5:2005. *Railway applications – Track - Track geometry quality - Part 5: Geometric quality assessment.* English version.

67. Profillidis, V. A. (2000). *Railway Engineering*. 2nd edition. Ashgate Publishing Limited.

68. Rao, S. (1992). Upgradation of track for higher speed and rectification of long wave length defects in track geometry. *Proceedings of the Conference Cost-effective Maintenance of Railway Track*, vol.1, pp. 51–62. London, UK.

69. Reddy, V., Gopinath, G., Kraik, L. and Doug, J. (2007). Modelling and analysis of rail maintenance cost. *International Journal of Production Economics*, vol. 105, pp. 475-482.

70. Remtech (2010). *Ballast Cleaning – REM Z45*. Available: http://www.remtech.info/REMZ45.htm [Accessed 20 December 2013].

71. Rosenberg, R., Amjad, M., Breeze, P., Brillinger, R. and Halliday, D.M. (1989). The Fourier approach to the identification of functional coupling between neuronal spike trains. *Prog. Biophys Mol Biol*, vol. 53, pp. 1–31.

72. Sadeghi, J. and Asgarinejad, H. (2007). Influences of track structure, geometry and traffic parameters on railway deterioration. *International Journal of engineering*, vol. 20, no. 3.

73. Sadeghi, J. and Asgarinejad, H. (2008). Development of Improved Railway Track Degradation Models. *International Journal of Structure and infrastructure Engineering*, vol. 3, Issue 4.

74. Sato, Y. (1995). Japanese studies on deterioration of ballasted track. *Vehicle system dynamic*, vol 24, pp. 197–208.
75. Selig, E. and Waters, M. (1994). *Track geotechnology and substructure management*. Thomas Telford, London.
76. Shenton, M. J. (1984). Ballast deformation and track deterioration. *Proceedings of a Conference on Track Technology*. University of Nottingham, pp. 253–265. Thomas Telford Limited, London.
77. Shimatake, M. (1997). *Track maintenance model for high speed rail: a systemic dynamics approach*. Master Thesis. Civil Engineering Department, Massachusetts Institute of Technology.
78. Song, K., Noh, H., and Choi, K., (2003). A new three-dimensional finite element analysis model of high-speed train-bridge interactions. *Engineering Structures*, vol. 25, pp. 1611–1626.
79. Sroba, P. (2006). *Rail Grinding Best Practice for Amtrak*, Revision 1. Available: http://www.arema.org/files/library/2003_Conference_Proceedings/0062.pdf [Accessed 20 December 2013].
80. Strauss, A. & Corbin, J. (1998). *Basics of qualitative research: Techniques and procedures for developing grounded theory*. Thousand Oaks, CA: Sage.
81. Talukdar, K., Arulmozhi, U., Prabhakar, K., and Satyanarayan (2006). *Project Presentation Improvement of TGI Value by Computer Analysis*. Ministry of Railways Indian Railways Institute of Civil Engineering, India.
82. Total Track (2013). *PTS-90-C Track Stabilizer*. Available: http://www.totaltrack.ca/pages/Dynamic%20Track%20Stabilizer.html [Accessed 20 December 2013].
83. Tzanakakis, K. (2013). The railway track and its long term behavior. *Springer Tracts on Transportation and Traffic*, vol. 2, pp195-197.
84. Unitedindustrial (2013). *Dynamic Track Stabilizer*. Available: http://www.unitedindsupply.com/dynamic-track-stabiliser.html [Accessed 20 December 2013].
85. Vale, C., Ribeiro, I., Calcada, R. (2010). Application of a maintenance model for optimizing tamping on ballasted tracks: the influence of the model constraints, *2nd International Conference on Engineering Optimization*. Lisbon, Portugal.

86. Witt, S. (2008). *The Influence of Under Sleeper Pads on Railway Track Dynamics*. Linköping University, LIU-IEITEK- A-08/00442-SE.

87. Xia, F. (2002). *The Dynamics of the Three Piece Freight Truck*. PhD thesis. Informatics and Mathematical modeling, Technical University of Denmark, DTU.

88. Xianmai, C., Wang, L., Xiaxin, T., Gaohang, C., Fengchun, Y., Xuesong, and Wangqing, W. (2008). Study on the Judgment Method for Track irregularity of the Main railway lines in China. *Journal of China Railway Science,* vol. 9, no. 4, pp. 22-27.

89. Yang, B., Yau, D. and Wu, Y. (2004). *Vehicle-Bridge Interaction Dynamics, with Applications to High-Speed Railway.* World Scientific.

90. Li, Z. and Lian, S. (2011) An Improved Method for Mitigating End Effects in Empirical Mode Decomposition and Its Applications to Track Irregularity Analysis. *International Conference of Chinese Transportation Professionals (ICCTP).* Nanjing, China.

91. Zarembski, A. M. (1991). Forecasting of track component lives and its use in track maintenance planning. *International Heavy Haul Association/Transportation Research Board Workshop*. Vancouver, B.C.

92. Zhang, J., Murray, H. and Ferreira, L. (1999). An Integrated Model for Track Degradation Prediction. *World Transport Research: Selected Proceedings of the 8th World Conference on Transport Research*, vol. 3, pp. 527–539. Elsevier Science, UK.

93. Zhang, Q., Vrouwenvelder, A. and Wardenier, J. (2001). Numerical Simulation of Train-Bridge Interactive Dynamics. *Computers & Structures*, vol. 79, pp. 1059-1075.

94. Zhang, Z., Lin, J., Zhang, Y., Zhao, Y., Howson. P., and Williams, F., (2010). Non-stationary random vibration analysis for train-bridge systems subjected to horizontal earthquakes. *Engineering Structures*, vol.32, no. 11, pp. 3571–3582. ISBN/ISSN: 0141-0296.

95. Zhiping, Z. and Shouhua, J. (2009). PSD Analysis of Slab Ballastless Track Irregularity of Qinhuangdao-Shenyang Dedicated Passenger Railway Line. *Intelligent Computation Technology and Automation. Second International Conference on ICICTA*, vol.3, pp. 669-672.

96. Zhiping, Z., Shouhua, and Zhiwu, Y. (2009). Analysis of Bogl Slab Track irregularities of Beijing-Tianjin intercity high speed railway. *Proceedings of the Second International Conference on Transportation Engineering*. Southwest Jiantong University, vol. 2, pp. 1408-1413. China.

97. Zhiqiang, L., Shihui, L., Weihua, M. and Rongrong, S. (2009). Application research of track irregularity PSD in the High Speed Train dynamic simulation. *Proceedings of the Second International Conference on Transportation Engineering*, vol. 4, pp. 2845-2850.

98. Zoetaman, A. and Esveld, C. (2005). State of the art in railway maintenance management: planning system, and their application in Europe. *Preceding paper in IEEE International conference on systems, man and cybernetics, v*ol. 5, pp. 4165-4170.

99. Zuo, Y. and Xiang, J. (2006). Correlation analysis of track irregularities of Zhengzhou - Wuhan Railway. *Journal of Railway Science and Engineering*. ISSN: 1000-2499.

100. Zwanenburg, W. J. (2006). Degradation Processes of Switches & Crossings. Railway Condition Monitoring. *The Institution of Engineering and Technology International Conference*, pp.115-119.

APPENDICES

A. THE DEGRADATION RATES OF LONGITUDINAL PROFILE

Block	Period 2 [Days 380 - 1232]								Degrad. Rate
	Left Profile				Right Profile				
	α	β	R^2	n	α	β	R^2	n	
1	0.0011	-0.27	0.98	11	0.0010	-0.07	0.97	11	0.0011
2	0.0009	0.02	0.97	11	0.0012	-0.41	0.97	11	0.0011
3	0.0014	-0.34	0.95	11	0.0011	-0.10	0.94	11	0.0013
4	0.0014	-0.52	1.00	7	0.0012	-0.09	0.98	7	0.0013
5	0.0003	1.52	0.73	7	0.0004	1.30	0.98	7	0.0004
6	0.0011	-0.25	0.91	11	0.0014	-0.33	0.95	11	0.0012
7	0.0009	0.76	0.98	4	0.0018	-1.10	0.99	8	0.0013
8	0.0009	0.24	0.73	11	0.0010	-0.44	0.89	11	0.0010
9	0.0015	-0.71	0.97	10	0.0022	-1.32	0.99	7	0.0018
10	0.0009	-0.08	0.92	10	0.0008	-0.14	0.84	10	0.0008
11	0.0018	-1.55	0.97	8	0.0024	-2.38	0.96	8	0.0021
12	0.0021	-1.58	0.86	10	0.0029	-2.43	0.93	10	0.0025
13	0.0013	-0.72	0.93	10	0.0019	-1.03	0.95	10	0.0016
14	0.0010	0.04	0.91	8	0.0021	-0.71	0.46	8	0.0016
15	0.0015	-0.23	0.66	8	0.0014	-0.42	0.93	8	0.0015
16	0.0018	-1.52	0.99	8	0.0008	0.44	0.91	7	0.0013

17	0.0007	0.30	0.98	11	0.0008	0.07	0.99	11	0.0007
18	0.0011	0.41	0.98	8	0.0010	0.26	0.97	8	0.0010
19	0.0014	-0.31	0.87	11	0.0013	-0.41	0.98	11	0.0013
20	0.0015	-0.46	0.99	11	0.0009	0.00	0.97	11	0.0012
21	0.0010	-0.12	0.76	10	0.0006	0.27	0.86	10	0.0008
22	0.0011	-0.22	0.99	11	0.0006	0.20	0.96	11	0.0008
23	0.0007	0.66	0.44	11	0.0009	0.09	0.89	11	0.0008
24	0.0010	0.41	0.75	11	0.0021	-1.26	0.96	8	0.0016
25	0.0017	-0.55	0.92	8	0.0014	-0.01	0.81	8	0.0015
26	0.0006	-0.09	0.96	11	0.0006	0.09	0.95	11	0.0006
27	0.0007	-0.22	0.98	11	0.0006	0.01	0.96	11	0.0007
28	0.0007	0.10	0.92	11	0.0007	0.11	0.97	11	0.0007
29	0.0005	0.07	0.94	10	0.0006	0.06	0.97	10	0.0006
30	0.0004	0.49	0.85	11	0.0005	0.19	0.93	11	0.0005
31	0.0009	0.01	0.97	11	0.0009	0.28	0.98	11	0.0009
32	0.0008	-0.04	0.89	5	0.0005	0.27	0.85	11	0.0007
33	0.0012	-0.39	0.95	11	0.0013	-0.30	0.98	11	0.0013
34	0.0008	-0.48	0.75	11	0.0016	-0.67	0.71	11	0.0012
35	0.0007	-0.22	0.97	11	0.0009	-0.21	0.98	11	0.0008
36	0.0012	-0.27	0.99	11	0.0007	0.20	0.94	11	0.0009
37	0.0008	-0.30	0.58	11	0.0010	-0.24	0.95	11	0.0009
38	0.0007	0.12	0.97	11	0.0006	0.04	0.95	11	0.0006

39	0.0007	-0.13	0.96	11	0.0009	-0.35	0.98	11	0.0008
40	0.0005	0.11	0.97	11	0.0007	0.05	0.98	11	0.0006
41	0.0016	-0.65	0.95	8	0.0016	-0.66	0.98	7	0.0016
42	0.0014	-0.68	0.84	11	0.0008	0.21	0.92	11	0.0011
43	0.0011	0.55	0.99	11	0.0010	0.71	0.98	11	0.0011
44	0.0005	0.65	0.98	11	0.0003	0.45	0.96	11	0.0004
45	0.0007	0.35	0.71	11	0.0005	0.10	0.79	11	0.0006
46	0.0007	0.79	0.97	11	0.0002	1.13	0.50	11	0.0005
47	0.0008	0.78	0.99	11	0.0004	0.43	0.97	11	0.0006
48	0.0007	0.56	0.93	11	0.0007	0.56	0.94	11	0.0007
49	0.0007	0.82	0.76	4	0.0008	1.30	0.83	4	0.0007
50	0.0007	0.99	0.94	10	0.0009	1.05	0.99	10	0.0008
51	0.0007	1.08	0.94	11	0.0006	0.89	0.95	11	0.0007
52	0.0007	0.49	0.97	11	0.0007	0.44	0.96	11	0.0007
53	0.0006	0.13	0.97	11	0.0004	0.55	0.93	11	0.0005
54	0.0006	0.01	0.95	11	0.0007	0.23	0.98	11	0.0007
55	0.0008	-0.11	0.94	11	0.0007	-0.03	0.96	11	0.0007
56	0.0009	-0.30	0.92	10	0.0005	0.52	0.90	10	0.0007
57	0.0009	-0.21	0.78	10	0.0013	-0.58	0.85	10	0.0011
58	0.0012	-0.50	0.97	11	0.0011	-0.48	0.98	11	0.0012
59	0.0007	0.14	0.92	11	0.0006	0.30	0.88	11	0.0007
60	0.0018	-1.48	0.85	11	0.0013	-0.43	0.82	11	0.0016

61	0.0010	-0.10	0.96	11	0.0007	0.01	0.96	11	0.0008
62	0.0003	0.50	0.61	11	0.0003	0.25	0.82	11	0.0003
63	0.0010	0.61	0.80	6	0.0010	0.20	0.89	8	0.0010
64	0.0005	0.25	0.85	9	0.0009	-0.11	0.75	8	0.0007
65	0.0008	-0.10	0.93	9	0.0006	-0.06	0.85	9	0.0007
66	0.0002	1.58	0.02	9	0.0003	0.68	0.26	9	0.0003
67	0.0023	-1.98	0.82	9	0.0016	-1.20	0.84	9	0.0019
68	0.0016	-0.84	0.88	9	0.0013	-0.89	0.88	9	0.0015
69	0.0005	0.26	0.95	9	0.0005	0.24	0.88	9	0.0005
70	0.0005	0.46	0.91	9	0.0006	0.48	0.86	9	0.0006
71	0.0009	-0.39	0.93	9	0.0006	0.24	0.79	9	0.0008
72	0.0010	-0.12	0.97	9	0.0010	-0.23	0.95	9	0.0010
73	0.0010	1.16	0.97	11	0.0008	1.14	0.96	11	0.0009
74	0.0006	0.87	0.99	11	0.0006	0.60	0.99	11	0.0006
75	0.0006	-0.15	0.97	11	0.0009	-0.27	0.91	11	0.0008
76	0.0010	-0.66	0.96	11	0.0010	0.10	0.97	11	0.0010
77	0.0005	0.27	0.90	11	0.0006	1.12	0.82	9	0.0005
78	0.0007	0.08	0.97	11	0.0007	0.15	0.96	11	0.0007
79	0.0009	-0.09	0.96	11	0.0009	-0.18	0.96	11	0.0009
80	0.0002	0.10	0.89	11	0.0006	0.00	0.94	11	0.0004
81	0.0004	0.08	0.93	11	0.0009	-0.37	0.99	11	0.0006
82	0.0006	0.00	0.98	11	0.0005	-0.09	0.98	11	0.0006

83	0.0005	0.33	0.95	10	0.0002	0.67	0.74	10	0.0003
84	0.0009	0.45	0.96	10	0.0007	0.75	0.80	10	0.0008
85	0.0002	1.15	0.64	8	0.0003	1.44	0.75	11	0.0003
86	0.0007	1.94	0.67	11	0.0002	2.59	0.48	11	0.0004
87	0.0014	2.05	0.97	6	0.0014	1.68	0.96	6	0.0014
88	0.0011	3.20	0.41	6	0.0010	2.55	0.73	6	0.0011
89	0.0010	1.34	0.97	10	0.0006	2.31	0.83	10	0.0008
90	0.0015	1.42	0.71	7	0.0033	-1.29	0.82	9	0.0024
91	0.0012	-0.62	1.00	11	0.0016	-1.11	1.00	11	0.0014
92	0.0013	-0.03	0.91	11	0.0013	-0.04	0.89	11	0.0013
93	0.0012	-0.60	0.96	11	0.0010	0.05	0.76	11	0.0011
94	0.0007	0.15	0.54	11	0.0008	0.18	0.51	11	0.0008
95	0.0014	-0.43	0.92	11	0.0012	-0.41	0.96	11	0.0013
96	0.0014	-0.78	0.96	10	0.0013	-0.79	0.97	10	0.0014
97	0.0020	-0.85	1.00	7	0.0010	-0.06	0.96	10	0.0015
98	0.0011	-0.37	0.98	10	0.0005	0.30	0.95	10	0.0008
99	0.0006	0.49	0.92	8	0.0007	0.50	0.85	9	0.0006
100	0.0013	-0.11	0.97	10	0.0009	0.10	0.94	10	0.0011
101	0.0012	0.17	0.92	10	0.0009	0.16	0.74	10	0.0010
102	0.0009	0.79	0.50	11	0.0007	0.50	0.44	11	0.0008
103	0.0010	0.40	0.95	11	0.0010	0.08	0.91	11	0.0010
104	0.0012	-0.56	0.96	11	0.0007	-0.18	0.88	11	0.0010

105	0.0010	-0.38	0.97	11	0.0001	0.43	0.70	11	0.0005
106	0.0011	-0.63	0.98	11	0.0007	-0.03	0.93	11	0.0009
107	0.0007	0.22	0.55	11	0.0012	-0.34	0.82	11	0.0009
108	0.0010	-0.43	0.95	11	0.0010	-0.40	0.95	11	0.0010
109	0.0007	0.16	0.93	11	0.0006	0.25	0.90	11	0.0007
110	0.0009	0.19	0.97	11	0.0008	0.30	0.94	11	0.0009
111	0.0009	0.60	0.91	6	0.0007	0.90	0.82	6	0.0008
112	0.0011	-0.01	0.97	11	0.0007	0.35	0.95	11	0.0009
113	0.0008	0.47	0.61	9	0.0010	0.31	0.72	8	0.0009
114	0.0010	-0.11	0.59	11	0.0005	0.69	0.65	11	0.0008
115	0.0005	0.17	0.93	10	0.0004	0.42	0.90	9	0.0004
116	0.0016	-0.66	0.83	4	0.0010	1.06	0.10	5	0.0013
117	0.0007	0.26	0.97	9	0.0005	0.38	0.92	9	0.0006
118	0.0005	1.00	0.93	10	0.0005	1.08	0.92	10	0.0005
119	0.0001	1.13	0.32	10	0.0002	1.03	0.76	9	0.0001
120	0.0004	0.88	0.92	10	0.0003	0.98	0.88	10	0.0004
121	0.0007	1.12	0.51	8	0.0011	0.64	0.61	6	0.0009
122	0.0012	-0.24	0.96	11	0.0010	-0.04	0.98	11	0.0011
123	0.0008	0.24	0.95	11	0.0007	0.48	0.93	11	0.0007
124	0.0024	-2.17	0.96	8	0.0027	-2.76	0.87	8	0.0025
125	0.0005	1.62	0.53	11	0.0009	0.96	0.84	11	0.0007
126	0.0014	-0.02	0.86	5	0.0011	0.56	0.66	8	0.0012

127	0.0013	0.23	0.94	6	0.0020	-1.31	0.98	6	0.0016
128	0.0030	-3.04	0.99	6	0.0047	-5.49	0.98	6	0.0038
129	0.0019	-0.66	0.78	7	0.0016	-0.23	0.92	8	0.0018
130	0.0008	0.79	0.75	10	0.0008	0.56	0.81	10	0.0008
131	0.0008	0.64	0.60	9	0.0013	0.09	0.61	9	0.0011
132	0.0019	-1.12	0.45	10	0.0005	0.64	0.57	9	0.0012
133	0.0016	-0.42	0.81	7	0.0018	-0.38	0.81	8	0.0017
134	0.0007	0.27	0.90	11	0.0008	-0.19	0.98	11	0.0007
135	0.0005	0.24	0.97	11	0.0005	0.30	0.90	11	0.0005
136	0.0016	-0.86	0.97	11	0.0013	-0.53	0.97	11	0.0015
137	0.0014	-0.78	0.96	11	0.0011	-0.40	0.97	11	0.0013
138	0.0008	0.11	0.95	11	0.0008	0.11	0.92	11	0.0008
139	0.0009	-0.29	0.90	9	0.0024	-1.95	0.79	10	0.0016
140	0.0010	-0.41	0.76	11	0.0014	-1.14	0.86	11	0.0012
141	0.0009	0.16	0.76	11	0.0015	-0.44	0.63	11	0.0012
142	0.0006	0.61	0.53	11	0.0009	-0.37	0.93	11	0.0007
143	0.0017	0.24	0.73	11	0.0007	0.29	0.82	11	0.0012
144	0.0008	0.59	0.77	11	0.0006	0.08	0.74	11	0.0007
145	0.0013	0.15	0.96	11	0.0012	-0.05	0.98	11	0.0012
146	0.0011	-0.75	0.70	11	0.0011	-0.69	0.89	11	0.0011
147	0.0008	0.67	0.10	11	0.0007	0.97	0.08	11	0.0008
148	0.0009	-0.23	0.99	10	0.0009	0.14	0.87	10	0.0009

149	0.0021	-2.32	0.80	8	0.0006	0.37	0.96	10	0.0013
150	0.0002	0.56	0.87	7	0.0008	0.31	0.93	10	0.0005
151	0.0010	0.33	0.87	10	0.0008	0.29	0.85	11	0.0009
152	0.0012	0.01	0.89	9	0.0009	0.72	0.96	9	0.0011
153	0.0009	0.92	0.41	7	0.0005	1.65	0.23	5	0.0007
154	0.0011	1.28	0.34	8	0.0008	2.57	0.41	4	0.0010
155	0.0010	1.07	0.98	5	0.0010	1.44	0.96	5	0.0010
156	0.0009	0.64	0.61	8	0.0009	1.07	0.73	8	0.0009
157	0.0015	-0.53	0.97	7	0.0014	-0.27	0.96	6	0.0015
158	0.0019	-1.03	0.50	6	0.0017	-0.51	0.30	5	0.0018
159	0.0004	0.92	0.85	4	0.0014	0.10	0.67	5	0.0009
160	0.0009	1.01	0.84	4	0.0011	0.86	0.52	6	0.0010
161	0.0011	0.96	0.98	10	0.0010	1.04	0.98	10	0.0010
162	0.0011	1.23	0.98	10	0.0006	1.34	0.94	10	0.0009
163	0.0005	0.71	0.98	10	0.0006	0.92	0.90	10	0.0005
164	0.0003	0.50	0.97	10	0.0002	0.63	0.94	10	0.0003
165	0.0004	0.49	0.97	8	0.0002	0.79	0.94	7	0.0003
166	0.0002	0.21	0.89	8	0.0001	0.36	0.49	8	0.0002
167	0.0001	0.30	0.98	5	0.0001	0.42	0.82	5	0.0001
	Average		0.86		Average		0.85		0.0010

B. THE DEGRADATION RATES OF ALIGNMENT

Block	Period 2 [Days 380 - 1232]								Degrad. Rate
	Left Alignment				Right Alignment				
	a	β	R^2	n	a	β	R^2	n	
1	0.0002	0.59	0.41	6	0.0003	0.20	0.70	9	0.0003
2	0.0008	-0.42	0.47	8	0.0007	-0.07	0.86	11	0.0007
3	0.0002	0.51	0.51	11	0.0004	0.22	0.78	11	0.0003
4	0.0005	0.10	0.80	7	0.0003	0.28	0.78	9	0.0004
5	0.0005	0.35	0.86	10	0.0004	0.16	0.79	9	0.0004
6	0.0012	-0.22	0.98	10	0.0010	-0.58	0.97	11	0.0011
7	0.0006	0.42	0.82	9	0.0005	0.10	0.90	7	0.0006
8	0.0003	0.51	0.82	8	0.0002	0.40	0.73	10	0.0002
9	0.0004	0.57	0.48	8	0.0004	0.89	0.49	8	0.0004
10	0.0008	-0.04	0.39	11	0.0009	-0.09	0.53	10	0.0008
11	0.0016	-1.18	0.63	7	0.0017	-1.30	0.93	7	0.0017
12	0.0014	-1.12	0.74	10	0.0015	-1.22	0.80	10	0.0015
13	0.0008	-0.02	0.67	10	0.0007	-0.38	0.86	8	0.0007
14	0.0007	0.39	0.60	9	0.0006	0.36	0.48	8	0.0006
15	0.0009	-0.06	0.51	10	0.0008	-0.39	0.53	10	0.0009
16	0.0006	0.11	0.64	10	0.0007	0.82	0.87	11	0.0007
17	0.0003	0.48	0.49	8	0.0004	0.70	0.78	11	0.0003
18	0.0004	0.36	0.84	7	0.0003	0.40	0.41	11	0.0003

19	0.0007	0.01	0.51	10	0.0007	-0.23	0.56	11	0.0007
20	0.0005	0.36	0.79	10	0.0008	-0.42	0.83	11	0.0006
21	0.0003	0.77	0.60	5	0.0006	-0.54	0.78	7	0.00044
22	0.0004	0.95	0.76	11	0.0005	-0.07	0.78	9	0.00046
23	0.0006	0.04	0.68	9	0.0002	0.57	0.56	11	0.00043
24	0.0005	0.30	0.67	7	0.0007	0.71	0.62	5	0.00062
25	0.0008	-0.11	0.77	8	0.0008	0.58	0.81	3	0.00082
26	0.0003	0.27	0.92	6	0.0005	-0.08	0.44	9	0.00042
27	0.0002	0.29	0.82	8	0.0006	-0.04	0.61	9	0.00041
28	0.0003	0.32	0.82	6	0.0003	0.24	0.79	8	0.00031
29	0.0002	0.62	0.78	5	0.0003	0.11	0.72	6	0.00023
30	0.0004	0.71	0.63	7	0.0003	0.12	0.63	10	0.00038
31	0.0004	0.19	0.73	11	0.0002	0.64	0.62	10	0.00028
32	0.0005	-0.06	0.77	11	0.0006	0.00	0.91	6	0.00055
33	0.0004	0.21	0.63	11	0.0004	0.21	0.83	9	0.00039
34	0.0006	-0.13	0.58	11	0.0007	0.33	0.90	10	0.00063
35	0.0004	0.31	0.84	11	0.0002	0.59	0.81	8	0.00029
36	0.0005	-0.10	0.68	8	0.0008	-0.60	0.79	9	0.00068
37	0.0007	-0.29	0.72	9	0.0007	-0.15	0.84	6	0.00067
38	0.0003	0.25	0.27	11	0.0006	-0.17	0.73	9	0.00042
39	0.0003	0.20	0.67	11	0.0004	0.17	0.77	8	0.00034
40	0.0003	0.27	0.80	7	0.0005	-0.10	0.67	9	0.00037

41	0.0002	0.41	0.54	11	0.0006	-0.43	0.73	11	0.00044
42	0.0002	0.60	0.58	10	0.0005	0.07	0.69	11	0.00034
43	0.0002	1.12	0.65	8	0.0004	0.39	0.84	11	0.00030
44	0.0003	1.11	0.84	5	0.0003	0.40	0.89	7	0.00027
45	0.0002	1.68	0.63	7	0.0006	-0.13	0.57	8	0.00037
46	0.0005	1.22	0.70	6	0.0006	0.10	0.73	11	0.00055
47	0.0002	0.80	0.43	6	0.0003	0.33	0.62	11	0.00028
48	0.0004	0.27	0.71	7	0.0004	0.05	0.63	10	0.00042
49	0.0006	0.38	0.71	7	0.0004	0.44	0.52	10	0.00047
50	0.0005	0.20	0.66	7	0.0003	0.28	0.56	11	0.00039
51	0.0002	0.70	0.78	7	0.0003	0.31	0.65	11	0.00023
52	0.0003	0.42	0.74	9	0.0004	0.28	0.71	11	0.00036
53	0.0002	0.27	0.63	10	0.0002	0.69	0.82	8	0.00021
54	0.0004	0.02	0.87	7	0.0002	1.08	0.56	8	0.00030
55	0.0003	0.14	0.56	7	0.0001	0.92	0.60	9	0.00022
56	0.0002	0.79	0.46	5	0.0007	0.20	0.69	8	0.00044
57	0.0002	0.55	0.58	4	0.0002	1.21	0.57	4	0.00016
58	0.0003	0.28	0.63	4	0.0002	0.84	0.89	4	0.00023
59	0.0006	-0.07	0.51	10	0.0002	0.93	0.50	7	0.00040
60	0.0006	-0.05	0.62	8	0.0002	0.82	0.40	6	0.00038
61	0.0001	0.57	0.58	10	0.0004	0.31	0.68	9	0.00025
62	0.0003	0.50	1.00	3	0.0004	-0.11	0.67	8	0.00036

63	NaN	NaN	NaN	NaN	0.0006	0.19	0.50	11	0.00064
64	0.0005	0.57	0.84	4	0.0006	0.11	0.66	9	0.00051
65	0.0002	1.39	0.57	4	0.0007	-0.22	0.61	11	0.00044
66	0.0004	1.30	0.57	6	0.0007	-0.10	0.47	7	0.00055
67	0.0007	-0.09	0.89	8	0.0007	-0.43	0.71	9	0.00071
68	0.0003	0.50	0.53	9	0.0003	0.28	0.84	9	0.00029
69	0.0003	0.59	0.63	10	0.0004	-0.08	0.76	9	0.00035
70	0.0007	-0.14	0.49	11	0.0004	0.01	0.68	9	0.00055
71	0.0003	0.64	0.74	7	0.0002	0.27	0.49	7	0.00023
72	0.0005	0.22	0.68	9	0.0004	0.00	0.76	9	0.00048
73	0.0003	0.38	0.81	8	0.0002	0.48	0.42	7	0.00028
74	0.0003	0.33	0.59	8	0.0003	0.51	0.60	11	0.00029
75	0.0002	0.21	0.47	10	0.0002	0.66	0.68	4	0.00022
76	0.0003	0.19	0.71	11	0.0005	0.46	0.91	4	0.00042
77	0.0004	0.10	0.63	9	0.0004	0.63	0.70	7	0.00041
78	0.0002	0.52	0.54	9	0.0003	0.44	0.89	6	0.00023
79	0.0002	0.33	0.59	6	0.0002	0.72	0.59	8	0.00020
80	0.0001	0.76	0.58	5	0.0002	0.22	0.62	11	0.00016
81	0.0002	0.75	0.65	7	0.0003	0.07	0.77	11	0.00025
82	0.0001	0.77	0.75	7	0.0002	0.18	0.76	11	0.00015
83	0.0002	0.40	0.80	5	0.0003	0.24	0.73	5	0.00024
84	0.0003	0.84	0.89	6	0.0005	0.44	0.70	10	0.00041

85	0.0003	2.04	0.88	5	0.0003	1.66	0.51	8	0.00033
86	0.0003	2.18	0.31	6	0.0010	1.42	0.39	4	0.00064
87	0.0001	1.57	0.13	5	0.0007	0.36	0.92	4	0.00037
88	0.0004	1.42	0.83	6	0.0011	0.06	0.91	4	0.00074
89	0.0007	1.89	0.66	6	0.0008	2.04	0.75	4	0.00077
90	0.0018	1.31	0.37	7	0.0030	-0.86	0.71	4	0.00240
91	0.0003	0.37	0.69	10	0.0004	0.83	0.86	10	0.00035
92	0.0004	0.85	0.67	10	0.0001	0.63	0.59	10	0.00029
93	0.0004	0.98	0.57	8	0.0003	0.74	0.72	10	0.00037
94	0.0007	0.04	0.94	7	0.0004	0.31	0.51	11	0.00057
95	0.0002	0.43	0.42	7	0.0003	0.22	0.67	7	0.00028
96	0.0006	-0.22	0.51	10	0.0006	0.03	0.72	9	0.00061
97	0.0005	0.15	0.57	6	0.0002	0.73	0.49	7	0.00035
98	0.0004	0.25	0.64	10	0.0002	0.48	0.69	9	0.00030
99	0.0004	0.70	0.75	8	0.0004	0.40	0.72	9	0.00042
100	0.0004	0.28	0.55	8	0.0005	0.19	0.52	8	0.00045
101	0.0007	-0.11	0.67	9	0.0004	0.85	0.45	11	0.00056
102	0.0003	0.44	0.66	10	0.0004	0.23	0.75	10	0.00036
103	0.0003	0.96	0.65	11	0.0003	0.74	0.41	9	0.00027
104	0.0004	0.28	0.68	11	0.0004	0.36	0.77	10	0.00042
105	0.0003	0.14	0.78	7	0.0002	0.76	0.67	5	0.00025
106	0.0003	0.18	0.83	11	0.0002	0.63	0.69	11	0.00029

107	0.0003	0.36	0.85	5	0.0002	0.45	0.69	7	0.00027
108	0.0003	0.72	0.69	9	0.0003	0.26	0.44	9	0.00031
109	0.0003	0.72	0.63	8	0.0003	0.29	0.68	11	0.00028
110	0.0002	0.87	0.47	8	0.0004	0.26	0.65	8	0.00031
111	0.0003	0.72	0.55	7	0.0005	0.18	0.77	10	0.00040
112	0.0002	0.89	0.66	6	0.0005	0.10	0.80	11	0.00034
113	0.0004	0.93	0.97	4	0.0005	0.47	0.67	8	0.00042
114	0.0005	0.12	0.78	9	0.0002	1.16	0.53	9	0.00034
115	0.0003	0.18	0.66	10	0.0002	0.65	0.68	10	0.00023
116	0.0008	-0.58	0.92	5	0.0010	-0.55	0.99	5	0.00089
117	0.0003	0.12	0.57	8	0.0002	0.67	0.51	7	0.00026
118	0.0002	0.41	0.56	6	0.0003	0.61	0.76	8	0.00027
119	0.0001	0.43	0.65	6	0.0004	0.53	0.66	9	0.00025
120	0.0003	0.32	0.65	6	0.0003	0.74	0.35	8	0.00029
121	0.0007	1.20	0.54	7	0.0006	1.16	0.46	11	0.00063
122	0.0004	0.17	0.79	9	0.0007	-0.02	0.50	9	0.00055
123	0.0001	0.90	0.52	6	0.0005	0.18	0.57	11	0.00030
124	0.0007	0.51	0.79	6	0.0006	0.14	0.60	10	0.00067
125	0.0006	1.50	0.75	6	0.0005	0.86	0.68	10	0.00057
126	0.0005	0.55	0.71	10	0.0005	0.42	0.77	11	0.00051
127	0.0002	1.33	0.63	5	0.0004	1.24	0.48	10	0.00028
128	0.0003	0.74	0.50	6	0.0005	0.37	0.82	7	0.00037

129	0.0007	0.25	0.94	7	0.0010	-0.23	0.86	9	0.00088
130	0.0004	0.62	0.61	11	0.0006	-0.11	0.77	10	0.00048
131	0.0006	0.25	0.84	9	0.0008	-0.14	0.52	10	0.00072
132	0.0006	1.08	0.61	9	0.0010	-0.46	0.88	6	0.00081
133	0.0002	0.98	0.64	10	0.0006	0.22	0.81	6	0.00036
134	0.0003	0.10	0.52	7	0.0004	0.44	0.60	5	0.00038
135	0.0006	-0.09	0.69	10	0.0002	1.00	0.65	9	0.00040
136	0.0005	0.06	0.59	6	0.0004	0.05	0.55	11	0.00048
137	0.0003	0.57	0.71	8	0.0005	-0.03	0.66	10	0.00041
138	0.0004	0.53	0.76	10	0.0003	0.48	0.60	11	0.00032
139	0.0005	0.15	0.57	11	0.0005	0.38	0.70	10	0.00049
140	0.0016	-1.26	0.72	11	0.0009	-0.03	0.48	11	0.00121
141	0.0003	0.82	0.51	10	0.0007	0.21	0.75	10	0.00046
142	0.0005	0.48	0.87	7	0.0004	0.26	0.49	11	0.00046
143	0.0010	0.34	0.84	11	0.0005	0.30	0.50	11	0.00075
144	0.0004	0.85	0.61	6	0.0003	0.45	0.33	11	0.00035
145	0.0003	0.55	0.74	7	0.0003	0.72	0.79	11	0.00027
146	0.0006	0.00	0.65	11	0.0004	0.46	0.55	8	0.00051
147	0.0006	0.22	0.73	7	0.0009	0.11	0.66	10	0.00072
148	0.0008	-0.36	0.58	10	0.0008	-0.12	0.40	11	0.00080
149	0.0011	-0.27	0.86	8	0.0004	0.27	0.67	5	0.00076
150	0.0007	0.47	0.55	4	0.0004	0.39	0.91	5	0.00055

151	0.0006	0.15	0.84	9	0.0007	-0.23	0.94	6	0.00067
152	0.0006	0.28	0.67	8	0.0006	0.09	0.84	9	0.00056
153	0.0005	0.28	0.64	8	0.0004	0.50	0.48	9	0.00042
154	0.0017	0.38	0.78	5	NaN	NaN	NaN	NaN	0.00167
155	0.0011	-0.15	0.83	4	0.0010	0.25	0.69	5	0.00106
156	0.0003	1.02	0.95	5	0.0005	1.02	0.62	8	0.00039
157	0.0004	0.31	0.65	4	0.0002	0.34	0.68	6	0.00035
158	0.0006	0.06	0.77	4	0.0007	0.21	0.81	5	0.00065
159	0.0004	1.41	0.54	4	0.0003	2.00	0.17	5	0.00034
160	0.0005	0.87	0.94	4	0.0004	1.00	0.53	7	0.00045
161	0.0001	0.48	0.84	9	0.0002	0.78	0.74	6	0.00016
162	0.0003	0.47	0.83	8	0.0004	1.02	0.52	5	0.00035
163	0.0001	0.89	0.77	6	0.0002	1.21	0.35	6	0.00017
164	0.0002	0.38	0.64	7	0.0004	0.02	0.86	5	0.00027
165	0.0002	0.72	0.70	7	0.0001	0.56	0.93	5	0.00014
166	0.0001	0.26	0.57	6	0.0001	0.22	0.34	8	0.00014
167	0.0002	0.27	0.84	5	0.0002	0.19	0.90	5	0.00023
	Average		0.67		Average		0.67		0.00047